INFORMATION TO USERS

This material was produced from a microfilm copy of the original document. While the most advanced technological means to photograph and reproduce this document have been used, the quality is heavily dependent upon the quality of the original submitted.

The following explanation of techniques is provided to help you understand markings or patterns which may appear on this reproduction.

1. The sign or "target" for pages apparently lacking from the document photographed is "Missing Page(s)". If it was possible to obtain the missing page(s) or section, they are spliced into the film along with adjacent pages. This may have necessitated cutting thru an image and duplicating adjacent pages to insure you complete continuity.

2. When an image on the film is obliterated with a large round black mark, it is an indication that the photographer suspected that the copy may have moved during exposure and thus cause a blurred image. You will find a good image of the page in the adjacent frame.

3. When a map, drawing or chart, etc., was part of the material being photographed the photographer followed a definite method in "sectioning" the material. It is customary to begin photoing at the upper left hand corner of a large sheet and to continue photoing from left to right in equal sections with a small overlap. If necessary, sectioning is continued again — beginning below the first row and continuing on until complete.

4. The majority of users indicate that the textual content is of greatest value, however, a somewhat higher quality reproduction could be made from "photographs" if essential to the understanding of the dissertation. Silver prints of "photographs" may be ordered at additional charge by writing the Order Department, giving the catalog number, title, author and specific pages you wish reproduced.

5. PLEASE NOTE: Some pages may have indistinct print. Filmed as received.

75-6546

PASKE, William Charles, 1944-
   MOLECULAR LIFETIME DETERMINATION VIA COLD
   CATHODE INVERTRON.

   The University of Oklahoma, Ph.D., 1974
   Physics, molecular

Xerox University Microfilms, Ann Arbor, Michigan 48106

THE UNIVERSITY OF OKLAHOMA
GRADUATE COLLEGE

MOLECULAR LIFETIME DETERMINATION VIA COLD CATHODE
INVERTRON

A DISSERTATION
SUBMITTED TO THE GRADUATE FACULTY
in partial fulfillment of the requirements for the
degree of
DOCTOR OF PHILOSOPHY

BY
WILLIAM C. PASKE
NORMAN, OKLAHOMA
1974

MOLECULAR LIFETIME DETERMINATION VIA COLD

CATHODE INVERTRON

APPROVED BY

....

....

....

....

....

DISSERTATION COMMITTEE

ACKNOWLEDGEMENTS

TABLE OF CONTENTS

TABLE OF CONTENTS (Cont'd.)

LIST OF TABLES

LIST OF ILLUSTRATIONS

LIST OF ILLUSTRATIONS (Cont'd.)

LIST OF ILLUSTRATIONS (Cont'd.)

STATEMENT OF PURPOSE

The purpose of this research is essentially twofold. First to validate the experimental apparatus and to determine in which ways the equipment could vitiate the results; and secondly, to use the improved apparatus to determine the lifetimes of SO_2.

In 1970 Copeland[1] developed the cold cathode invertron for lifetime studies of molecules easily dissociated by the thermally heated cathode of the Holzberlein invertron (see the works of Holzberlein[2], Johnson[3], Shaeffer[4] and Thompson[5]). Copeland's studies dealt with nitric oxide, atomic and molecular oxygen, and in his work he reported lifetimes with as much as 20% uncertainty. Anderson[6] has used a similar device and reported lifetimes of the $C^3\Pi_u$, and $B^2\Sigma_u^+$ states of N_2 and N_2^+, with rather large experimental scatter. It was felt that design improvements and a better understanding of the experimental equipment could eliminate much of this scatter.

To this aim, the rather excellent data which Johnson[3] ($\pm 2\%$ in most cases) presented for the $C^3\Pi_u$ and $B^2\Sigma_u^+$ states of N_2 and N_2^+ have served as a standard. The first section of this paper then will deal with the development of the experimental apparatus (where different from Copeland) and the effects of the following on lifetime measurements: data acquisition rate, discharge voltage, applied external magnetic field, cathode structure (geometry), the addition of a quenching gas and finally, the problems caused by an improperly functioning photomultiplier tube.

The remaining sections will deal first with the measurements made on nitrogen to give an overview of the system's accuracy and finally a discussion of the lifetime measurements made on sulfer dioxide will conclude this report.

CHAPTER I

INTRODUCTORY COMMENTS

Why measure the lifetimes or the transition probabilities of excited atomic or molecular systems? The answer to this question is intended to provide an overview for this chapter, i.e. why directly measured lifetimes are useful to various fields of physics. A few obvious examples of fields which can make good use of lifetime measurements are spectroscopy, astrophysics (similarly for environmental physics), and lasers. It should be noted that lifetimes themselves are not needed in these fields, but the Einstein transition coefficients A_{ik} are, and these are related to the measured lifetime by the relation

$$\tau_k = 1/\Sigma_i A_{ik} \qquad\qquad 1$$

For example, the intensity of a given emission (similarly for absorption) line is related to the Einstein transition coefficient by the expression

$$I_{kn} = A_{kn} N_k \hbar \omega_{kn} \frac{V}{4\pi} \qquad\qquad 2$$

where $\omega_{kn} = (E_k - E_n)/\hbar$, E_k and E_n are the energies of the k and n levels, $V/4\pi$ is the solid angle extended and N_k is the number of molecules in the state of interest k. By knowing the transition coefficient A_{kn} and measuring the relative intensities of the various emission lines, relative populations of the excited states can be determined.

In astrophysics (as well as in the environmental monitoring of the atmosphere) a knowledge of the oscillator strength f_{kn} will allow a calculation of the absorption coefficients of a gas of atoms or molecules through which the observed light is propagating. The oscillator strength is a dimensionless constant which expresses the absorptive power for each characteristic frequency as a function of the total absorptive power of the electron, i.e. it is a measure of the Fourier coefficient of the particular harmonic of the electron oscillator. It is related to the transition coefficient by the equation

$$f_{kn} = -A_{kn}mc^3 (2e^2\omega_{kn}^2)=\frac{mc}{8\pi^2 e^2} \frac{g_k}{g_n} \lambda^2 A_{kn} \qquad 3$$

where g_k and g_n are the statistical weights of the levels involved; e.g. $g_k = 2J_k + 1$, J_k is the total angular momentum number of the system.

In the case of lasers, it is necessary to have some knowledge of the ability to maintain a population inversion which is dependent on the decay rate of the lower laser level. This level obeys the inequality

$$dN_k/dt > A_{kn}g_k/g_n. \qquad 4$$

A knowledge of these levels and their transition probabilities then can be of great help in determining the direction of laser research.

One way to obtain the transition coefficients is to calculate them. It is well known that electromagnetic radiation interacts with atomic systems, in that an atom in level k of energy E_k described by ψ_k has a non-zero probability of finding itself in level n of energy E_n described by ψ_n if the electromagnetic radiation was of

wavenumber $\nu = (E_k - E_n)/hc$ (assuming k and n are non-degenerate).
This interaction may be considered as an interaction between an
electromagnetic wave having an electric vector $\underline{E}$, and an atomic sys-
tem, which in a first approximation is an interaction with an elec-
tric dipole of moment $\underline{M}$. When this interaction, $\underline{M} \cdot \underline{E}$, is treated by
quantum mechanics, it is found that the probability of a transition
is proportional to the square of the matrix elements of the electric
dipole moment, i.e.

$$A_{kn} = \frac{4e^2 \omega_{kn}^3}{3\hbar c^3} \frac{1}{g_k} \sum_{m_n m_k} |\underline{R}^{kn}|^2 \qquad 5$$

where

$$\underline{R}_i^{kn} = \int \psi_n^* M_i \psi_k dt \qquad i = x, y, z. \qquad 6$$

This assumes equal population of the k levels, a valid assumption
for most gas discharges.

If $|\underline{R}^{km}|^2 \neq 0$, the two states have a finite probability of
interaction with the emission or absorption of radiation. If
$|\underline{R}^{km}|^2 = 0$, then the electric dipole transition is forbidden; that
is to say, in the absence of external fields it must go by higher
order electric multipoles or by magnetic multipole transitions.
Note, however, that the magnetic dipole transitions and the elec-
tric quadrapole transitions are down by a factor of 10^{-5} and 10^{-8}
with respect to electric dipole radiation.

For a diatomic molecular system, we may consider the mole-
cule to have electronic configuration k, vibrational quantum number
v' and rotational quantum number J'. Then, if we assume (i) separ-
ability, i.e. $\psi = \frac{1}{r} \psi_k \psi_{v'} \psi_{J'm'}$, and (ii) that the electronic por-

tion $\psi_k(\underline{r}_i)$ does not depend appreciably on the internuclear separation $\underline{r}$, that is to say we assume that the transition occurs sufficiently rapidly that the nuclei do not have time to rearrange themselves during the interaction, we find

$$A_{kn',\ v'v'',\ J'J''} = \frac{4e^2\omega^3_{kn',v'v''}}{3\hbar\,c^3 g_k}\ |\underset{\sim}{R}_e^{kn}|^2\ |R_{vib}^{v'v''}|^2 \underset{m'm''}{\Sigma}|\underset{\sim}{R}_{rot}^{J'J''}|^2 \frac{}{2J'+'} \qquad 7$$

where

$$R_e^{kn} = \int \psi_k \Sigma r_i\ \psi_n d\underline{r}_i$$

$$R_{vib}^{v'v''} = \int \psi_{v'}^* \ \psi_{v''} d\underline{r} \qquad \{\,|R_{vib}^{v'v''}|^2 \equiv \text{Frank-Condon factors}\,\}$$

$$R_{rot}^{J'J''} = \int \psi_{J'm'}^* \psi_{J''m''} \sin\theta d\theta d\phi$$

Now, by summing over all transitions from a given vibrational level and using the sum rule

$$\underset{J''}{\Sigma} \underset{m'm''}{\Sigma} |R_{rot}^{J'J''}|^2 = 2J' + 1 \qquad 8$$

we find for the transition probability $A_{kn'}$,

$$A_{kn',\ v'v''} = \frac{4e^2\omega^3_{kn,v'v''}}{3\hbar c^3 g_k}\ |\underset{\sim}{R}_e^{kn}|^2 |\underset{\sim}{R}_{vib}^{v'v''}|^2 \qquad 9$$

Using this equation, calculations can be made to determine the Einstein spontaneous transition probability (and from this the absorption probability) which may then be used in the manner sketched earlier in other branches of physics. Unfortunately many of these calculations have rather large errors associated with them, some as high as 50%[7]).

However, the lifetime (or mean life) of the above vibrational band is given by

$$\tau_k = 1/\sum_{nv''} A_{kn,v'v''} \qquad\qquad 10$$

and if this lifetime can be directly measured, significant reduction in the errors of the system can be made, thereby reducing the error in the subsequent manipulations.

From a probabilistic standpoint, we could consider the time rate of change of the population of a given excited level N_k by the relation

$$\frac{dN_k}{dt} = -N_k \sum_n A_{kn} = -N_k/\tau_k \qquad\qquad 11$$

which is simply

$$N_k(t) = N_k(o)e^{-t/\tau_k} = N_k(o)e^{-\sum_{n,v''} A_{kn,v'v''} t} \qquad\qquad 12$$

This implies that a straight forward observation of the decay rate of the excited state would yield the transition probability via the mean life or the lifetime of that state.

In actuality, the time rate of change should be written

$$\frac{dN_k}{dt} = -N_k \sum_n A_{kn} + \sum_\ell N_\ell A_{\ell k} - N_k \sum_\ell B_{k\ell} U(v_{k\ell}) + \sum_n N_n B_{nk} U(v_{nk})$$

$$- \quad -N_k \sum_n B_{kn} U(v_{kn}) + \sum_\ell N_\ell B_{\ell k} U(v_{\ell k}) - N_o v N_k \sum_n \sigma_{kn} + N_o v N_k \sum_n \sigma_{nk}$$

$$-N_o v \sum_\ell \sigma_{k\ell} N_\ell + N_o v \sum_\ell \sigma_{\ell k} N_\ell + n_e N_o \sigma_k v_e + n_e v_e \sum \sigma_{kn} N_n - D_k \nabla^2 N_k$$

$$-\alpha_a N_e N_k - \alpha_r N_e N_k^+ \qquad\qquad 13$$

where: B_{mn} = Einstein transition probability: induced absorption, m<n; induced emission, m>n.

A_{kn} = Einstein spontaneous emission transition probability.

$U(v_{kn})$ = radiation density of photons .

σ_{mn} = cross section for radiationless collisional transition from m to n

N_o = Neutral ground state molecules

$n_e v_e$ = excitation electric current density

$\alpha_{\dot{a}}$ = attachment coefficient (electron)

v = mean velocity of neutral ground state molecules

α_r = electron recombination coefficient

D_k = diffusion coefficient

σ_k = electron excitation cross section

σ_{nk} = electron excitation due to metastable or other excited states

and where ℓ refers to higher energy levels, n refers to lower energy levels with respect to the level k.

Verbally, this equation could be written as the following:

rate of change of the population of level k =

    spontaneous emission from
- level of interest to lower state

    spontaneous cascade from
+ upper state to level of interest

    induced absorption from
- level of interest to higher level

    induced absorption from
+ lower level to level of interest

    induced emission from
- level of interest to lower level

    induced emission from
+ higher level to level of interest

    collisional depopulation
- from level of interest to lower level

    collisional depopulation
- from level of interest to higher level

    collisional population
+ from lower level to level of interest

    collisional population from
+ higher level to level of interest

production due to
+ electron bombardment
of neutrals

production due to
+ electron bombardment
of metastables

collisional depopula-
- tion due to diffusion
to walls

depopulation by electron
- quenching

depopulation due to
- recombination

In practice however, the following simplification is usually used, all other terms in Eq. 13 being ignored

$$\frac{dN_k}{dt} = -N_k \sum_m A_{kn} + \sum_\ell N_\ell A_{\ell k} - N_k N_o <v> \sum_n \sigma_{kn}$$ 14

and in the event that there are no cascading levels present, we have

$$N_k(t) = N_k(o)e^{-A't}$$ 15

where A' now includes the pressure depopulation term, i.e.

$$A' = \sum_n A_{kn} + N_o <v> \sum \sigma_{kn}$$ 16

This type of system will give a pressure dependent lifetime such that $1/\tau_k$ plotted vs the pressure will yield a slope which is proportional to the collisional depopulation cross section and the intercept will be the zero pressure lifetime of the excited state. A useful relationship between the second term of Eq. 15 and the pressure is

$$N<\sigma v> = 1.404 \ p\sigma \frac{(m_1 + m_2)}{(m_1 m_2 T)}^{1/2} X10^{23} \ sec^{-1}$$

where pressure p is in torr, σ is in cm^2 and the m's represent the masses of the respective atoms.

The following sections will deal with the development of the experimental apparatus with Eq. 12 and 13 in mind, i.e. have we left

anything out that we should not have and have we biased the results in any way by the manner in which we conduct the experiments? For example:

cathode structure: any geometrical dependence present? Also, can any new information be collected as to the depopulation of excited states by means other than neutral molecule collisions?

magnetic field: the field is necessary to initiate the discharge at low pressures...does it effect the observed lifetimes in a systematic way?

quenching or attaching gas: how big a role do recombination and attachment play?

discharge voltage: can varying the applied voltage effect the results in any manner?

count rate: does the data acquisition rate have any effect on the lifetimes?

pressure dependence: is there anything other than the usual pressure dependence?

Further discussion of the transitions probabilities may be found in ref. 8-16 and many related works.

CHAPTER II

EXPERIMENTAL APPARATUS

A
Vacuum System

The vacuum system was built to insure sample purity and to
provide variable flow rates since the gases intended for study will
dissociate rather easily. The system consists of two vacuum sys-
tems, one for purity and maintainance of the base pressure $(10^{-5}$
torr) and the second for the removal of the waste gases. This sec-
ond system allowed for special handling of the SO_2. Fig. 1 illu-
strates the total system and the dashed line AA' indicates the divi-
sion of the two.
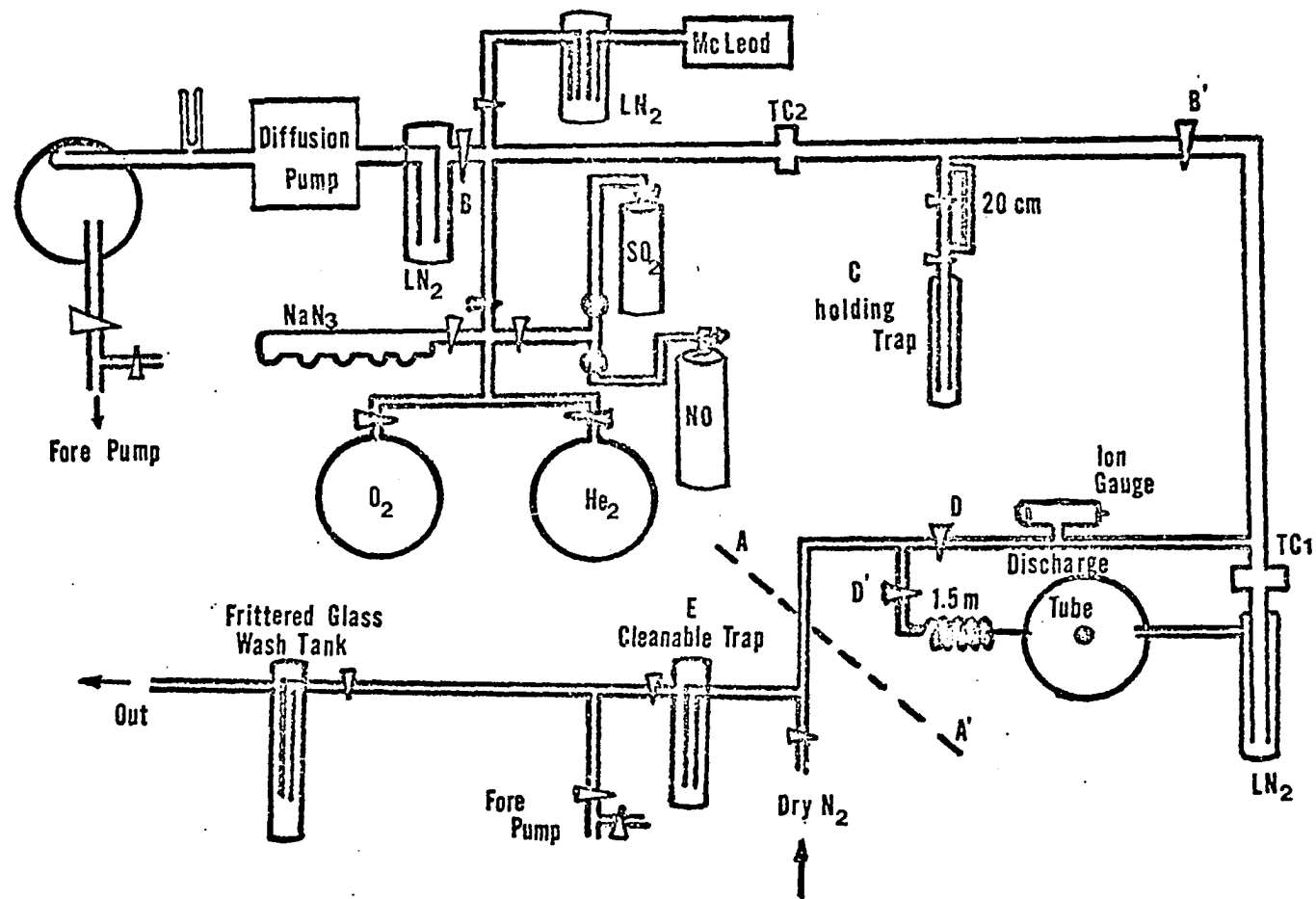
Fig. 1. Vacuum System

The main components of the system are discussed below. Both the forepumps are standard mechanical-oil roughing pumps capable of pumping 100 liters per minute and have a base pressure of approximately 10^{-4} torr. These pumps were connected to the Pyrex system via Tygon tubing. All stopcocks, including the main stopcocks on the pumps were of high vacuum quality with pumpable bores. Apiezon N vacuum grease was used throughout the system and in the final version, no Black Wax or Glyptol was used.

The mercury diffusion pump was a two stage water cooled Eck and Krebs which was isolated from the main system by a liquid nitrogen trap.

Pressure in the system was monitored by two CVC type GTC-004 thermocouples (TC1, TC2) and a Bayard-Alpert type ion gauge which were maintained by a GIC-110B gauge pack. The thermocouples were calibrated for each gas with the mercury McLeod gauge in a static system.

The gas sampling units consisted of Matheson research quality Pyrex liter flasks of oxygen and helium which were used in the quenching experiments, a Matheson bottle of 95% pure NO, a lecture bottle of anhydrous sulfur dioxide and a special nippled tube (see Fig. 1) for sodium azide which provided high quality nitrogen after treatment.

The frittered glass wash tank provided a means of disposing of the used SO_2 safely without dumping the waste gas out the window and also prevented the gas from coming in contact with the hot mercury in the diffusion pump.

The dosed gases were handled in the usual manner with the exceptions of the N_2 and the SO_2. To produce the N_2, the sodium azide tube was pumped down and _gently_ heated to remove any moisture. The system was then closed off and heated vigorously until the NaN_3 decomposed in a milky-grey cloud. This N_2 charge was then used as any standard bottle of gas would be. A gram of NaN_3 produces approximately one liter of nitrogen at one atmosphere.

When SO_2 was used, the charge was dosed into the system up to point B' making sure that the stopcock at B was _closed_. Liquid nitrogen was then used to freeze the SO_2 into the holding trap at C. After freezing, the valve at B was opened and the residual gases pumped off. The stopcock above C was closed and the holding trap allowed to warm up. The gas was then again cooled with liquid nitrogen and the stopcock above C opened and the residual gases were again pumped off. In this way, trace amounts of dissolved nitrogen were removed from the SO_2 spectrum.

To use the SO_2, B was closed, B' opened, D closed, D' opened and the bypass valve on the holding trap was closed. The collection trap at E was cooled to liquid nitrogen temperature and the first valve above the holding trap opened. In this manner, flowing SO_2 can be obtained at pressures varying from 0.015 torr to 0.500 torr for up to six hours. After the gas has been collected, the collection trap is isolated from the rest of the system by closing D' and then allowed to warm up to room temperature. Once warm, the trap is back filled with dry nitrogen to atmospheric pressure and then bled through the water trap.

In this fashion, the SO_2 is dissolved by the water (3940 cc or 11.28 of SO_2 will dissolve in 100 cc of water) and sulfurous acid is produced, thereby containing the toxic gas in solution. The collection trap is then roughed out by the second fore pump to ensure no water gets into the main system, after which it is pumped to base pressure by the main pumps.

The NO bottle was not used in this experiment.

B
Excitation Electronics

The excitation electronics in this section were designed to produce essentially a square pulse of 600 to 1500 V peak and from 100 ns to a few microseconds duration at variable repetition rates from 60 Hz to 3KHz with fall times on the order of 5 to 10 ns. This has been accomplished in much the same way as described by Copeland. However, three of the circuits have been altered to allow for a more complete energy transfer and faster repetition rates. The modified circuits are: the high voltage power supply, the pulse forming generator (PFG) and the crowbar unit. All circuits, however, will be presented for completeness.

Fig. 2 shows the essential parts of this system in block form, the primary components are in double lines.

The high voltage power supply, Fig. 3, consists of a power line transformer rated at 35 KV-A, i.e. will deliver 7000 volts at 5 amps. This unit is normally only required to provide around 3 KV. The AC output of this unit is fed via high voltage standoffs and high voltage cable to a separate unit (indicated by the dashed line in the figure) where it is rectified by the silicon bridge and fed to a 14 µf 40KV oil filled capacitor which provides the main power for the discharge when fed through the pulse forming generator. The silicon rectifiers shown in the figure consist of three diodes in series (1 amp 4KV PIV), each of these in parallel with a 0.005 µf ceramic disc capacitor and a
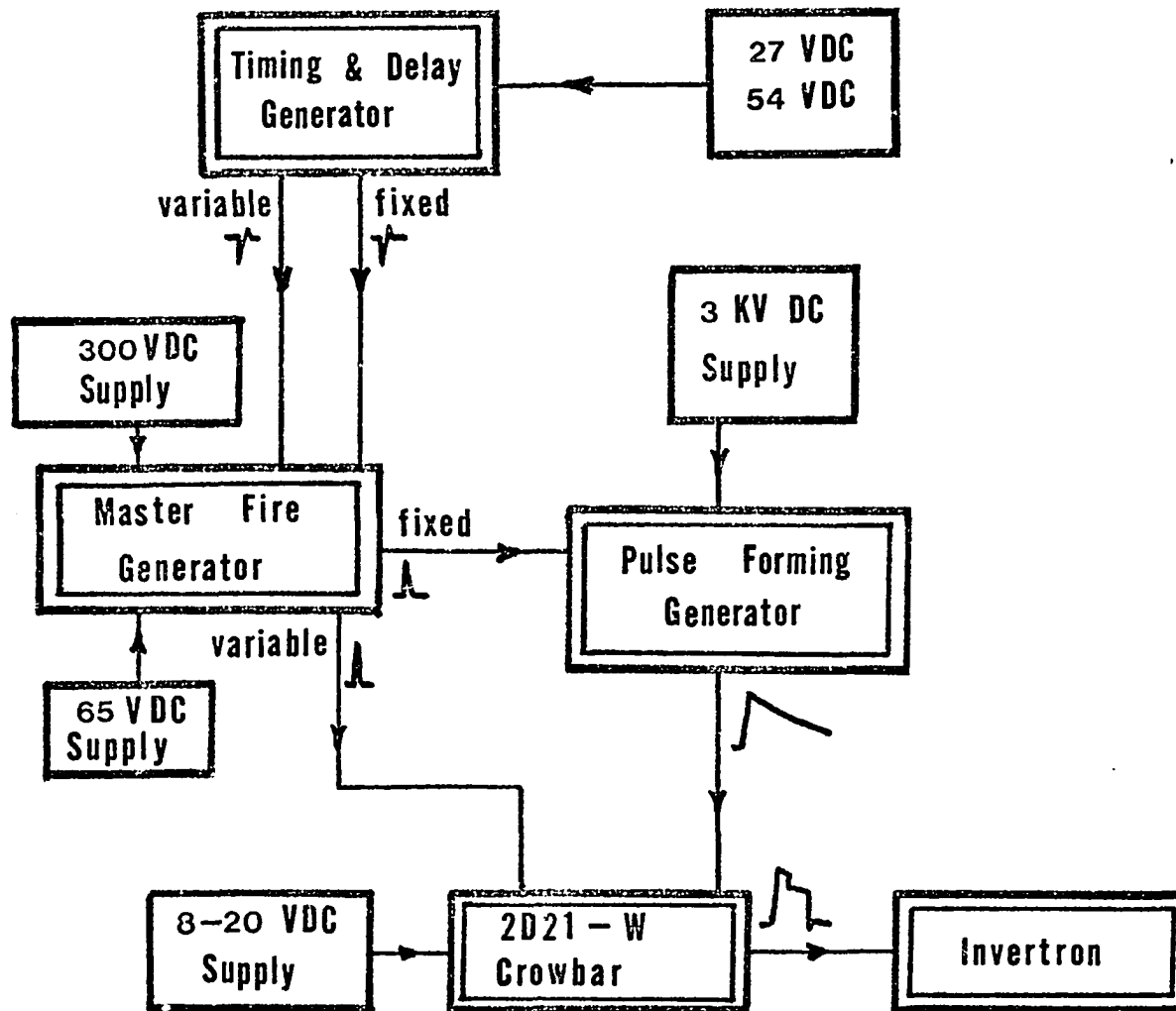
Fig.2. Excitation System
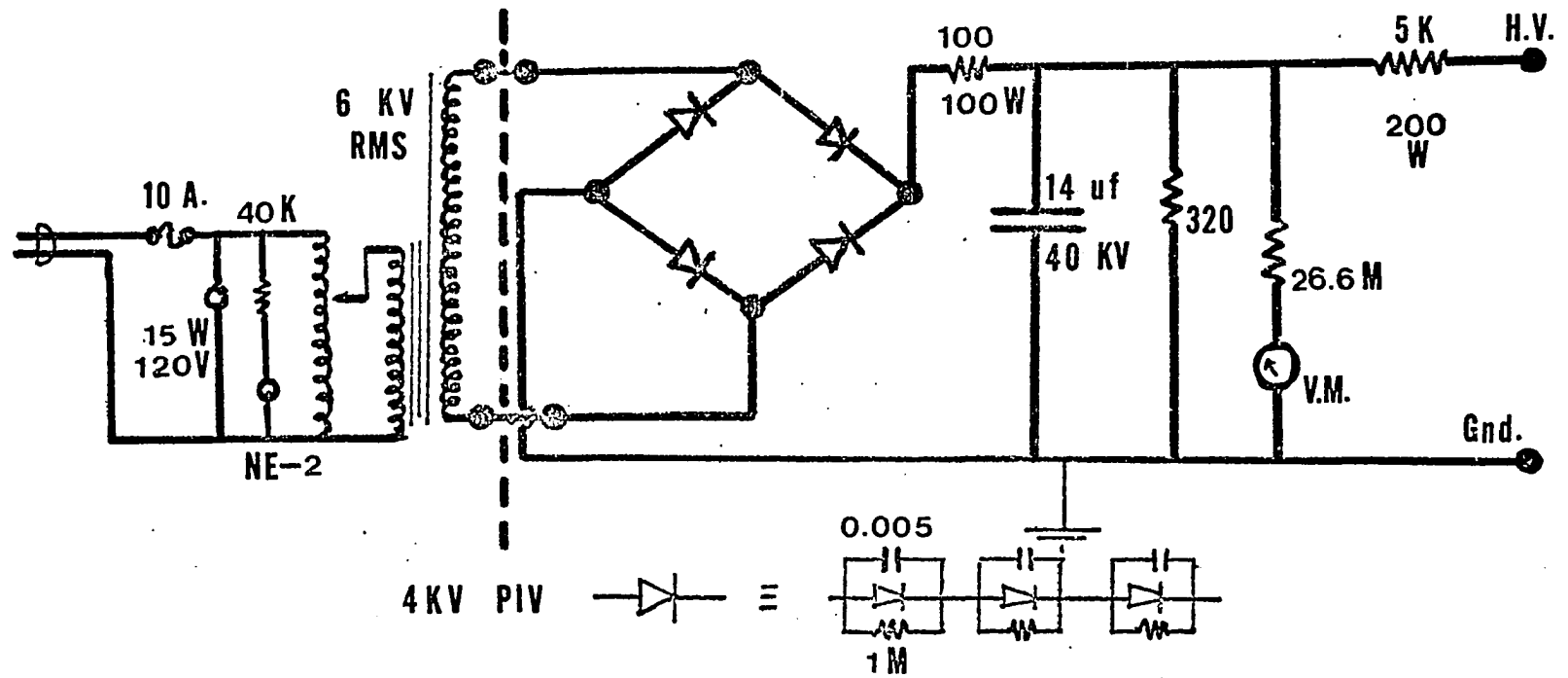
Fig. 3: High Voltage Power Supply

5W 1M resistor to reduce the spike amplitudes in the diodes and to provide a bleeder circuit to ground. The 320K resistor provides a bleed to ground on the 14 μf capacitor for safety.

Instead of the 80K load resistor, the system now uses a 5K load resistor (200W) which allows the 14 μf capacitor to recharge at faster repetition rates (2-3Khz). This insures that the 3C45 in the PFG will have sufficient voltage to fire everytime it is triggered by the master fire generator (MFG).

The output of this power supply is then fed to the PFG via high voltage cable to high voltage standoffs. This unit, shown in Fig. 4, was found to function much more efficiently and at much higher repetition rates if the 500Ω developing resistor was replaced by 47Ω (150W), the characteristic impedance of the 3C45. This system will fire, without missing, for repetition rates up to 3KHz, but this tends to reduce the usable lifetime of the hydrogen thyratron considerably. Consequently, a repetition rate of 1KHz was generally used. The 250Ω carbon resistor was comprised of four 1K carbon resistors and was used to reduce the inductance of the system.

The third circuit modified was the crowbar unit. This was designed to clamp or short the RC decay provided by the PFG into a square pulse at variable times after the inception of the pulse. This unit, see Fig. 5, did just that with a fall time from 5 to 10ns. The crowbar was placed in direct proximity with the discharge tube via UHF connectors to reduce stray inductance. The differentiated output was used to provide a voltage trigger to the time amplitude converter (TAC) in coincidence with the cessation of the excitation pulse. It was noticed
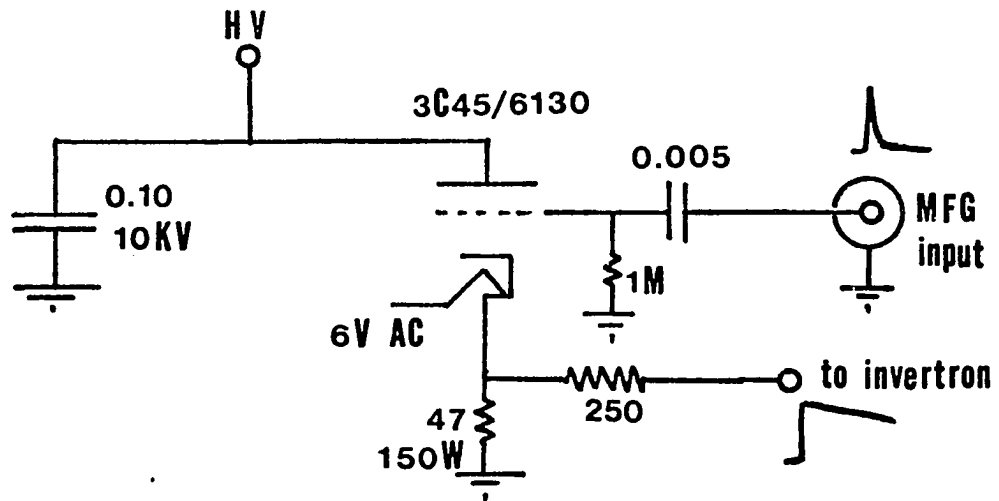
Fig. 4:   Schematic for Pulse Forming Generator
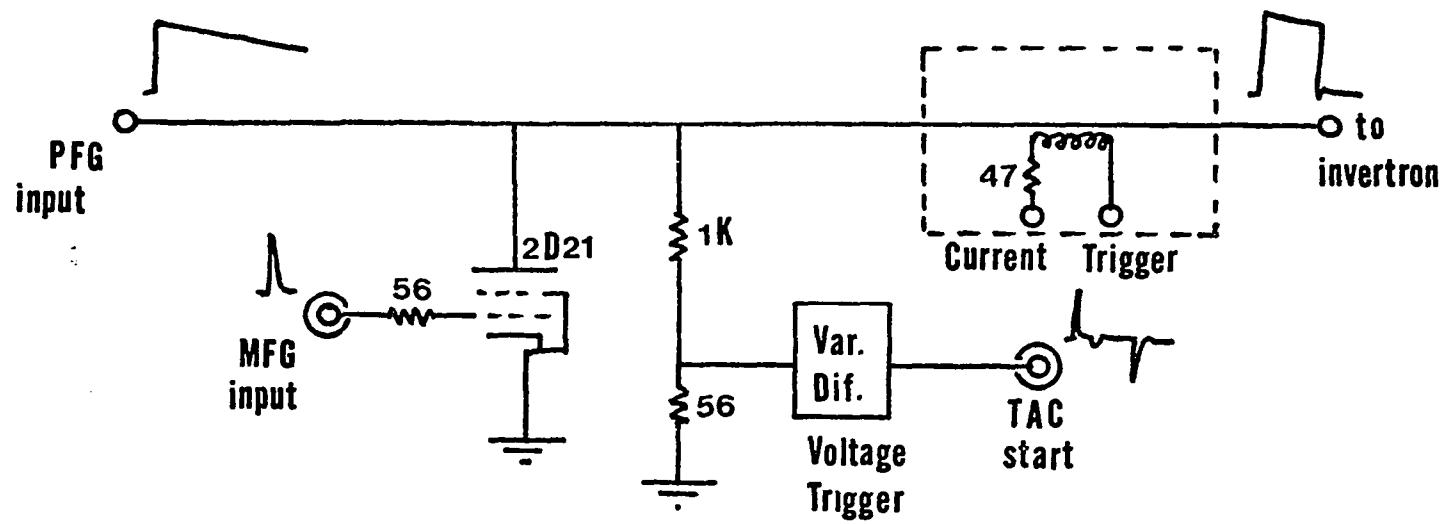
Fig. 5: Schematic for Crowbar Unit

that this 'start' pulse had some rather subtle structure as shown in

Fig. 6. Further experimentation indicated that it was this second

fall, not the first, which was the true cut-off of the glow discharge

(note the statistical nature of this second pulse), and that in severe

cases of slow cut-off, e.g. 30+nsec, see Fig. 7, this fine structure

could vitiate the experimental results since either of the pulses

could trigger the TAC clock 'on'. This then appears as a smeared onset

of the decay as shown in Fig. 8a and 8b, and can mask short lifetimes

on the order of 20nsec.
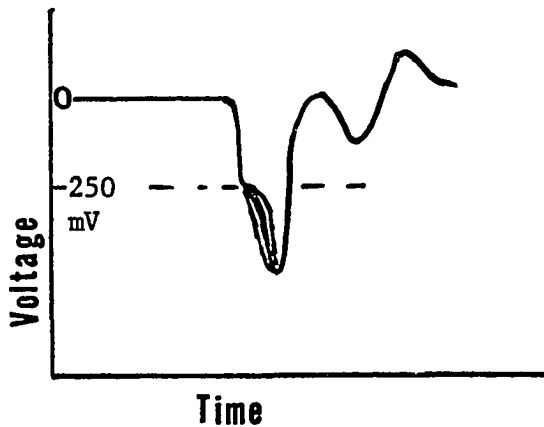
Fig. 6: fine structure of
         start pulse.
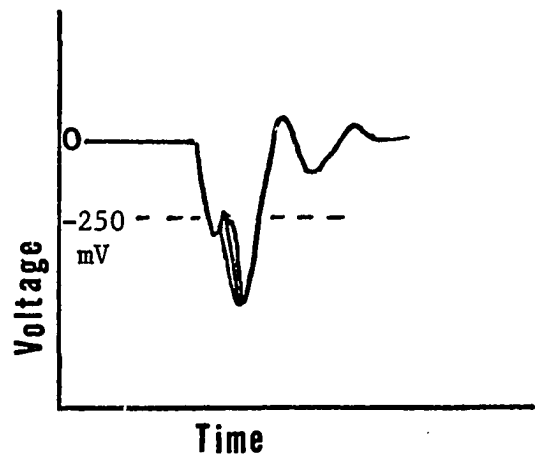
Fig. 7: start pulse with
         slow, 30+nsec,
         cut-off
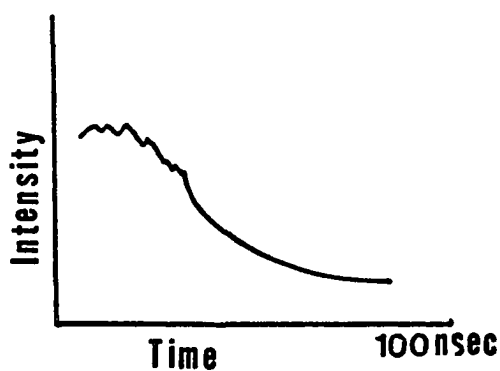
Fig. 8a: decay curve using
         voltage trigger
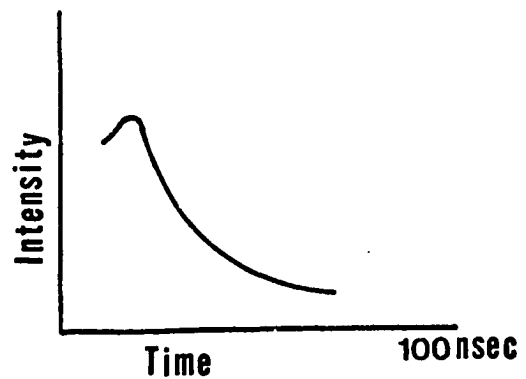
Fig. 8b: decay curve using
         current trigger

Fig. 8b was compiled using the current trigger which is shown in the dashed box in Fig. 5. This trigger only fired when the glow cut-off, and also coincided with the second pulse of the voltage trigger when superimposed. However, this current trigger could not be used with confidence as it altered the cut-off characteristics of the discharge and consequently biased the observed lifetimes for lifetimes around 30 to 40 nanoseconds. It did show legitimate lifetimes for fast states however, as we checked the 3^1P (5016Å) level of He and the $4P-^4D^o$(4650Å) level of OII and found lifetimes compatable with those reported in the literature (~10ns). It should be stressed that this problem is only important when measuring fast lifetimes, i.e. on the order of 20 nanoseconds or faster. For longer lifetimes, even those as short as 40 nanoseconds, this distortion in the lead channels due to false starts is of no consequence, adding only a small percentage of random error to the observed lifetime.

The cut-off could be altered for the above experiment by varying the filament voltage of the 2D21 in the crowbar unit from 8 to 16 volts, the higher the filament voltage, the faster the cut-off appeared. It was also found that the 2D21 filament could be increased to as high as 24 Vdc before the tube burned out.

The 1K carbon load resistor was also inserted to improve cut-off characteristics. It was noticed that while the $C\ ^3\Pi_u$ state of N_2 gave the appropriate lifetime, the $B^2\Sigma_u^+$ state of N_2^+ did not. Fig. 9a, b, show the observed decay curves for these states. Note the poor fit in the lead channels for the ionized molecule. Fig. 10 shows the same

sample except with a 500 ohm load resistor. Not only is the plateau reduced, i.e. the cut-off is truely faster, the lead channels do not appear as distorted. See also the section on cathode inserts for further discussion of this problem.

The rest of the circuitry, the master fire generator (MFG) Fig. 11, the timing and delay generator (TDG) Fig. 12a, b, the two power supplies, +27 and +54 Vdc Fig. 13, and +65 Vdc Fig. 14 are all the same as described by Copeland and are included for completeness. The ± 310 Vdc regulated power supply was a surplus unit manufactured by the U. S. Science Corporation.

Fig. 9a. Decay curve for

N_2^+ B $^2\Sigma_u^+$ 3914 Å

τ = 53.1 nsec

p = 220 u Hg

Ln Intensity

Channel (Time)

Fig. 9b. Decay curve for

$N_2 \; C^3\pi_u \quad$ 3371 Å

τ = 38.7 nsec

p = 220 u Hg

Fig. 10. Decay curve for

N_2^+ B $^2\Sigma_u^+$ 3914 Å,

altered load resistor

τ = 55.4 nsec

p = 220 u Hg

Ln Intensity

Channel No.

+65 V DC

+310 V DC

50K

TDG
fixed
input

0.001

1N198

200K

2N3440

30K
4W

0.01

2D21

0.005

-310V
DC

250K

50K

0.1

47

output
to
PFG

+65V DC

50K

TDG
variable
input

0.001

1N198

200K

2N3440

30K
4W

0.01

2D21

0.005

-310V
DC

250K

50K

0.1

47

output
to
Crowbar

Fig. 11: Master Fire Generator

Fig. 12a: Timing and Delay Generator
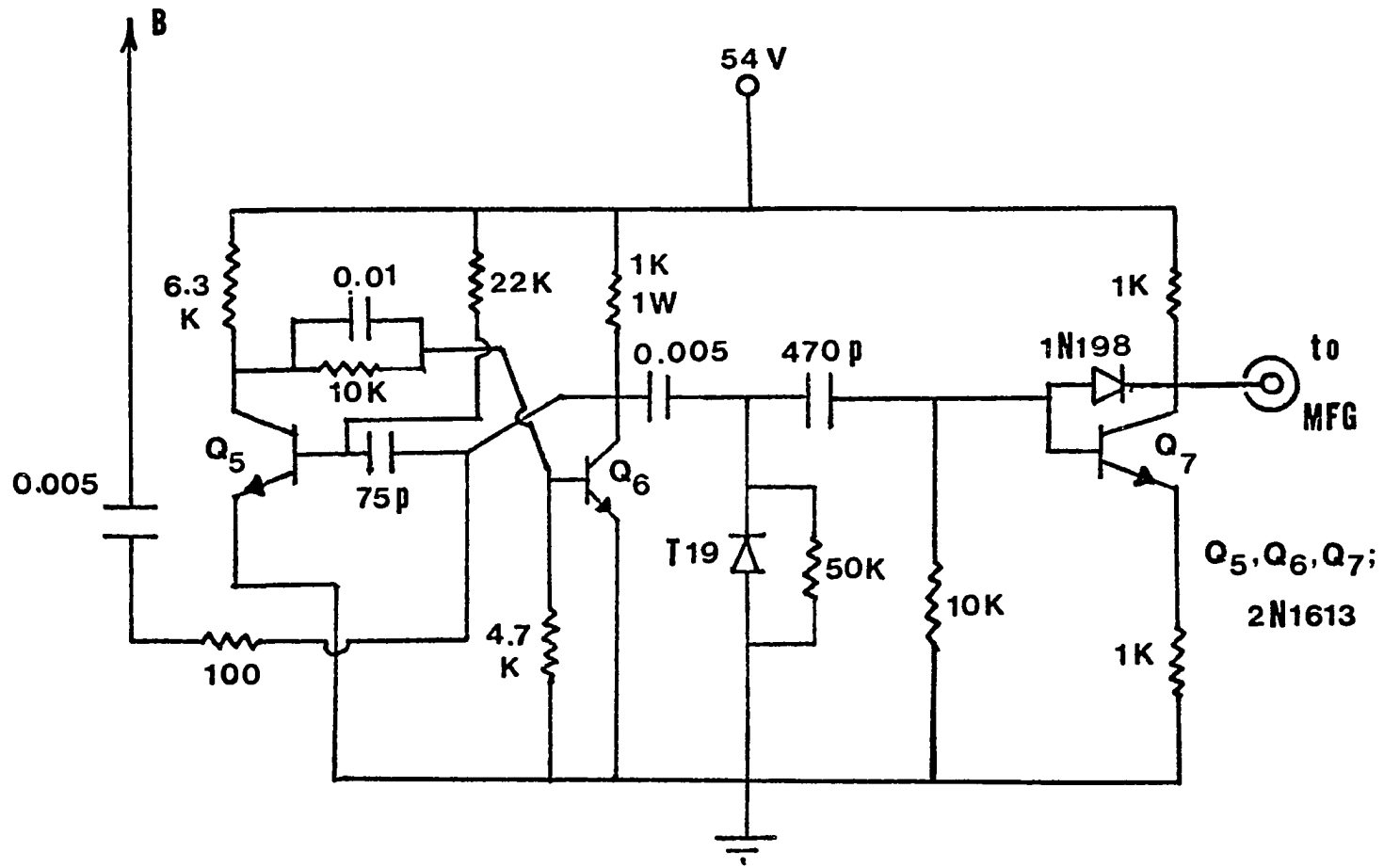
Fig. 12b: Timing and Delay Generator
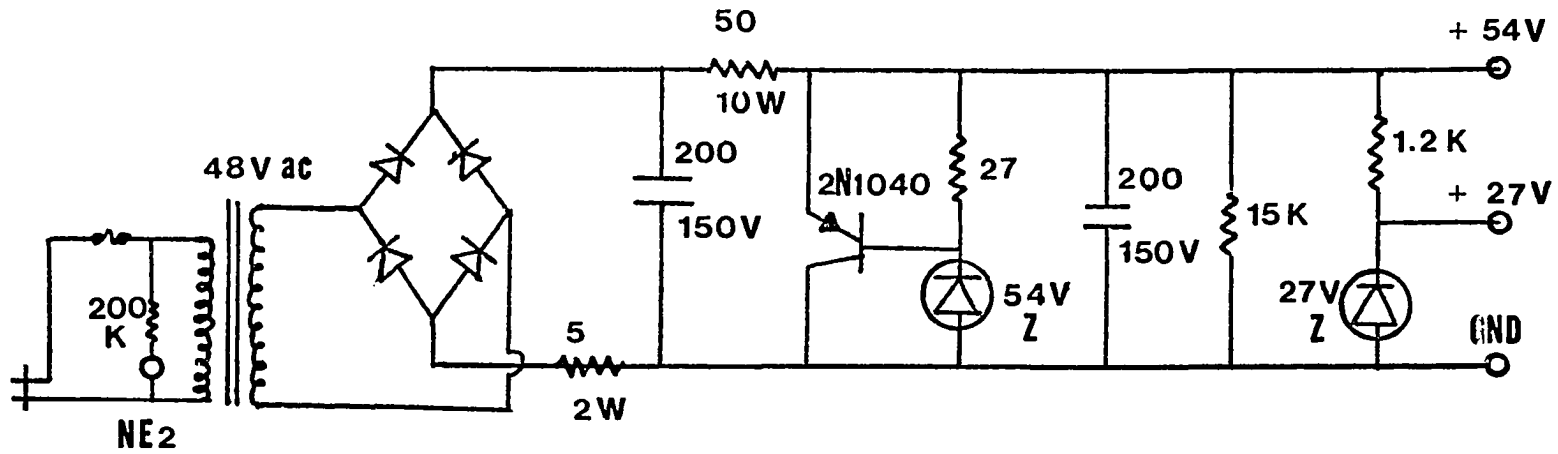
Fig. 13:   +27 and +54 VDC Power Supply

C
Detection System

The experiments described in this paper are based on the probability of observing a photon of appropriate wavelength after the excitation system has been turned off; hence, the technique is known as delayed coincidence photon counting. The system is shown in block form in Fig. 15.

A typical event would proceed as follows: the excitation system clamps the discharge off, and the differentiator produces a positive and negative spike coincident with the on-set and cut-off of this pulse. The differentiated signal is sent to the ORTEC time to amplitude converter (TAC) as a 'start' signal, where only the negative spike (minimum -250 mV and 5 nsec fwhm) will start the internal clock, and to the ORTEC delay gate generator (416A) where the positive spike is used to generate a positive logic pulse (approx. 3V) which is then delayed sufficiently to coincide with the cut-off of the excitation pulse and serves as a gate to the TAC. This insures that the system will not trigger on from the differentiated portion of the discharge pulse which is due to the statistical break-down of the glow discharge as shown in Fig. 16. The first Canberra scaler provides the number of times that the system is fired in a given experimental run.

After cut-off of the excitation, the first photon of appropriate wavelength that the photo-detection system 'sees' will produce a sharp negative pulse (-800 mV, 6 nsec fwhm) which is sent to the TAC
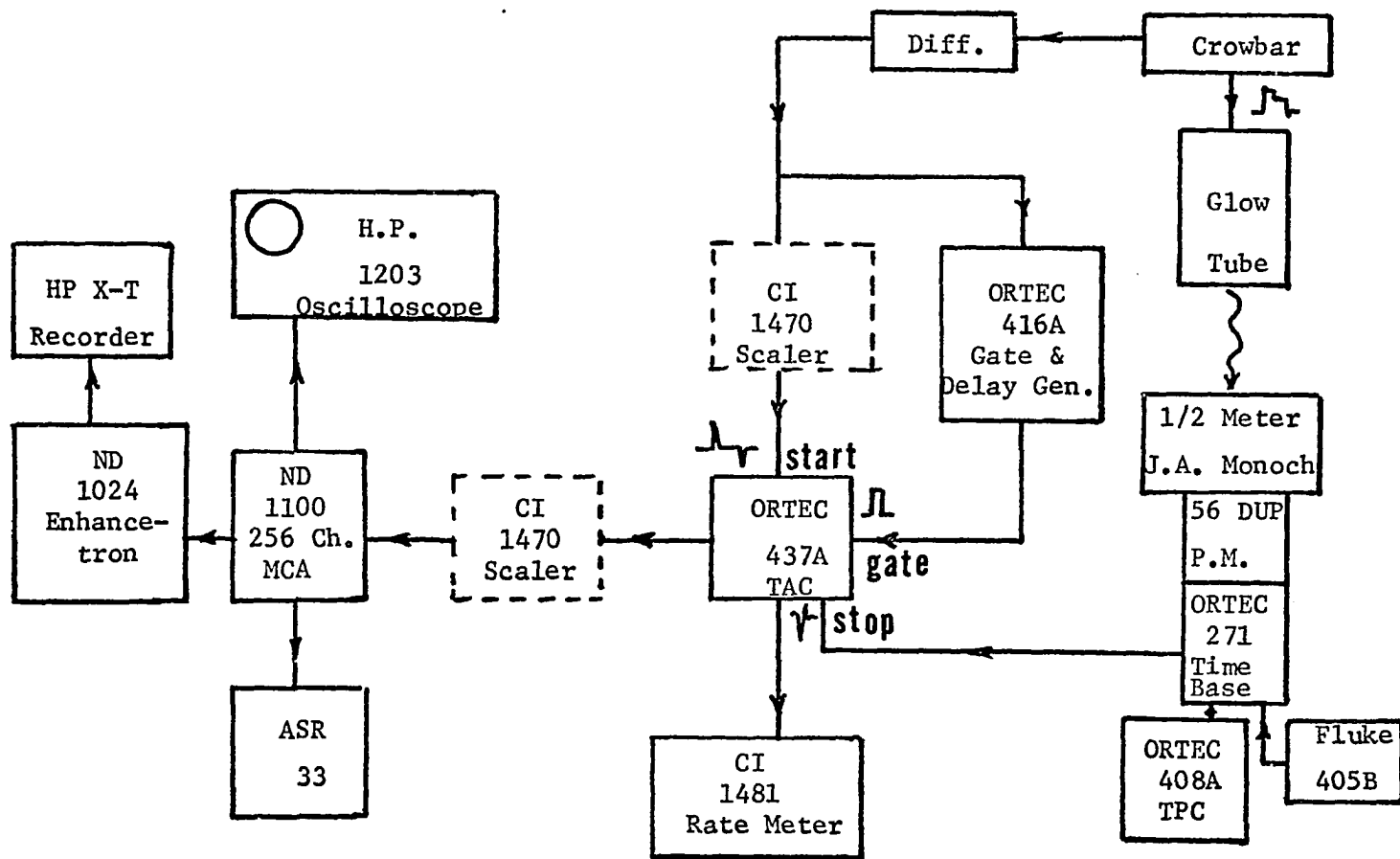
Fig. 15: Block Diagram of Detection System
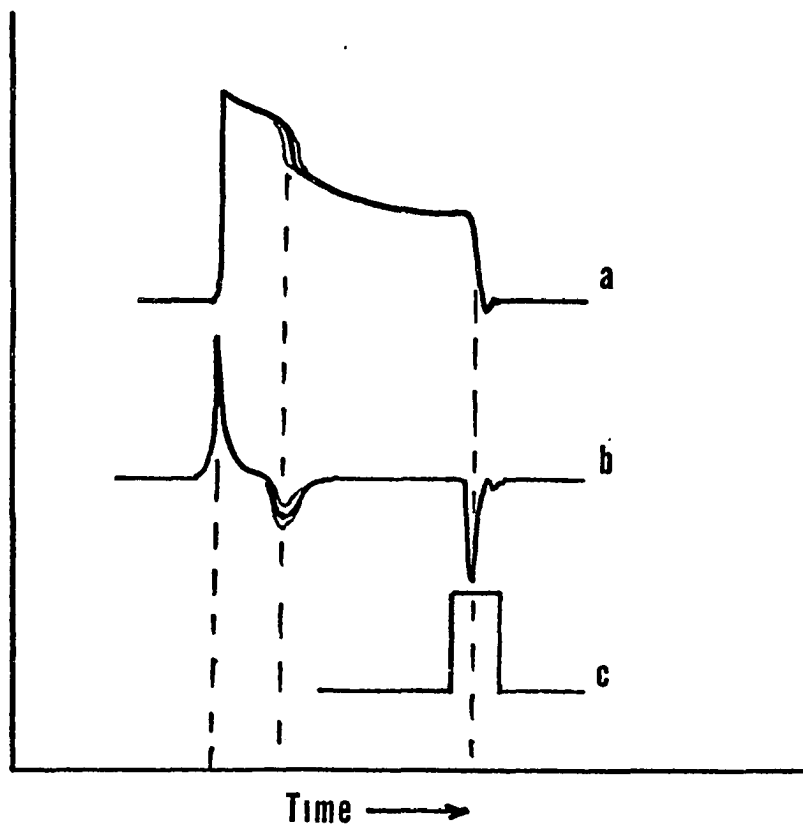
Fig. 16:   Time Sequence of Gate Pulse

a)   Excitation Pulse

b)   Differentiated Pulse

c)   Logic Gate Pulse

as the 'stop' signal. The time delay from the receipt of the start

pulse until the arrival of the stop pulse is then converted to a vol-

tage pulse whose amplitude is proportional to this time delay. The

output from the TAC is sent to a ND-1100 256 channel multichannel an-

alyzer (MCA) where the amplitude of the voltage pulse determines in

which channel of the memory the signal belongs. This process is re-

peated several hundreds of thousands of times until a probability de-

cay curve is developed with sufficient statistics for analysis. The

second Canberra scaler is used to determine the total number of events

which comprise a given experiment. This is useful in determining

data acquisition rate corrections. See later discussion of this prob-

lem, Chapter IV.

The Canberra rate meter (model 1481) provides an on-line ac-

quisition rate which is useful in adjusting the experiment to a given

count rate. The Hewlett-Packard model 1203 oscilloscope provides a

visual monitor of the decay curves as they are acquired and the ASR-33

teletype provides printed and punched paper-tape output from the MCA

memory.

The timing-calibration procedures used in these experiments

are identical to those described by Copeland. The timing delay cables

are listed in Table 1.

Table 1: Time delay cables

CABLE	TIME DELAY (nsec)*
1	28.0±0.30
2	44.0±0.20
3	88.09±0.90
4	88.7±0.77
5	101.4±0.50
6	183.2±1.6
7	378.5±2.2

* errors are one standard deviation

The photo-detection system for these experiments consisted of the following various photomultipliers: three RCA 8575's, one 56TUVP Amperex, and one 56DUP Amperex. These PM's were coupled to an ORTEC 271 constant fraction timing base. It was found during the experiments that some rather subtle distortion of the data, and some not so subtle distortion, stemmed from this system. The blatant distortions were observed with the RCA 8575's which varied in age but for the most part were older than five years. These tubes would exhibit unusually high noise levels (greater than 20%) which the computer had difficulty in analyzing; It could not tell if the noise level was linear or exponential in nature and frequently failed to give any usable analysis on known molecular lifetimes. Also, when the same data was collected on a longer time scale (800 nsec instead of 400 nsec) the probability decay curves would exhibit a rather interesting plateau around 350nsec as shown in Fig. 17. This phenomenon can be explained by considering 'afterpulses' produced inside the phototubes by ionized perfused helium which drifts back to the cathode, producing a burst of secondary electrons delayed in time from the parent primary electron (delayed time due to drift velocity of the ions). This effect primarily causes an increase in the observed lifetime as well as an increase in the noise level. For example, the observed decay of the $C\ ^3\Pi_u$ state of N_2 with an improperly functioning PM was found to be 44nsec, while the same state would be observed with a lifetime of 38.5nsec with a properly dunctioning PM. While this may not seem very important, being only an error of 15%, it is a systematic error and it would tend to make it very difficult to analyze properly a decay on the order of 300 to 400nsec.
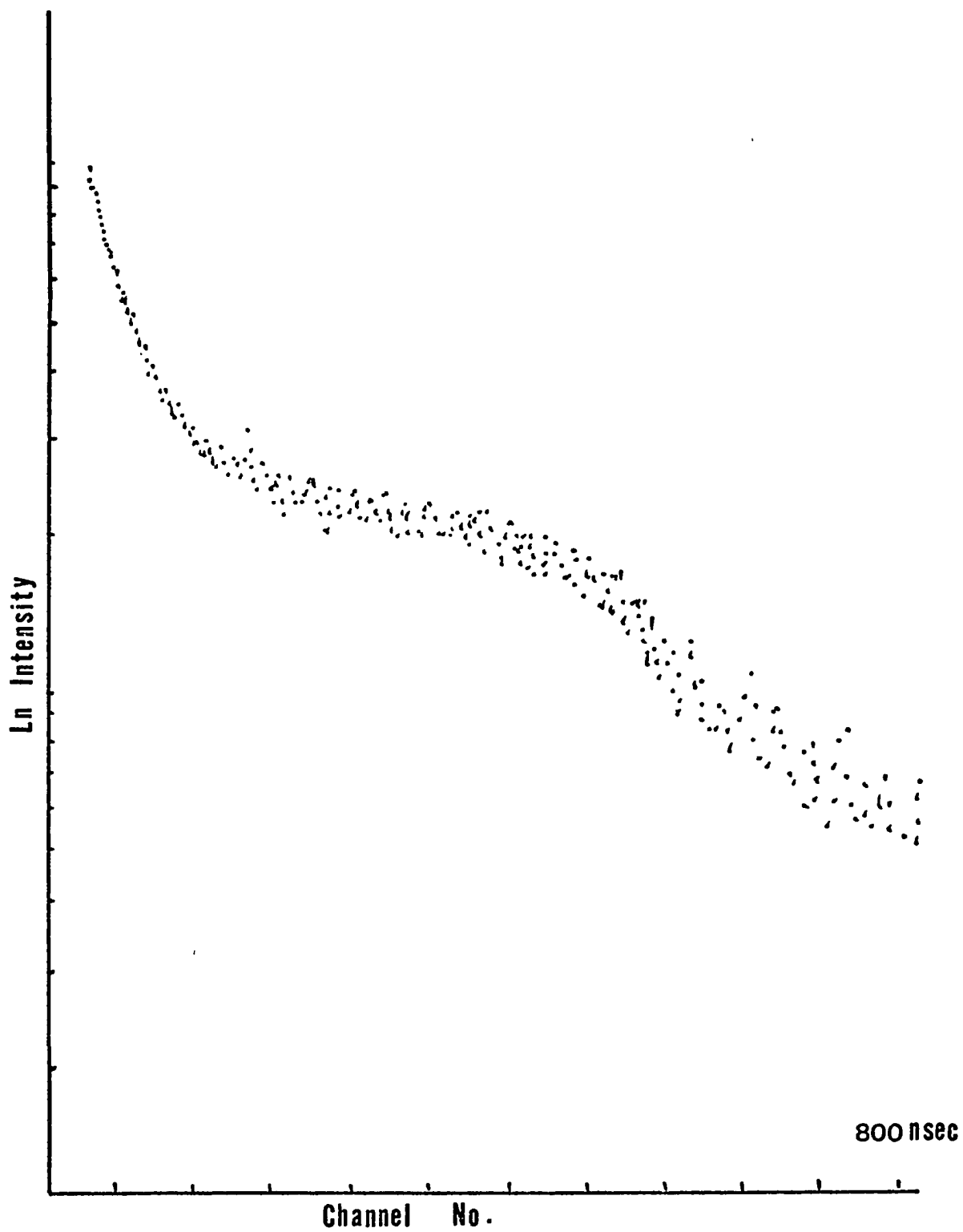
Fig. 17:   Distorted Decay Curve Due to Faulty PM

This problem can reach extremes, i.e. the PM can contain so much perfused helium that dynode bursts are also seen.[20] These tend to vitiate the results in the opposite sense, in that they tend to produce lifetimes that are too short. One of the RCA 8575's, for example, produced invalid lifetimes for both the C $^3\Pi_u$ and the B $^2\Sigma_u^+$ states of N_2 and N_2^+ of 20nsec, independent of pressure. Both these problems, the afterpulses and the dynode bursts, can be explained with the aid of Fig. 18. Trace 'a' represents the true radiative decay of the excited source. Note the apparent RC decay of the equilibrium region before cut-off. This follows the decay of the excitation pulse and is instrumental in producing the plateau apparent in Fig. 17. Trace 'b' represents the buildup of afterpulses with a time delay of approximately 350nsec after cut-off. The decay of these pulses after this 350nsec delay is not exponential but gaussian due to the time-of-flight statistics, and makes analysis of this data utterly misleading.

Trace 'c' represents the light curve obtained for the dynode bursts and is essentially the same as that above for the afterpulses except that the time of flight to the dynodes is only on the order of 15-20nsec. These dynode bursts can be very annoying in that they provide the same 'lifetime', i.e. 20 nsec, regardless of the light source. This would of course make for easy recognition if it were not for the fact that this distortion is light sensitive, in that without the light source present, the PM appears noise free. Consequently, an experiment run on an unknown gas would produce false lifetimes which
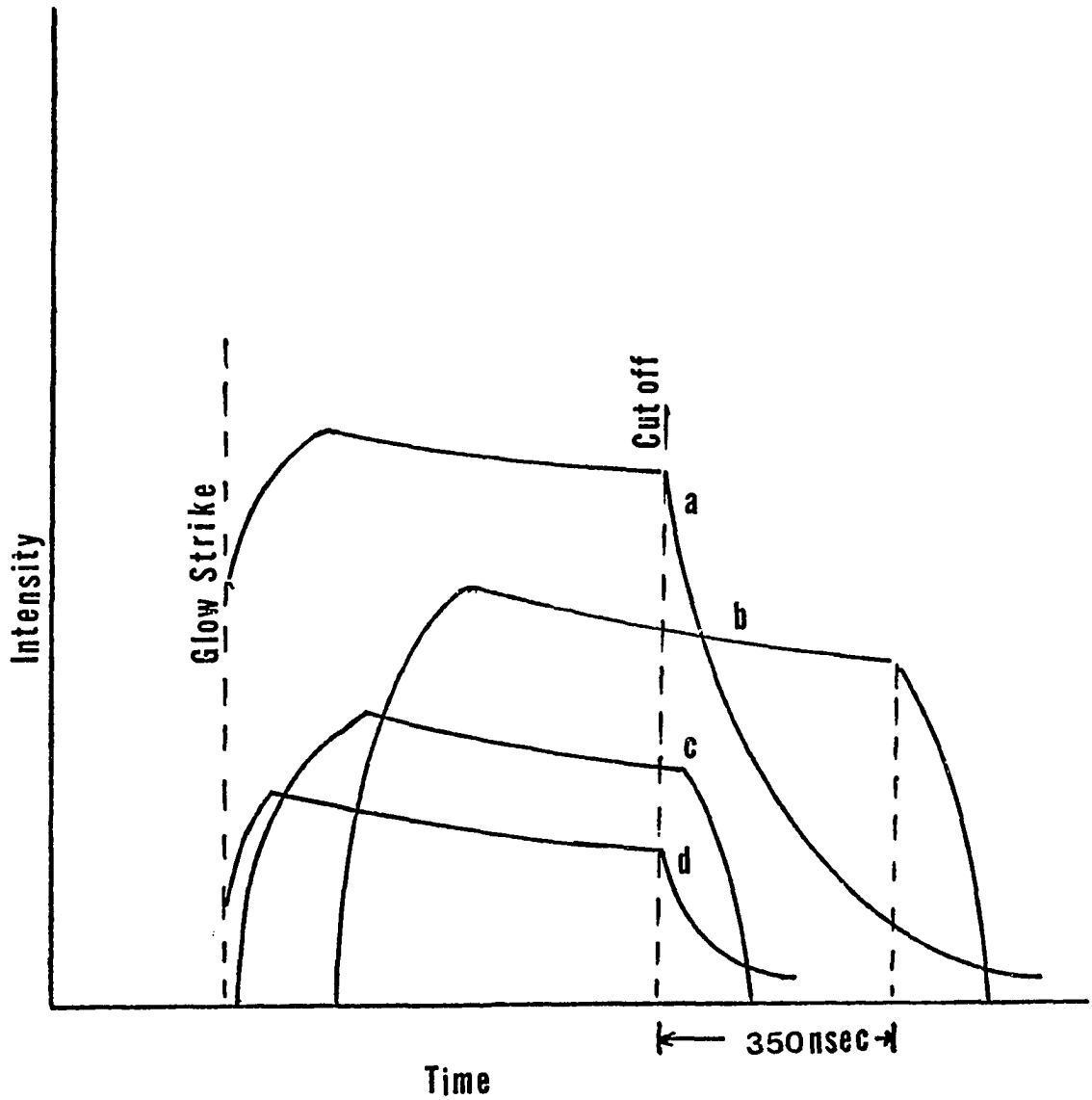
Fig. 18: Light Curve Compostion During And
After Excitation Pulse Cessation

would not be recognized as false. For a complete discussion of this subject, see ref. 20.

Another type of PM related distortion is caused by undervolting the PM dynode chain. Although this effect does cause shorter apparent lifetimes, it does so in a much different manner than the dynode bursts. While the dynode bursts give a constant 20nsec decay curve, regardless of the decaying source, the undervolted PM produces an apparent two-exponential decay; the 'correct' decay curve plus a fast component which appears to depend on the radiating source. Examples of two such curves are presented for the C $^3\Pi_u$ and B $^2\Sigma_2^+$ states of N_2 and N_2^+ in Fig. 19, 20. Increasing the dynode voltage eliminates this problem.

Since the Amperex 56DUP does not have a quartz window, a pilot 'B' scintillator was placed in front of the window for all UV work. This was accomplished by using Dow-Corning 20-057 Optical Coupling Compound as a glue to afix the scintillator directly on the face of the PM window. Tests with and without it showed the coupler to be free of objectionable characteristics such as flouresence.

This total system could be adapted to spectral investigation by using the MCA in the multiscale (MS) mode instead of the pulse height analysis (PHS) mode. The MS mode allowed a spectrum to be obtained based on the time dependent relative intensity of emission lines. The channel dwell time of the MCA in the MS mode was variable but was usually operated at 800 μs/channel. Fig. 21 is an example of the type of spectra obtainable with this system.

One other means of obtaining spectra was available. By using a ND Enhancetron 1024 multiscaler, much more detailed spectra were

possible. This was achieved by replacing the MCA in Fig. 15 with the

Enhancetron. The output was plotted via an X-T Hewlet-Packard recorder

and a sample is shown in Fig. 22.
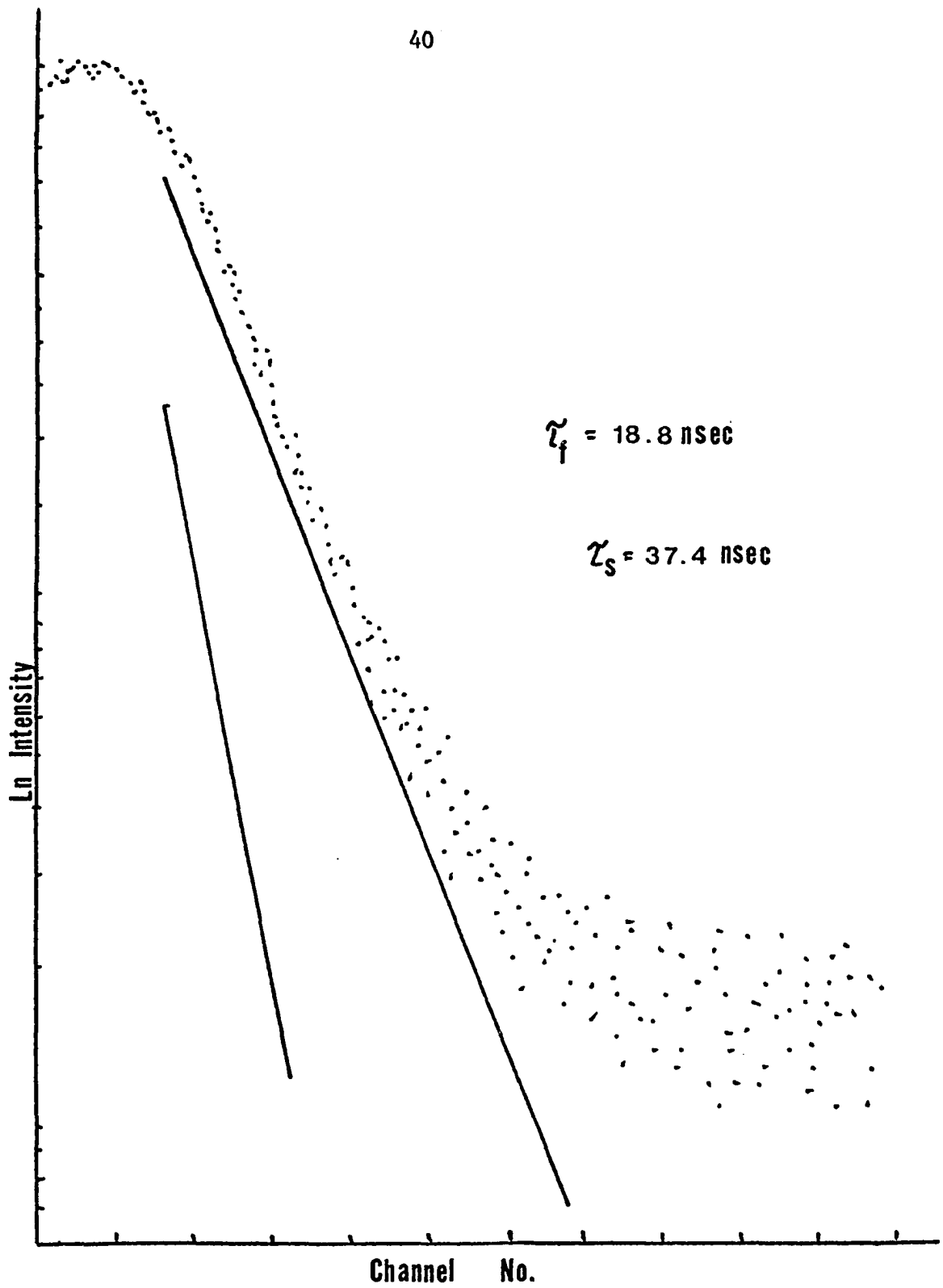
Fig. 19: Decay Curve N_2 C $^3\Pi_u$ With Undervolter PM

$\tau_f = 28.4\, nsec$

$\tau_s = 54.6\, nsec$

$p = 190\, u\, Hg$
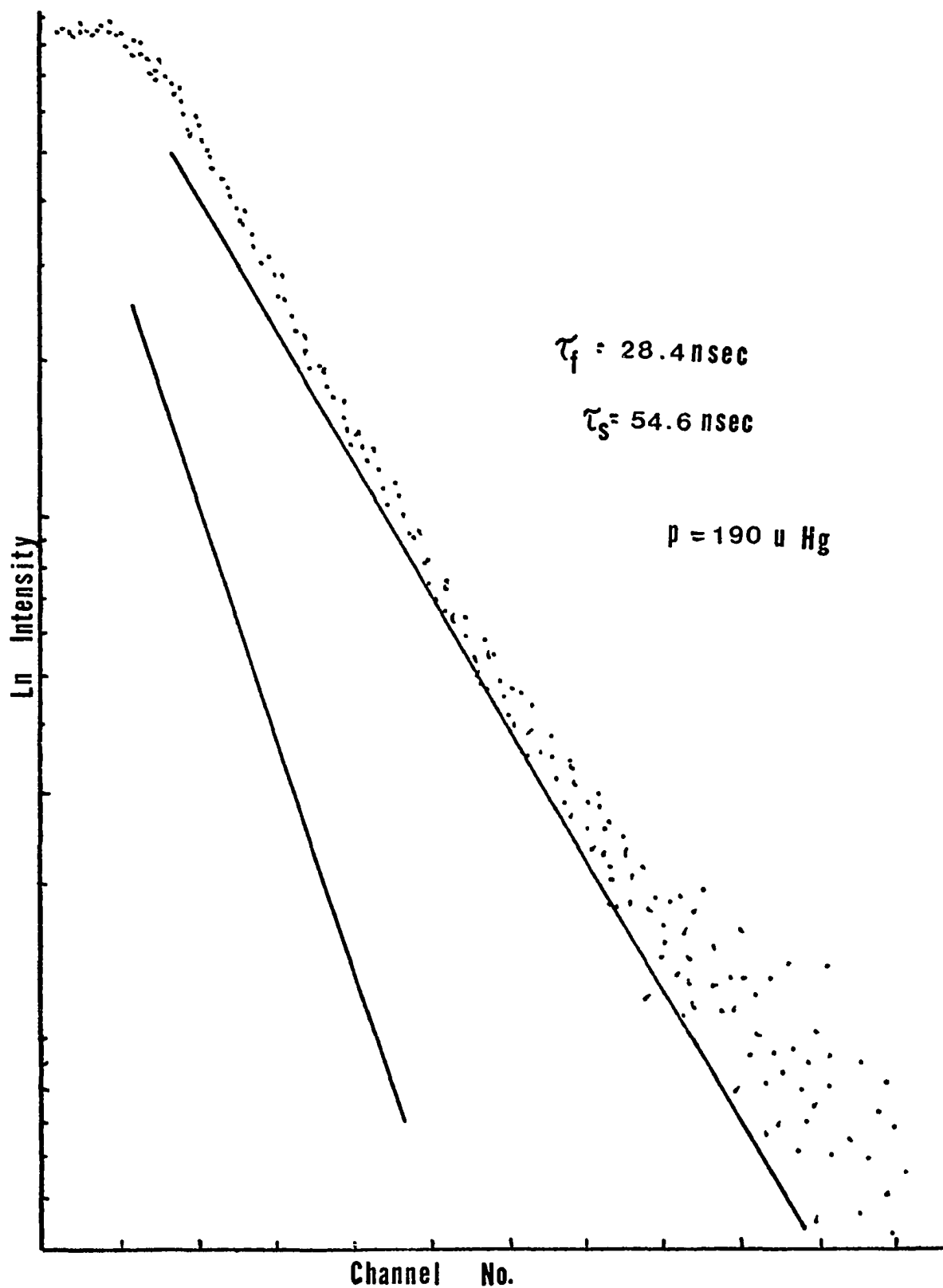
Fig. 20: Decay Curve N_2^+ B $^2\Sigma_u^+$ With Undervolted PM

(3,5)   (2,4)   (1,3)   (0,2)   (1,1)   (0,0)   (2,5)
3672Å   3943Å

N$_2$ C$^3\Pi_u$ N$_2^+$ B$^2\Sigma_u^+$

(1,0)

(3,3)   (0,0)   (2,3)   (1,2)   (0,1)
3371Å   3577Å
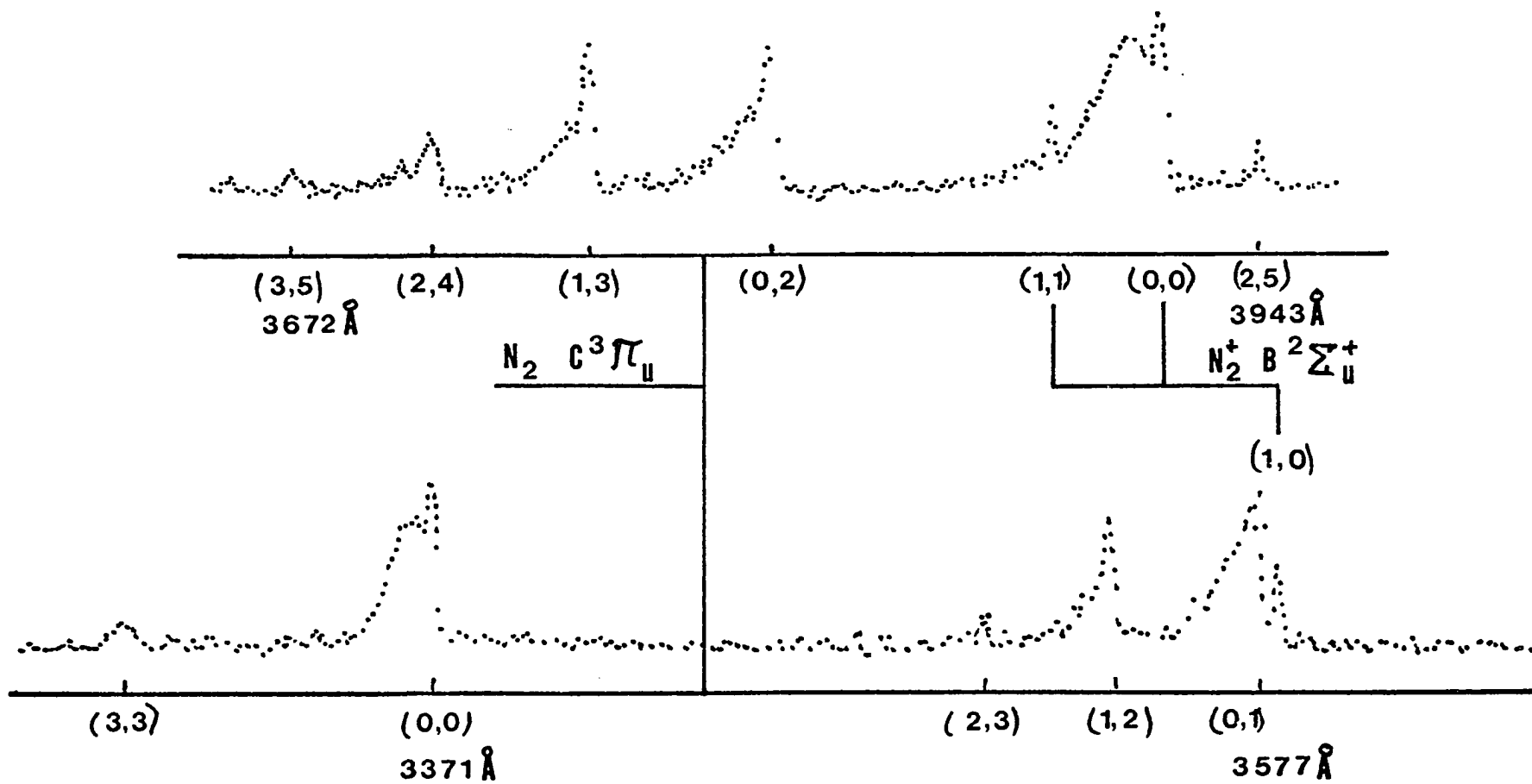
Fig. 21: Ms Spectra for N$_2$: 3300 – 4000Å
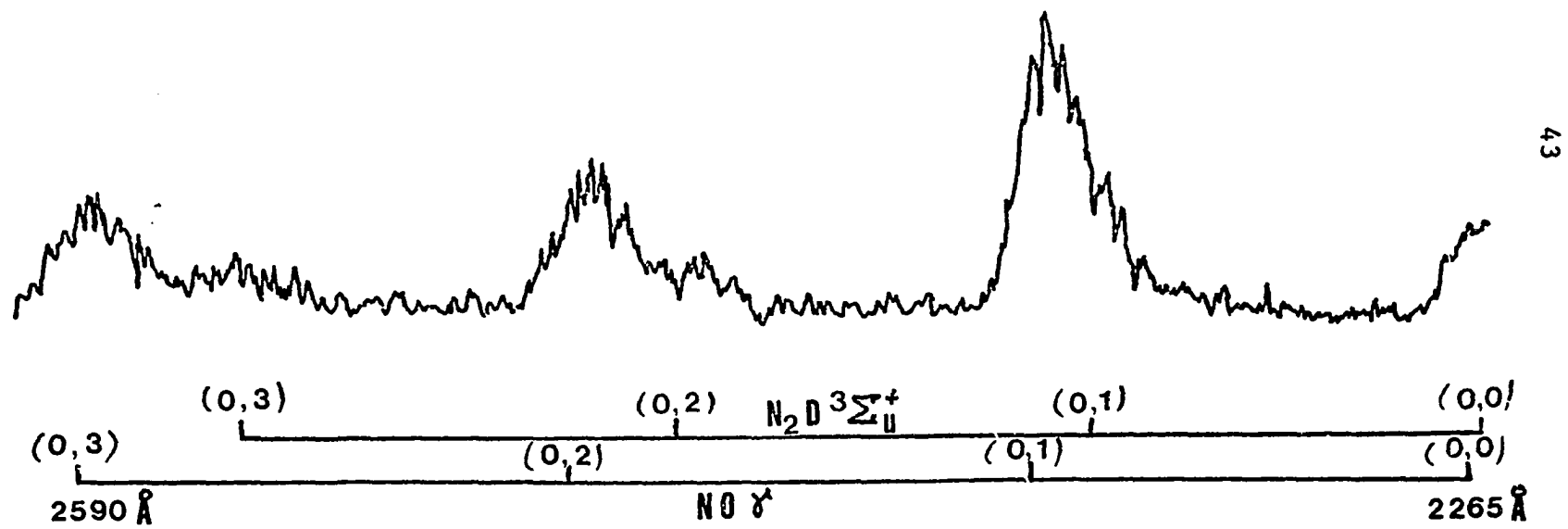
Fig. 22: 1024 ND Enhancetron Spectra For N_2: 2270 - 2590 Å

D
Discharge Tube

G. E. Copeland developed the cold cathode invertron in 1970 for the explicit application to easily dissociated polyatomic molecules and those which tend to poison oxide coated heated cathodes. A complete description of the apparatus can be found in ref. 1 and 21. The first part of this experiment was intended to validate and improve the accuracy of this instrument.

In its present form, the invertron is essentially the same as Copeland's although it has been modified to allow for experimentation to insure that geometrical factors have not biased the experimental results. Figure 23 illustrates the modified system. The dimensions of the stainless steel invertron are approximately seven inches long by three inches outer diameter and two and a half inches inner diameter at the constriction. The upper inlet serves as the main pumping port and as the flow entrance port during experimentation. This port fits 8mm pyrex tubing to facilitate primary evacuation. The lower port in the figure is for gas exhaust during the flow runs.

The window is a fused quartz disc three inches in diameter and a quarter inch thick which was sandwitched between two viton 'O' rings. The pyrex backing plate facilitated cleaning the instrument and served as an insulating plate to the back wall of the discharge tube.

The anode is a stainless steel rod eight and three quarters inches long by an eighth inch diameter. It is inserted through two
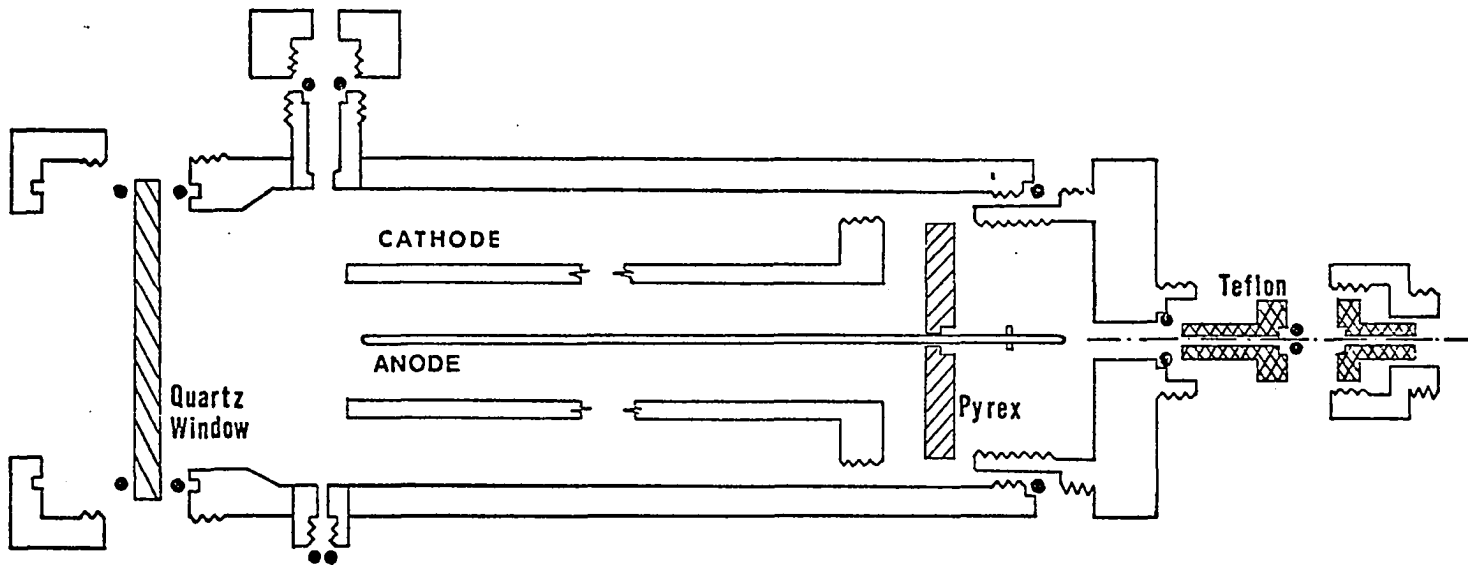
Fig. 23:   Modified Invertron
          (All Viton 'O' Rings)

Teflon sleeves for electrical insulation as shown. The cathode inserts are normally aluminium cylinders which varied in diameter and configuration as will be discussed in the next section.

E
Cathode Structure

It is very important that the electronics used in a given experiment do not bias the results of that experiment, or it they do, it is important to know, at least, how and preferably why. This section is intended to cover the development of the cathode structures used in our experiments and to answer the question of experimental bias due to the glow discharge.

The cold cathode invertron is a glow discharge device which depends on electron collisions to produce the excited molecular states of interest for study. Fig. 24 illustrates the primary parts of the glow in cylindrical geometry.

The first part of this study was intended to determine if the size (diameter) or the geometry of the cathode structure effected the observed lifetimes in any way. Also, a larger diameter cathode would allow us to work at lower pressures since Paschen's law indicates that the applied voltage necessary to initiate a glow is governed by the product of pressure times diameter (pd). This increased separation of the anode and the cathode should require a slightly larger applied voltage to sustain the discharge and the positive glow should expand to fill the larger region while the negative glow should remain unaltered[23].

An increase in the cathode diameter would also reduce the effect of diffusion in the system. Consider for example the following simplified rate equation

47
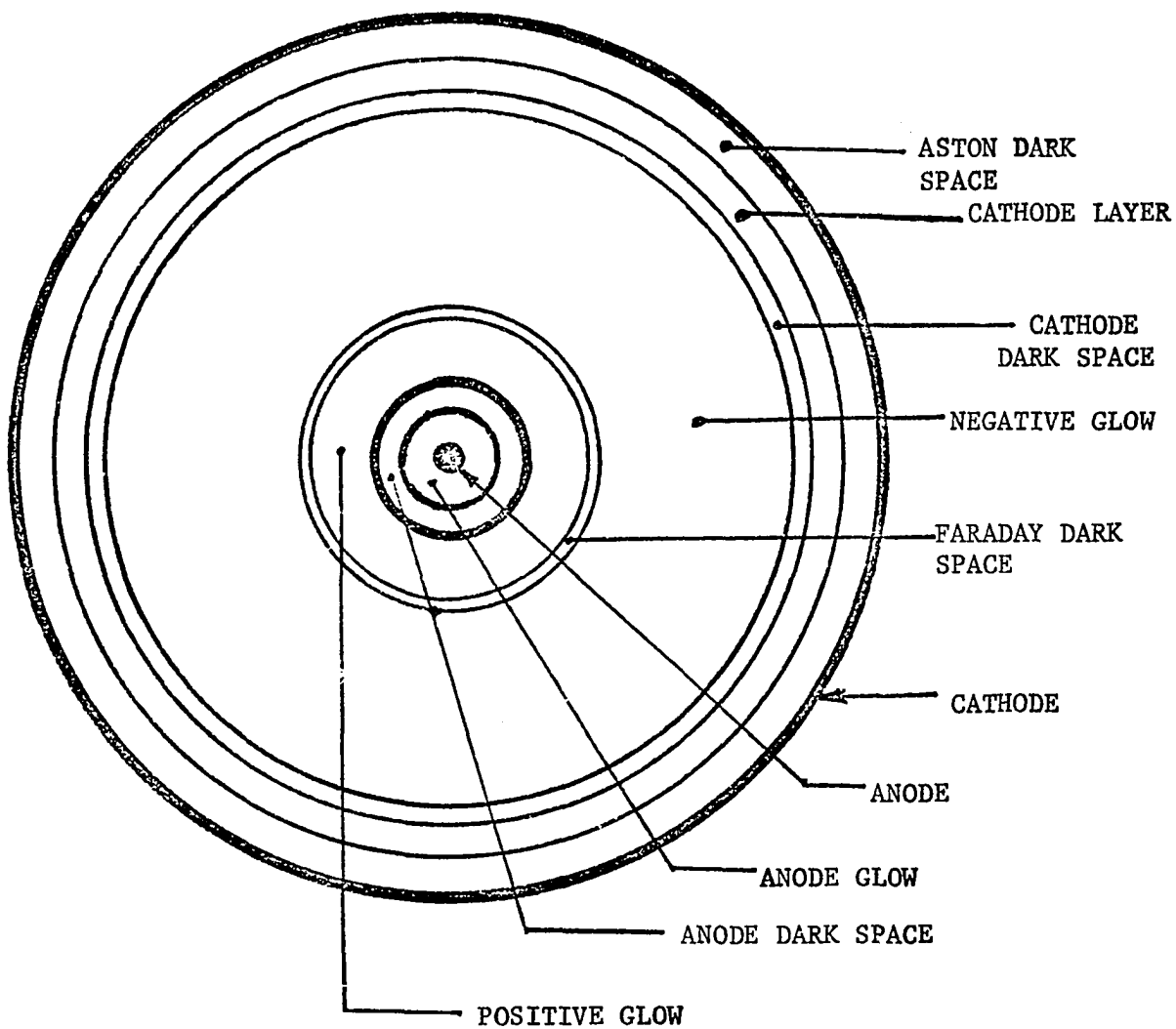
Fig. **24** . Glow region of discharge tube (cylindrical geometry).

$$\frac{dN_k}{dt} = -AN_k - N_o \sigma \bar{v} N_k + D\nabla^2 N_k \qquad \qquad 18$$

where ∇^2 will be expressed in cylindrical coordinates and we assume
no axial or angular dependence of the excited molecular density, i.e.
a uniform distribution exists along the length of the discharge. We
then have

$$N_k = R(r) \ T(t) \qquad \qquad 19$$

and by using the separation constant $- \rho^2$, we find

$$dT/dt = -(\rho^2 + A + N_o \sigma \bar{v})T$$

$$\qquad \qquad 20$$

$$r^2 \frac{d^2R}{dr^2} + r\frac{dr}{dr} + \frac{\rho^2 r^2}{D} R = 0$$

which has the general solution

$$N_k = C \exp \ \{-(\rho^2 + A + N_o \sigma \bar{v})t\} \ J_o \ (\rho r/\sqrt{D}) \qquad \qquad 21$$

where J_o is the zero order Bessel function. After imposing the bound-
ary conditions (a = radius of discharge tube)

$$t = 0 \quad \begin{array}{ll} N_k = N_k(0) & r < a \\ \\ N_k = 0 & r > a \end{array}$$

we find that the effect of diffusion on the system is the addition of
$\Lambda^2 = (2.405/a)^2 D$ in the effective transition probability, i.e. an ef-
fective decrease in the true lifetime, as shown below.

$$A' = A + N_o \sigma \bar{v} + \Lambda^2 \qquad \qquad 22$$

This implies that as the separation of the electrodes in-
creases, the effect of this term, Λ^2, decreases as $1/r^2$. As this
effect was reportedly small for the hot cathode invertron[3], it
should be even smaller for the large cold cathode invertron.

It was therefore very surprising to find that not only was there an effect when the larger cathode was used, but the effect went the wrong way!!! Longer lifetimes were observed, e.g. $B^2\Sigma_u^+$ states of N_2^+ were observed at false lifetimes as long as 110nsec, which when observed at comparable pressures in the small cathode system were only 50nsec (uncorrected for pressure dependence).

This coupled with the fact that as the pressure was decreased this effect became even more pronounced led to the conclusion that this problem had to do with improper field quenching after the excitation voltage was clamped off. That is, with larger cathodes, a larger surface area was available to produce electrons while insufficient means were present to sweep these additional electrons out of the excitation region where they were continuing to produce excited molecules after the field was supposedly turned off. Consequently, while the cut-off appeared to be 10nsec on the monitor, it was probably as long as 50nsec, or longer.

This conclusion seems to be born out by the following experiments. A rod structure was inserted just inside the cathode shell, in electrical contact with the cathode as shown in Fig. 25. This structure did indeed bring the observed lifetimes back down to 50 nsec at the appropriate pressure but a very long plateau now existed as shown in Fig. 26. It was found that removal of every other rod in the cathode structure made the plateau twice as long as before. If this plateau was indeed due to insufficient electron collection, it seemed reasonable to expect an increase in the duration of the discharge pulse would produce a similar result. Fig. 27 indicates that this exactly what happens.

CATHODE SHELL

ROD END PLATE

PARALLEL RODS

ANODE
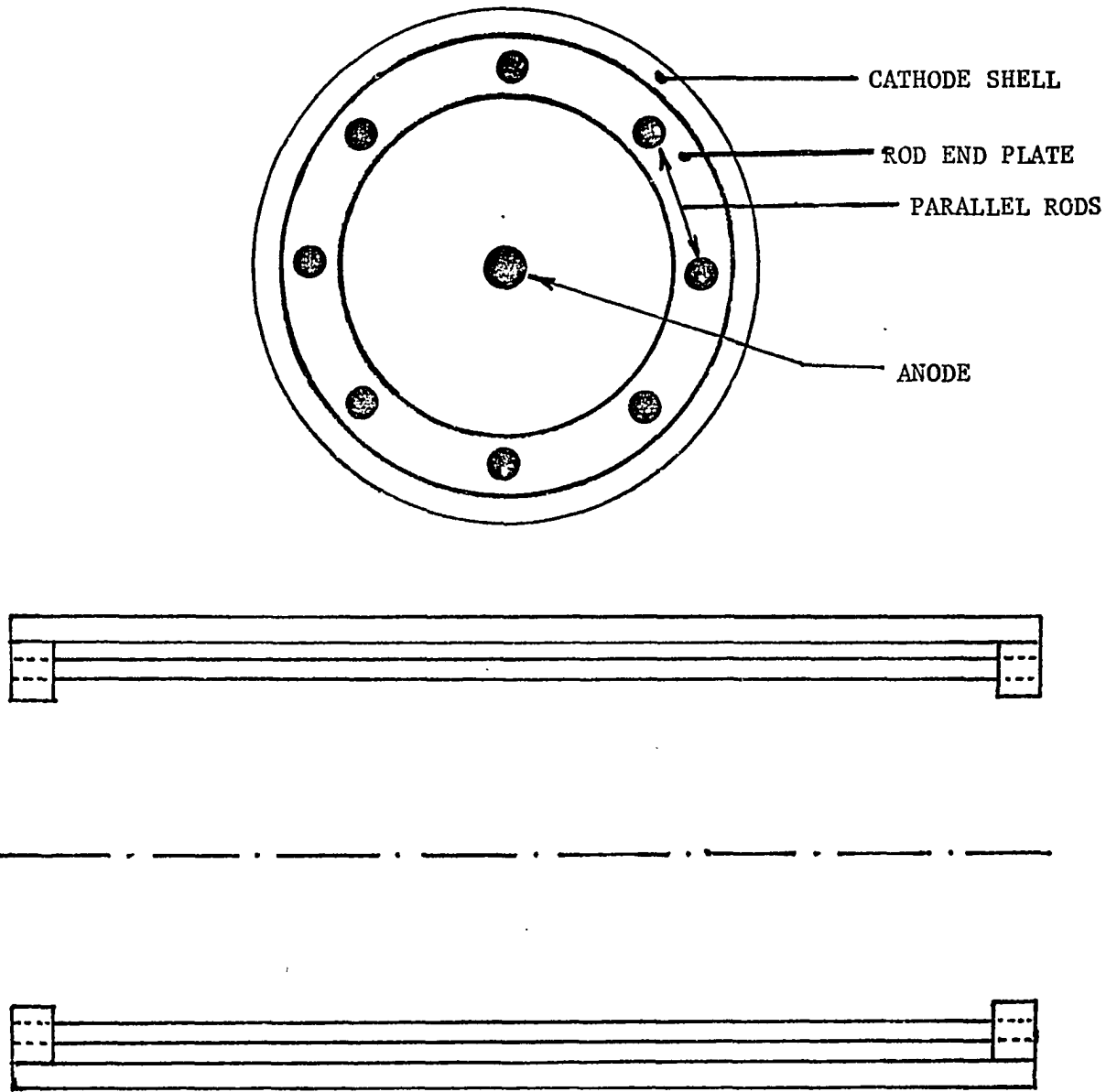
Fig. 25   Parallel rod cathode cenfiguration
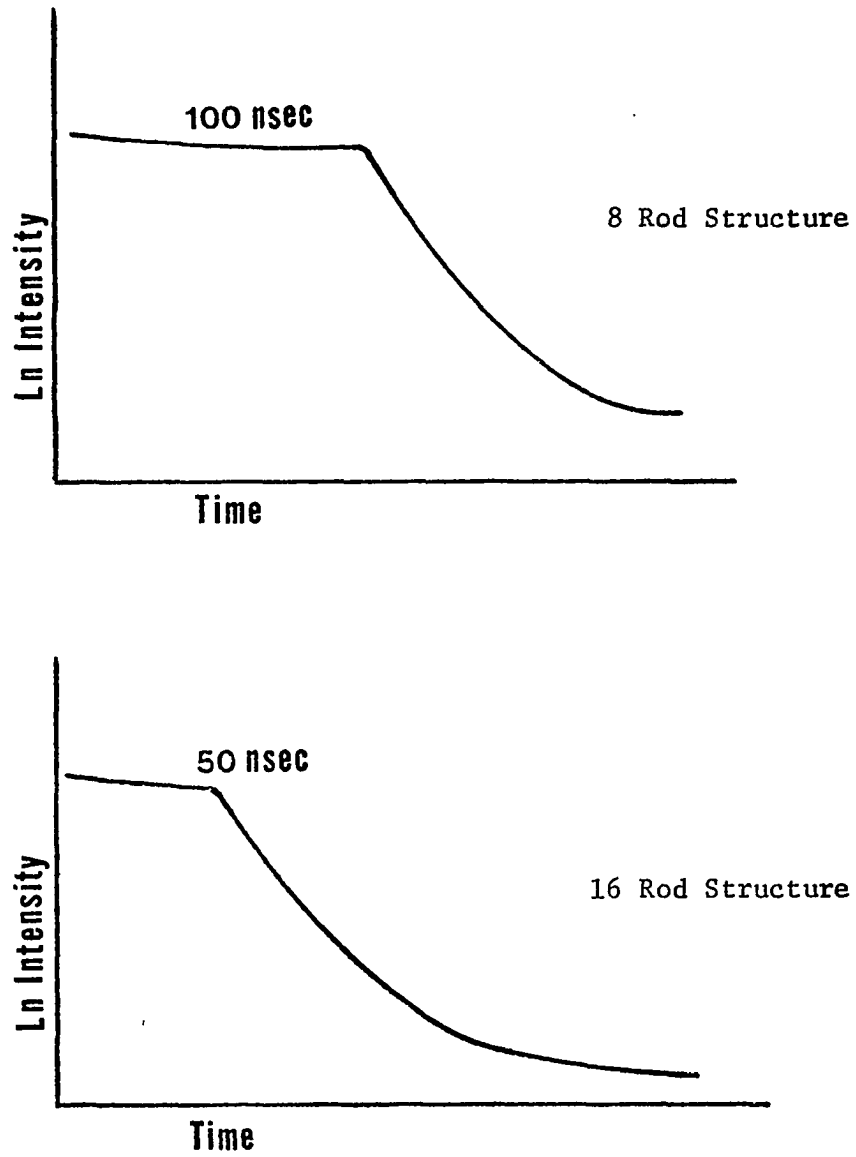
Fig. 26: Effect of the Parrallel-Rod Cathode on the Apparent Cut-Off of the Decay Curve.
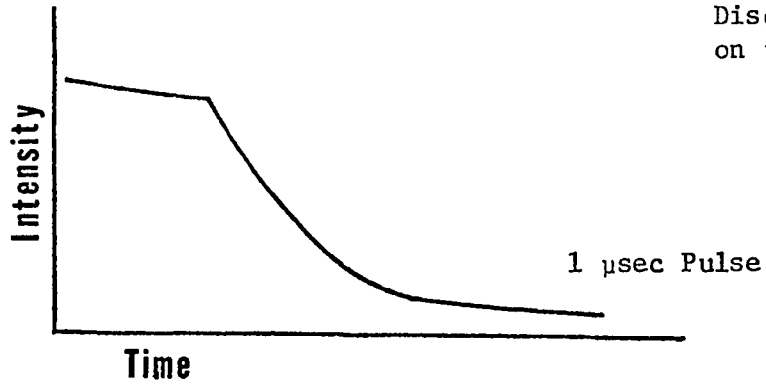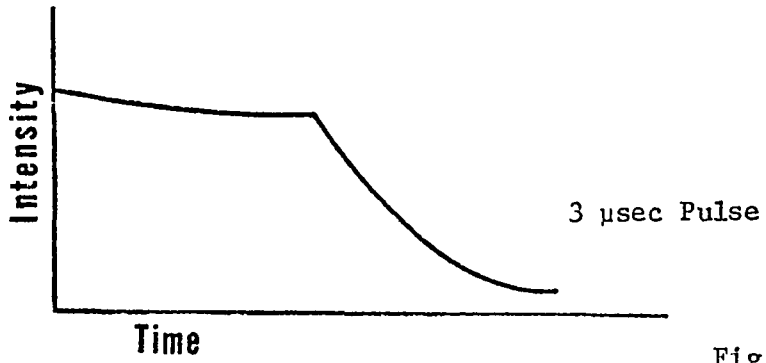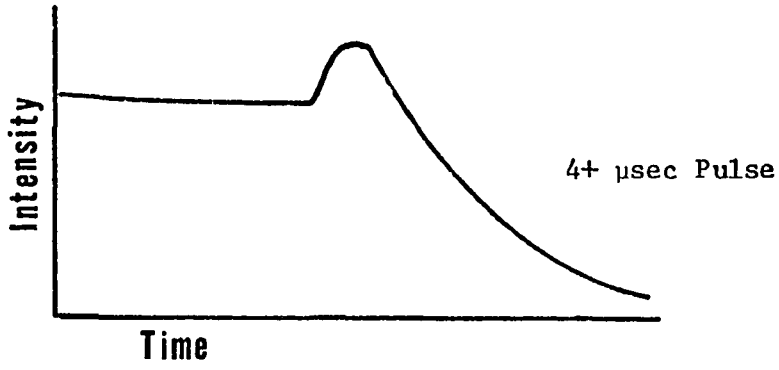
Fig. 27: Effect of the Discharge Pulse Duration on the Decay Curve Plateau
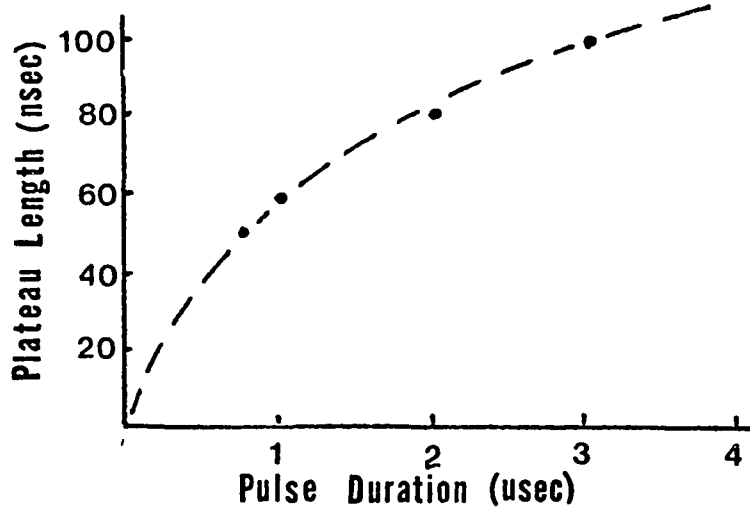
As a result of this study, it was determined that the cathode structure must accomplish two ends...first, it must be able to produce sufficient electrons to maintain the glow discharge, and second, it must be able to retrieve those electrons rapidly (10nsec or better) when clamped off. The parallel rod structure and a later developed helically-grooved structure accomplished this end independent of their large surface areas needed for electron production by the presence of short radius field points (rods or helix corners) near the cathode to provide strong retrieval field lines.

This problem is also related to the ability of the electronics to provide sufficient current on demand to give complete cut-off. This is a small problem but is probably responsible for the small amplitude oscillations present in the computor analyzed data (it was present in the hand analyzed data also, but is not as noticable). Fig. 28a, b, are decay curves taken on $B^2\Sigma_u^+$ where only the crowbar circuitry was altered. This may indicate an interesting phenomenan as this effect was always stronger for the B state of N_2^+ than for the neutral molecular state C $^3\Pi_u$. This may indicate a forced diffusion (or field diffusion) of the N_2^+ molecules as their lifetimes seem to be reduced very slightly in the lead channels, while the 'true' lifetime is still present in the later channels of the experiment.

Another interesting fact from these studies was the overall effect of the various cathode diameters on the observed lifetimes as illustrated in Fig. 29. This plot represents the data acquired from the original small smooth cathode, the large diameter parallel-rod cathode and the large diameter helical-groove cathode. Note that

Fig. 28a. Decay curve for

N_2^+ B $^2\Sigma_u^+$ 3914 Å

τ = 53.1 nsec

p = 220 u Hg

Ln Intensity

Channel (Time)

Fig. 28b. Decay curve for

N_2^+ $B\,^2\Sigma_u^+$ 3914 $\overset{o}{A}$,

altered load resistor

τ = 55.4 nsec

p = 220 u Hg
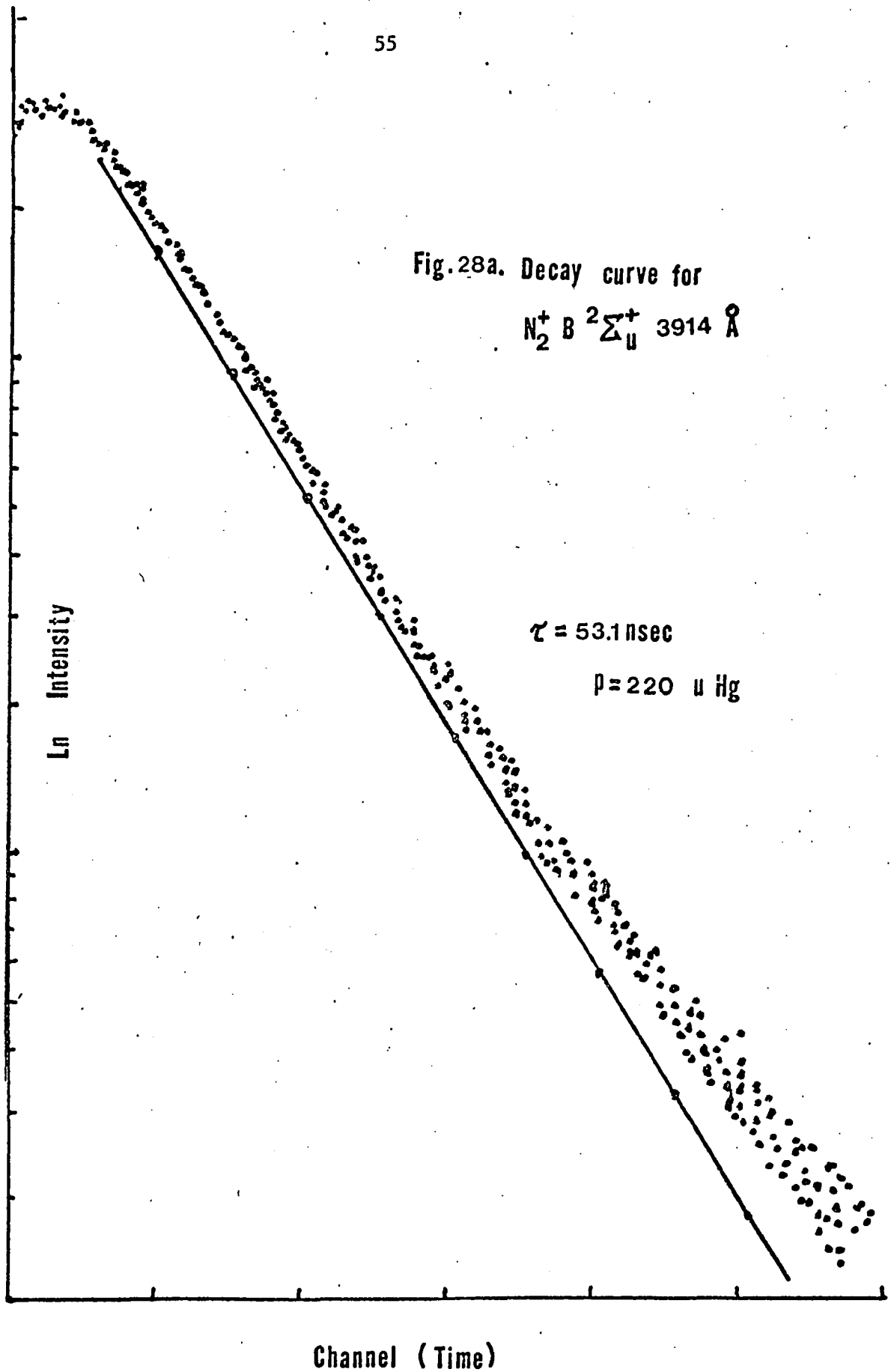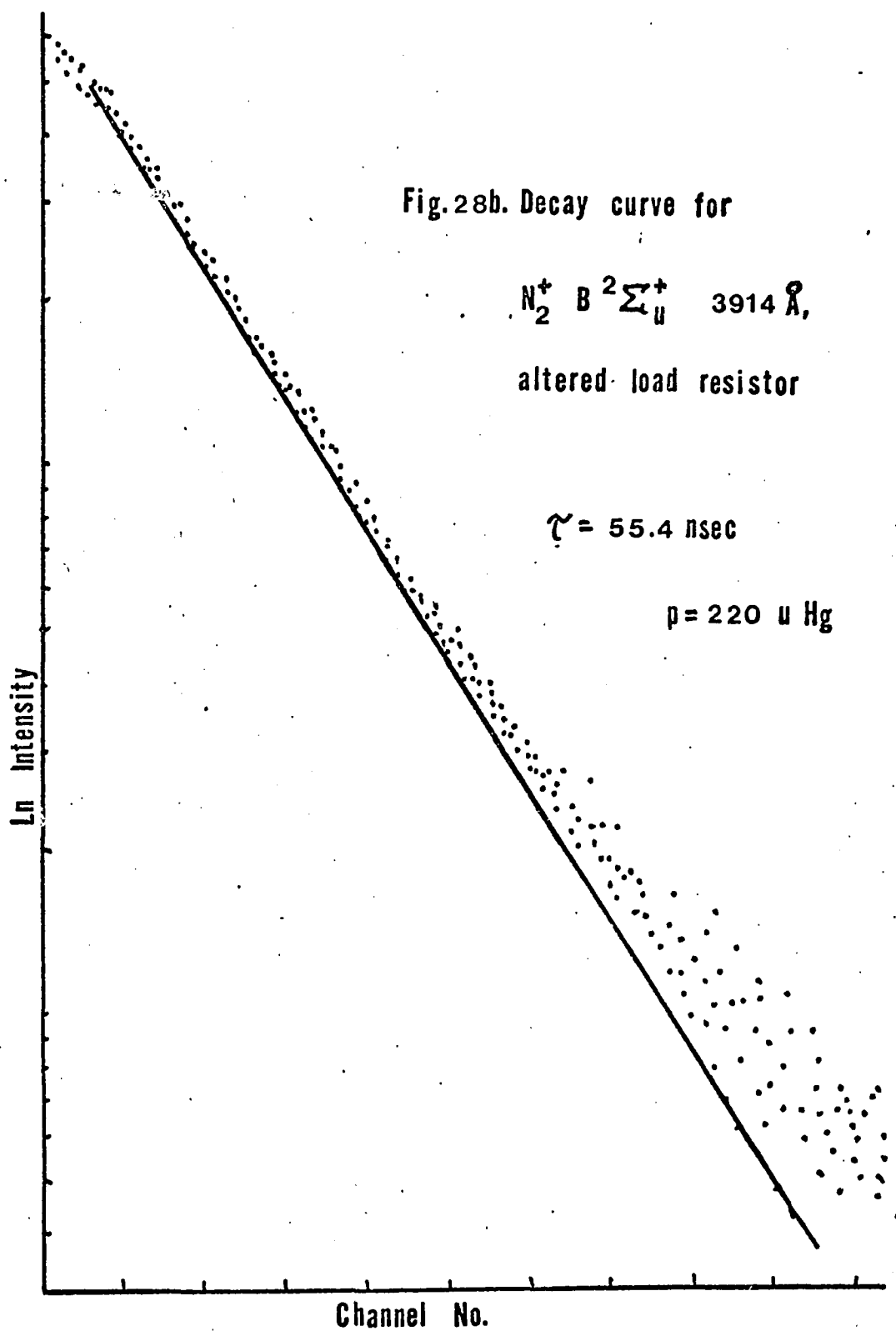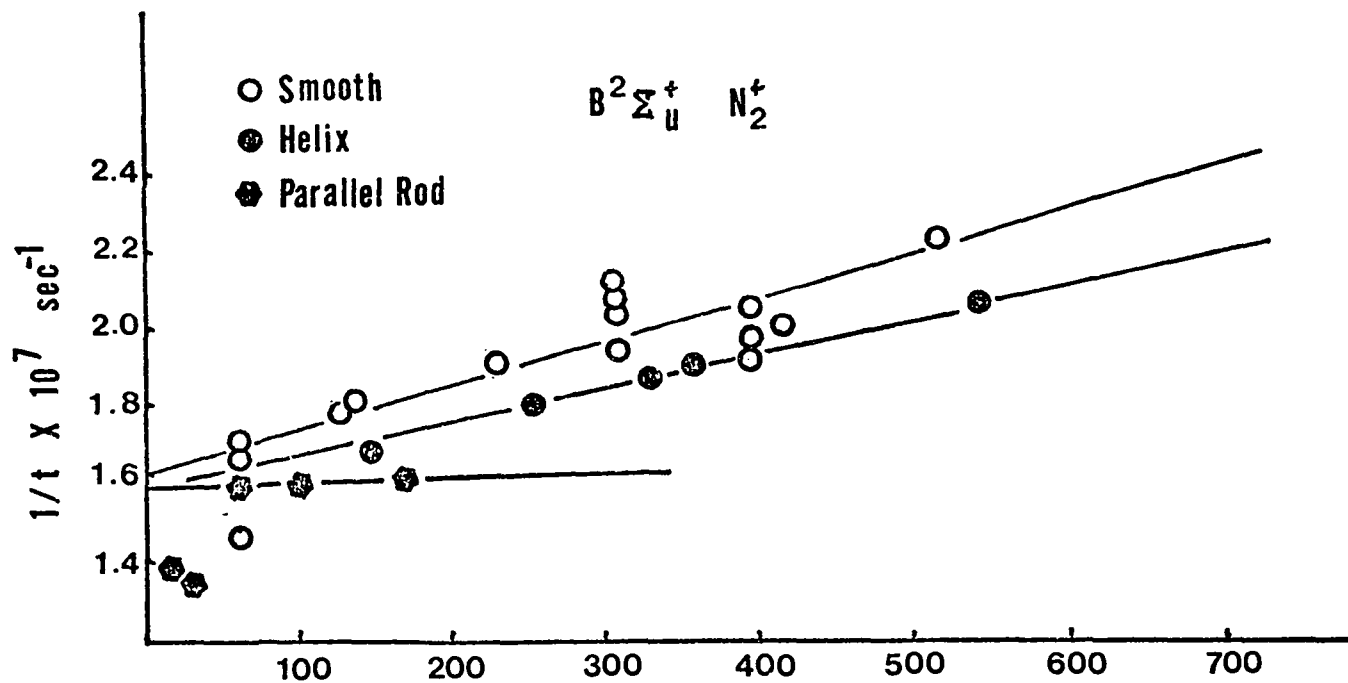
Fig. 29: Inverse Lifetime VS Pressure Curves for Different Cathode Structures

while their slopes are quite different, their zero pressure intercepts
are quite similar.

This indicates that the form of Eq. 16, Chapter I, is incomplete;
i.e.,

$$A' = \sum_n A_{kn} + N_o <v> \sum_n \sigma_{kn} \qquad 16$$

does not describe the curves properly. For a given pressure, excita-
tion voltage, etc., the only factor changed in these experiments was
the cathode geometry. This can only alter the electron concentration.
The different cathodes have demonstrated varying efficiencies for
sweeping the electrons from the active region of the excitation tube
(e.g. Fig. 26) and the excitation pulse duration has also been shown
to effect the decay curves (Fig. 27). These experiments point to re-
sidual electron concentrations which must be accounted for.

By considering the recombination and attachment loses given in
Eq. 12, Chapter I, we have,

$$\frac{dN_k}{dt} = -N_k \sum_n A_{kn} -N_o N_k \sum_n <v\sigma_{kn}> -\alpha_r n_e N_k -\alpha_a n_e N_k. \qquad 23$$

However, we can almost discount the attachment term out of hand since
pure nitrogen does not attach electrons. Air on the other hand will
attach, with an attachment coefficient of $\alpha_a = 6.3 \times 10^{-7}$ sec.[22]
Consequently, a leaky vacuum system may require this factor to be in-
cluded.

Electron recombination might appear as a questionable factor
since the calculated recombination coefficient is on the order of 10^{-14}
cm^3/sec. However, this value has been observed much larger (10^{-8} cm^3/
sec)[23] for cases when the time for the disposal of the recombination

energy is much shorter than the average life of an excited molecule.

The dissociation of a molecule will occur within a time interval of

one vibration (10^{-13} sec) and according to the Frank-Condon rule, the

electron changes from one state to another in an excited molecule

within a time which is negligible compared to this vibration. This

would seem to imply that dissociative recombination might then be

an important factor. Von Engel[24] states that this dissociative re-

combination coefficient is proportional to the pressure. With this

in mind, and using the assumption that after cut-off of the dis-

charge tube, with only the external magnetic field to influence them,

electrons and ions should be in a fairly equal concentration, constant

with respect to the nanosecond decays of the excited state, we will

have

$$N_k(t) = N_k(o) \exp\{-(\sum_n A_{kn} + N_{on}\sum<v\sigma_{kn}> +\alpha_r n_e)\}. \qquad 24$$

So, instead of depopulation by collision with neutrals only,

we should also include the depopulation by collision with electrons

in the form of dissociative recombination. The data would then imply

that the smooth cathode is very inefficient in removing the electrons

after cut-off, while the helix cathode and the parallel-rod cathode

are much more effecient. This is an additive factor, linear in pres-

sure and consequently it will not detract from the validity of the

experiment.

Magnetic Field

The cold cathode invertron discharge tube is a glow discharge
tube which relies on electron impact on the target gas for electri-
cal breakdown. This is at best a statistical process and in a fixed
diameter tube Paschen's Law limits the target gas pressure.

In order to promote the breakdown at lower pressures, one needs
to find a means of artifically increasing the electron-target colli-
sion frequency. This can be done by applying a coaxial magnetic field
to the discharge tube as Copeland did. (see also ref. 25, 26, 27)
This causes the electrons to spiral around the magnetic lines of force,
thus increasing their effective path length in the active region of the
discharge tube. A weak field, around one hundred gauss, will allow
workable discharges to gas pressures as low as 5 millitorr in this
apparatus.

The field is provided by a selenoid wound around a copper
sleeve to allow water cooling of the coil (typically 75 watts of power
is generated by the coil). This copper sleeve fits over the discharge
tube shell, as shown in Fig. 30. The current supplying the field was
normally supplied by a Western Electric power supply (48 volts dc);
however, for the tests to determine the effect of the magnetic field
on the observed lifetimes, the current was provided by the main 100
volt dc generator in the physics building.

Since we are observing the radiation parallel to the magnetic

field, we would not really expect any effect of the field on the life-times. However, we do see some effect with increasing field as shown below in Figure 31. While the average value is the same, the experimental scatter increases. This data was taken on the vibrational levels of C Π_u (v'=0,1) (3371,3159 $\overset{o}{A}$) of nitrogen.
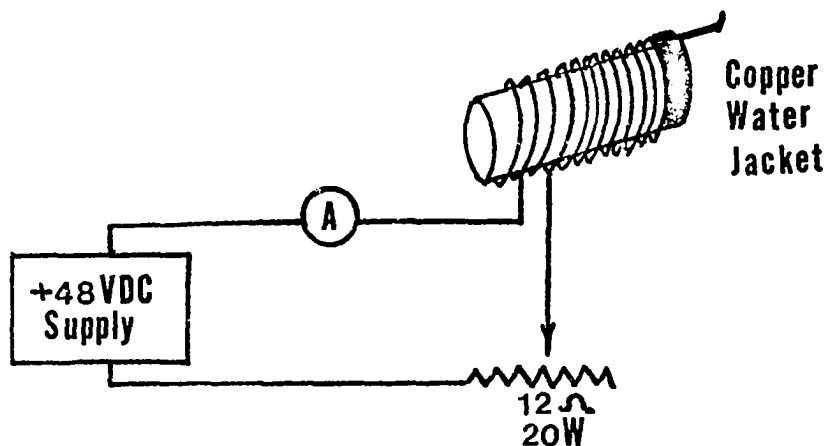
Figure 30: Magnetic field system
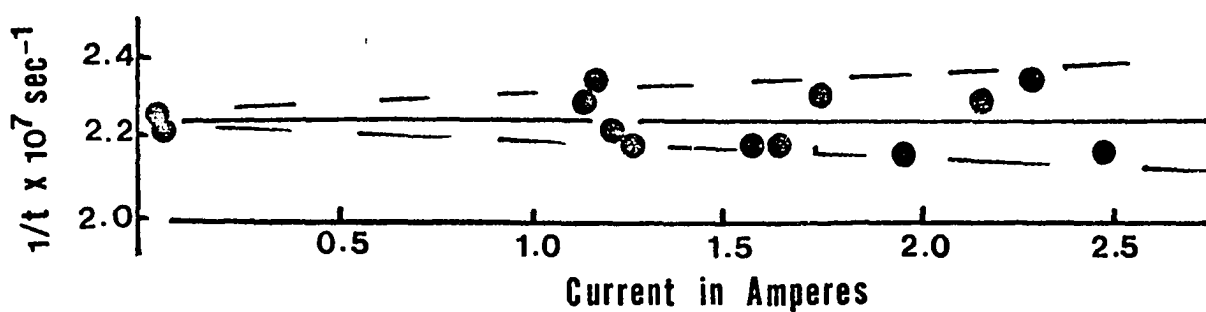
Figure 31: Effect of the magnetic field on lifetimes.

This effect is certainly not due to the interaction of the magnetic field with the decaying state, i.e. precession of the radiating dipoles around the magnetic lines of force with Larmor frequency $\omega_L = g_J \mu_0 H/h$ (g_J = Landé factor), but is probably related to interference of the increasing field with the electrical cut off of the discharge.

Evidence may be found for this in the increase of the "plateau" of the decay curves as shown in Fig. 32. This plateau represents a stable region after cut off which indicates the inability of the inqertron to sweep the electrons from the field on application of the 2D21 crowbar (see pulse generation section). See also the section on cathode assemblies for similar results. This increasing plateau then increases the uncertainty of the measured lifetime, but on the average, does not bias the results.

We may then conclude the applied field offers no systematic error to the system but indicates that we should keep the field as low as possible to reduce the overall error of the system.
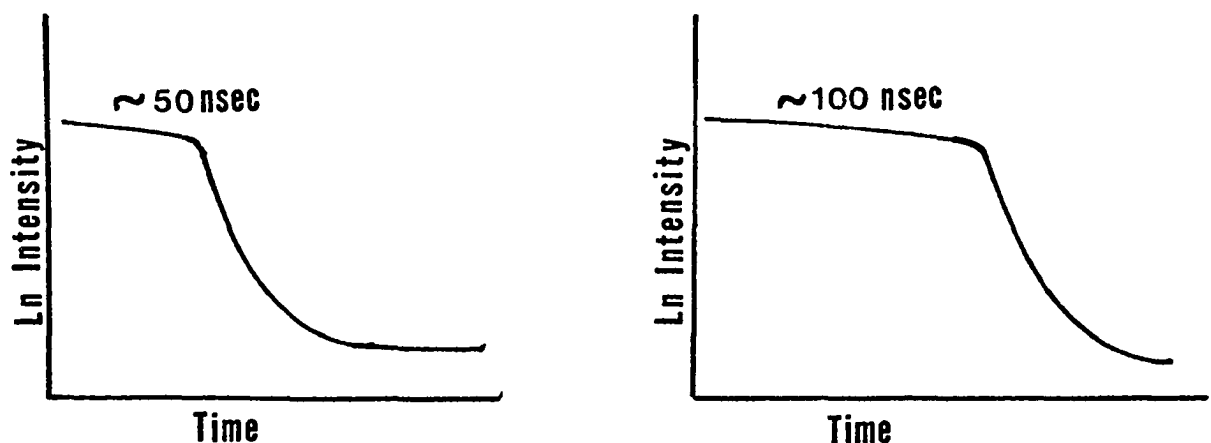
Figure 32: Effect of the magnetic field on the decay curves
a) low field, I=1.3 amp (~150g)
b) high field, I=2.5 amp (~300g)

CHAPTER III

DATA ANALYSIS

Within the limits descussed in the first chapter the data may

be considered as consisting simply of the sum of several exponentials,

the actual number determined by the number of cascading states plus

an additive constant due to random noise. We then have for the time

dependent intensity

$$I(t) = Be^{-A_1 t} + Ce^{-A_2 t} + \dots + K \qquad\qquad 25$$

where the decay constants, A_1, A_2 are the Einstein transition coeffi-

cients plus the pressure dependent quenching rates $A_1 = \sum_i A_{ki} + N_o \sigma <v>$,

B and C are the respective amplitudes and K the constant background term.

Exponential curve fitting is at best an educated guess if more

than two exponentials are present since in the presence of errors prac-

tically _any_ combination of three exponentials can be made to fit a

given data set involving three or more exponentials. However, if strict

attention is paid to the 'clues' presented by the data, two exponential

data curves can be handled with relative ease if the long lived compon-

ent is much longer than the short lived one (a factor of 5 or more).

Two techniques were used in evaluating the lifetime data in this

work, graphical stripping, and computer stripping. These techniques

will be discussed separately below.

Graphical Analysis

This method can give remarkably good results if the following

technique is followed. After the data is plotted on semi-log paper,

63

a constant amount representing the noise is subtracted from the data point by point. This is perhaps the most critical step. It too much, or too little is subtracted, the exponential overlying the background will be distorted. If this distortion is not ignored however, it will clearly indicate to the operator the proper amount to be called noise as is indicated in Fig. 33. This technique breaks down if too short a time scale is used for the data acquisition, i.e. the time scale used should be sufficiently long for at least 4 e-foldings of the decay to have occurred. For example, a 60 nsec decay should be acquired on the 400 nsec time scale and not on the 200 nsec scale. This insures also that the curve in Fig. 33b is not due in part or wholly to a real long-lived cascade component.

If two exponentials are present, where one is of rather weak amplitude, and an attempt is made to fit only one exponential to the data, a slight but rather persistent oscillation will be present as shown in Fig. 34a. This effect is obvious in the computer analysis (LASL) as the background also varies (see appendix A for sample LASL run #2).

If the two exponentials are of approximately equal amplitude and only one exponent is used to fit to the data, a noticable 'break' will occur as shown in Fig. 35. If the fast exponential is of much greater amplitude than the slow component, no problem should arise as a double exponential fit should be obvious.

One final point should be mentioned. Regardless of all else, the stirpping process MUST fit in the lead channels with a high degree of accuracy. This is an additional clue as to the misinterpretation of the data in Fig. 34a, where a noticable discrepancy exists

Fig. 33: Illustration of improper background subtraction. (Simulated data)
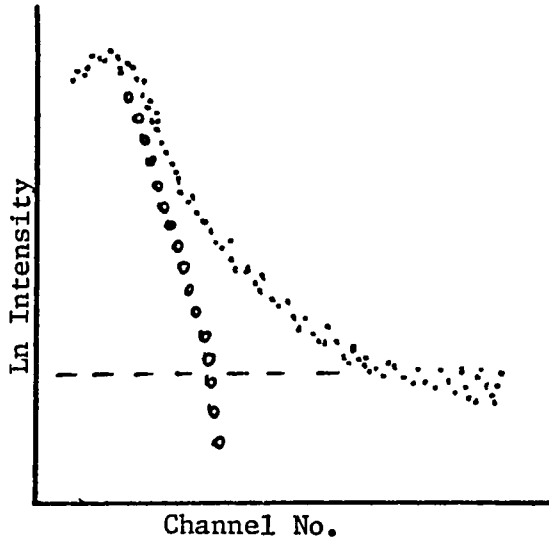
a) too much subtraction
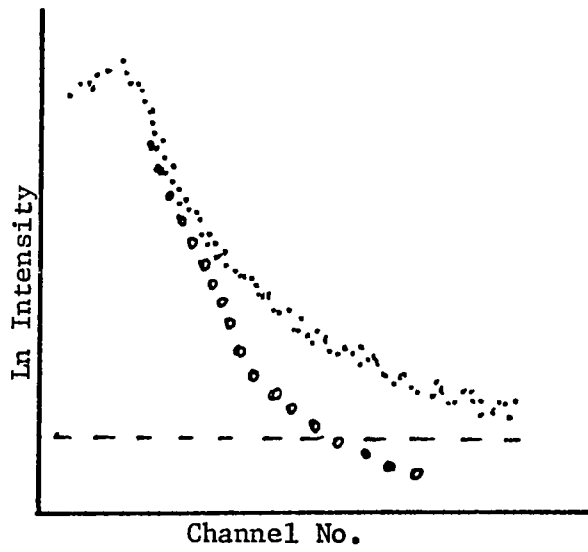
b) too little subtraction

c) proper subtraction

a) Improper Fit – Resultant Lifetime too Short.
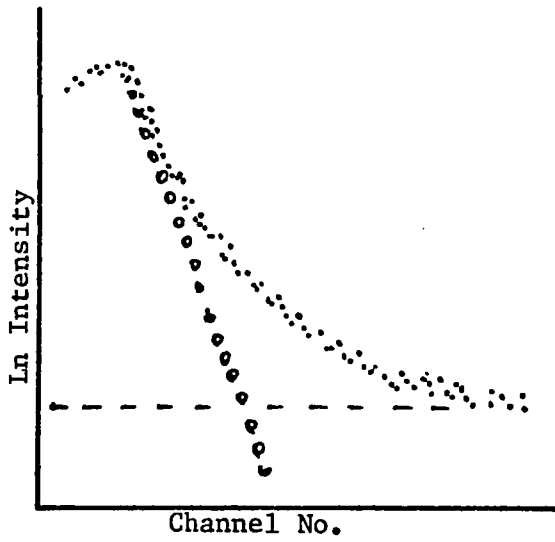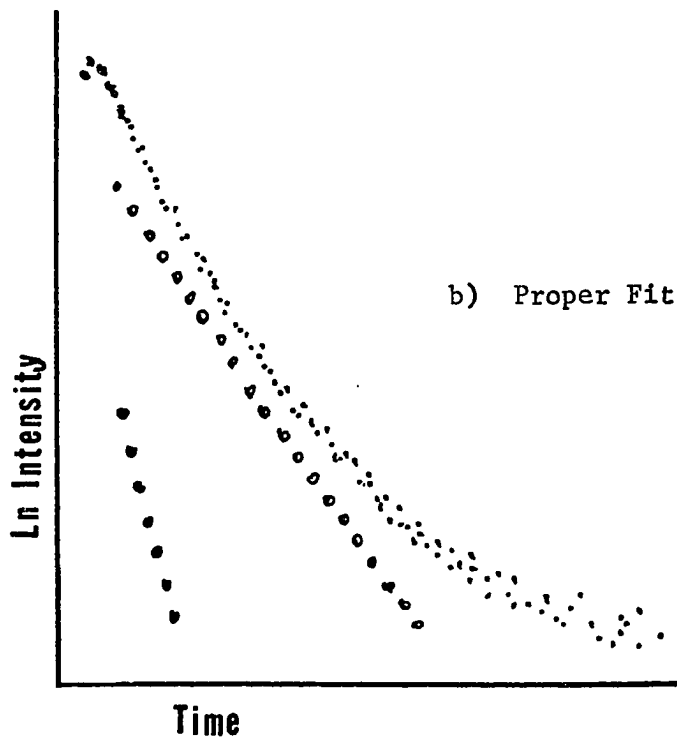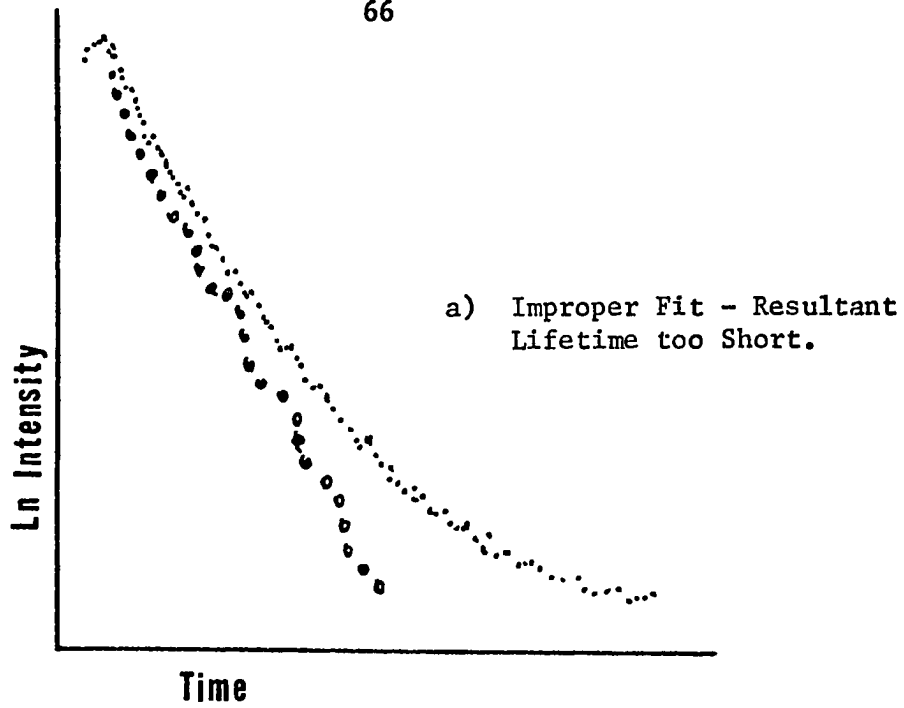
b) Proper Fit

Fig. 34: Improper Fit for Small Amplitude Second Exponential

a) Improper Fit: Note 'Break' in Data Curve.
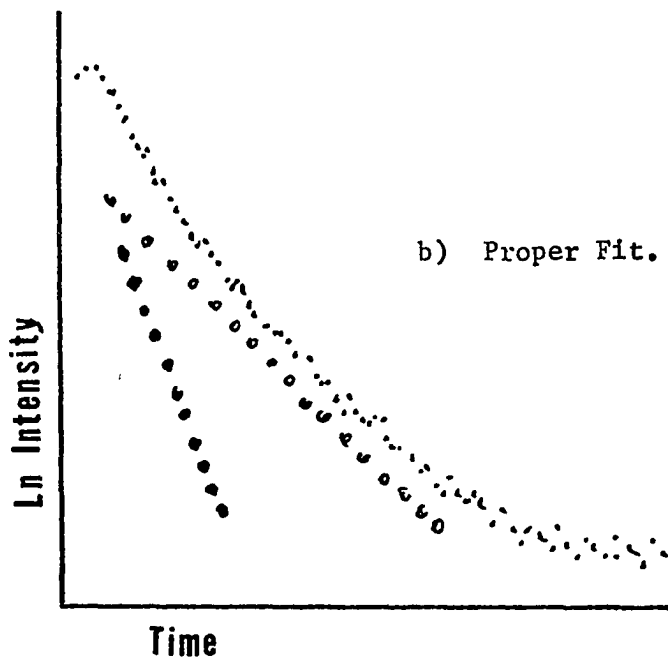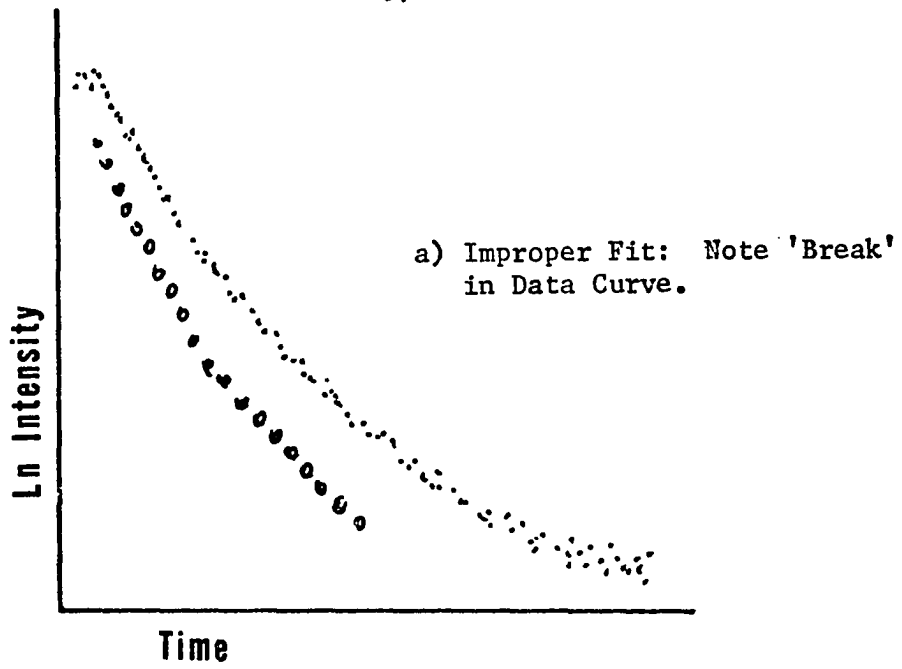
b) Proper Fit.

Fig. 35: Improper Fit For Equal Amplitude Second Exponential

between the data curve and the linear fit.

Computer Technique

It should be stressed at the onset that the computer cannot handle data which cannot be treated by hand graphical methods, as the computer does does essentially the same thing except that instead of averaging the data by 'eye', the computer uses a linear (or non-linear) least squares fit. Therefore, while the PRECISION stated by the machine looks better, the ACCURACY cannot be any better than that achieved by an experienced individual. Also, the machine cannot discount datum errors as the eye can, and consequently a 'dropped' channel (one in which the number of counts is several standard deviations lower than the surrounding channels or even zero) might be weighted incorrectly to the point of distorting the decay curve unless a χ-square or similar test is built into the program. This is a costly CPU procedure. However, the computer offers the advantage in that it reduces the experimental error due to the experimenter's bias about his preferred answer. However, since he can select weight factors, etc., for the program, bias still may not be entirely eliminated.

Two computer programs are used in these experiments in addition to the above mentioned 'hand' techniques. These are the programs LPLOT and LASL (both Fortran G-level).

LPLOT is a semi-logarithmic plotting routine which will also reproduce the data file in punched deck form for later re-use and permanent storage of the data. This program is used to provide information as to how many exponentials are present; where to start the fitting routine; where to stop the routine (channel number); how

much experimental error to expect in the reduced data. Apendix A

contains a program listing for LPLOT followed by a sample data run.

LASL is a non-linear least squares program which through

iteration techniques adjust the parameters (see equation III-1) until

a best fit is reached. The program was initially developed by the

Los Alamos Scientific Laboratory and has been extensively modified

for use in the IBM 360-40 (currently being run on the IBM 370-158).

The least squares technique used is that of Gauss-Newton which has

been modified by Thompson[5] to provide a steepest path of descent as

described by Marquardt[28]. Proofs of the technique may be found in

ref. 29, 30 and 31. A thorough description of this program and its

limitations may be found in R. T. Thompson's dissertation[5]. A pro-

gram listing is provided in Appendix A along with two sample data

runs.

CHAPTER IV

COUNT RATE DISTORTION

It was noticed by Johnson[3] that the rate at which data is acquired in pulse height analysis (PHA) could cause distortions in the decay probability curves. This is illustrated in Fig. 36 a-d, which represent the decay curves observed for the $B^2\Sigma_2^+$ state of N_2^+ which were obtained at count rates of 4, 11, 17 and 25%.

In order to better understand why large count rates distort the data taken in delayed coincidence photon counting, it would be useful to look at why data acquired in the MS mode used for nuclear half-lives is not distorted handling the same effective count rates. Consider the time rate of change of the population N(t) of a given radionuclide

$$dN(t)/dt = -AN \qquad\qquad 26$$

or the number of nuclei at any given time t is

$$N(t) = N(o)\ e^{-At} \qquad\qquad 27$$

which gives the time dependent distribution as follows:
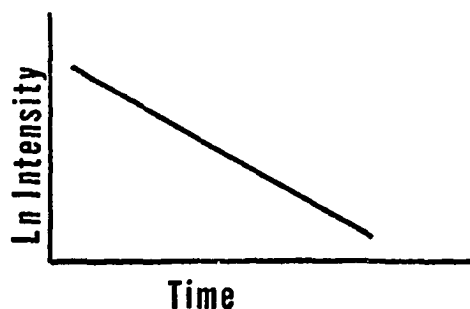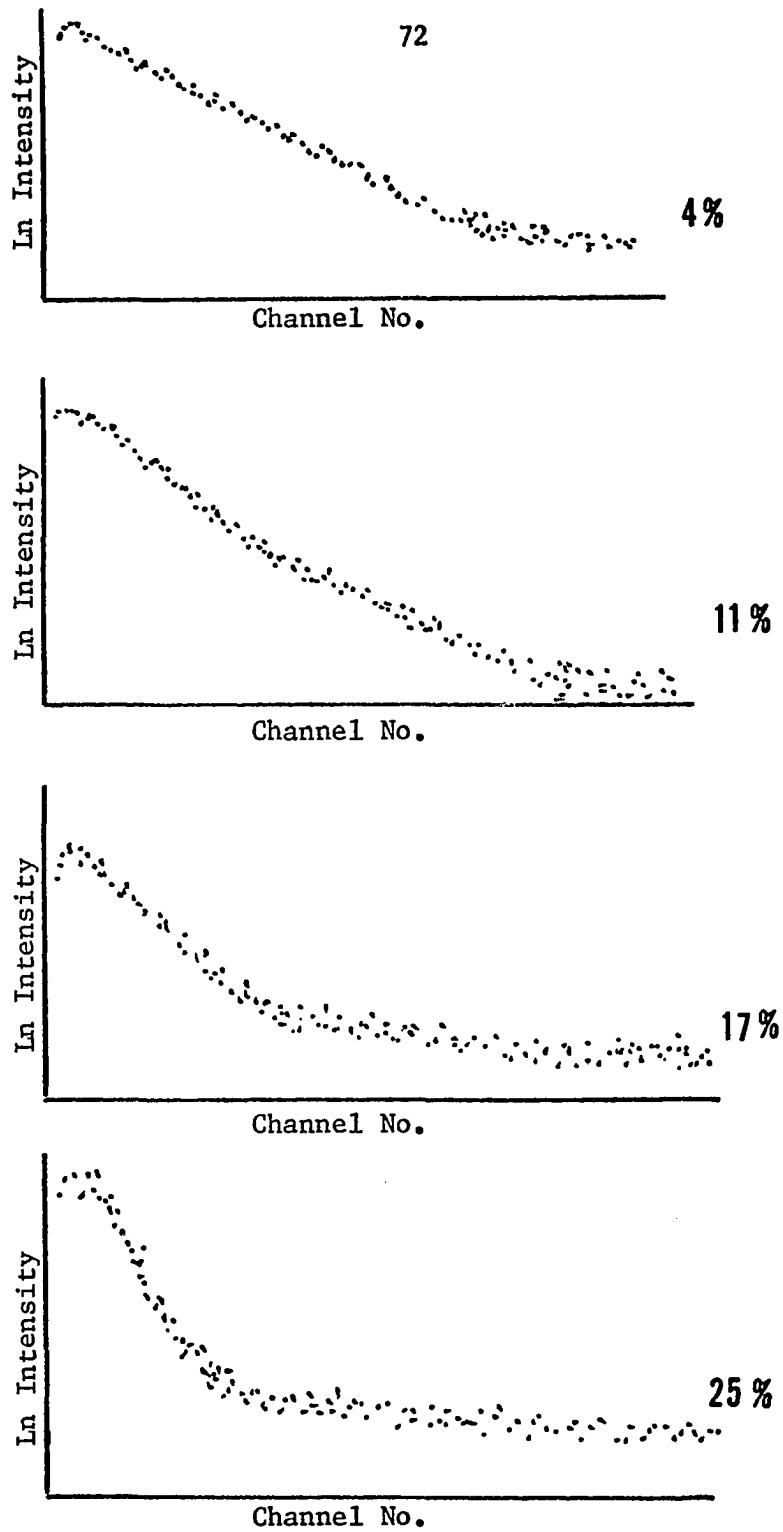
Time

Fig. 36. Decay curves at various count rates.

Now, consider the probability distribution obtained by a MCA

in the MS mode, i.e. all counts delivered in a prescribed time t⎯⎯

$t+\tau_\omega$, are accepted (ignoring MCA dead time which is a different type

of distortion) and the analyzer goes on to the next channel τ_ω. We

need to know if the distribution is indeed that which is predicted

by Eq. 27.

Since intensity $I(t)$, is the number of events per unit time we

should have

$$I(t) = N_o \; dp/_{dt} \qquad\qquad 28$$

where N_o is the population of possible events (number of radionuclei),

dp/dt is the probability an event will occur per unit time (or $dp/$

$d\tau_\omega$ per unit channel) and $dp = p_e p_s dP_d$ where Pe is the probability that

the nuclei exist $\exp\text{-}At = (e^{-At})$, p_s is the probability that we detect it

(effeciency, etc.) and dp_d is the probability of decay Adt (or $Ad\tau_\omega$).

Therefore

$$I(t) = N_o p_s A e^{-At} \qquad\qquad 29$$

and at $t=0$ we have $I(0) = N_o p_s A$ so we can write

$$I(t) = I(0)e^{-At} \qquad\qquad 30$$

This is of the same form as Eq. 27 and therefore indicates that the

data acquisition technique does not inferfer with the experimental

results.

Now, whereas the above technique uses one initial population

to determine the halflife, the mean lifetimes of molecules must be

determined from many different initial systems, where only one decay

per initial system is observed, all others are ignored. The prob-

ability decay curve is then the collection of many hundreds of thou-

sands of separate events, each contributing at most only one count.
Therefore, we will have for the intensity

$$I(t) = N \; dp/_{dt} \qquad\qquad 31$$

where N is the number of events sampled (invertron pulses), dp/dt is
the probability that the event will occur per unit time (channel)
and now

$$dp = PePsPm^d P_d \qquad\qquad 32$$

where p_e is the probability that the molecule exists exp(-At), p_s
is the probability that it is detected (efficiency etc.), p_m is the
probability that the event was missed, and dp_d is the probability
that the molecule will decay in t———— t+dt.

The factor p_m is required since we are basing our measurements
on the time a pulse is seen after the excitation is effected, all
subsequent pulses from that excitation being ignored. This is not
done in the MS mode and consequently no correction is required as
missed events are assumed accountable in the detection efficiency of
the equipment. The question then is how much bias does this factor
cause.

Consider the probability of seeing an event

$$p_s (1-e^{-At}) \qquad\qquad 33$$

Then the probability of missing the event is simply

$$1 - p_s (1-e^{-At}). \qquad\qquad 34$$

For n possible decay events (in the direction of the detection
apparatus) we see only 1 decay event before the TAC turns the sys-
tem off, so we miss

$$\{1 - p_s (1-e^{-At})\}^{n-1} \qquad\qquad 35$$

The intensity is thus given by

$$I(t) = NAp_s e^{-At} \{1-p_s(1-e^{-At})\}^{n-1} \qquad 36$$

and for $t=0$, we have $I(0) = NAp_s$ or

$$I(t) = I(0) \, e^{-At} \{1-p_s(1-e^{-At})\}^{n-1} \qquad 37$$

which indicates a deviation from the curve of interest by the term in braces. But note if we consider only one possible event and we detect it, i.e. $n-1=0$, we get the undistorted curve.

Here n represents the number of events which did get through the apparatus and could have been detected but were not recorded by the method of counting employed, since all but the first were ignored. The value of n can be artificially kept low by keeping the count rate low. The count rate is the number of measured counts divided by the number of times the system (or invertron) is cycled. By keeping the count rate around 10%, we imply that the probability of two simultaneous events is 1%, that of three events 0.1% etc. Therefore we could write for a "double event":

$$I(t) = I(0)\{(1-p_s)e^{-At}+p_s e^{-2At}\} \qquad 38$$

and for a "triple event":

$$I(t) = I(0)\{(1-p_s)^2 e^{-At}+2p_s(1-p_s)e^{-2At}+p_s^2 e^{-3At}\} \qquad 39$$

To reiterate, corrections are required not because events are missed by the system, but because one event is detected and another selectively ignored. This biases the data to the earlier channels and appears as a fast exponential in the data curve as illustrated in Fig. 36

A much more convienent analytical form may be obtained by rewriting the probability of lost events as follows.

$$P_m = \{1-p_s(1-e^{-At})\}^{n-1}$$

$$= 1-(n-1)\left[1-e^{-At}\right]p_s - \frac{(n-1)\ (n-2)}{2!}\ p_s^2\ \left[1-e^{-At}\right]^2 + \ldots \tag{40}$$

which is approximately

$$\approx \sum_{i=0}^{\infty} \frac{(np_s)^i\left[1-e^{-At}\right]^i(-1)^i}{i!} \tag{41}$$

since $\left(\frac{np_s}{i!}\right) \ll 1$, i an integer, is correct for much smaller values of i than is the expression $(n-i) \ll n$. See ref. 3, 32.

Now, by defining $m = np_s$, we have

$$P_m = \sum_{i=0}^{\infty}(-1)^i\ \frac{m^i\left[1-e^{-At}\right]^i}{i} = \exp\{-m\left[1-e^{-At}\right]\}.$$

Consequently Eq. 37 becomes

$$I(t) = I(o)e^{-At}e^{-m(1-e^{-At})} \tag{42}$$

where $m = \ln\ (1-\frac{C_m}{C_p})$ and C_p is the number of counts measured (total number of events seen by the MCA), and C_m is the total number of counts possible (number of times the system fires since only one count is allowed per excitation).

Fig. 37 shows how Eq. 42 fits the experimental data compiled on the $C\ ^3\Pi_u$ state of nitrogen. Currently, additional work is being conducted on this problem and will be reported later by others.

$$I \propto e^{-At} e^{-m(1-e^{-At})}$$
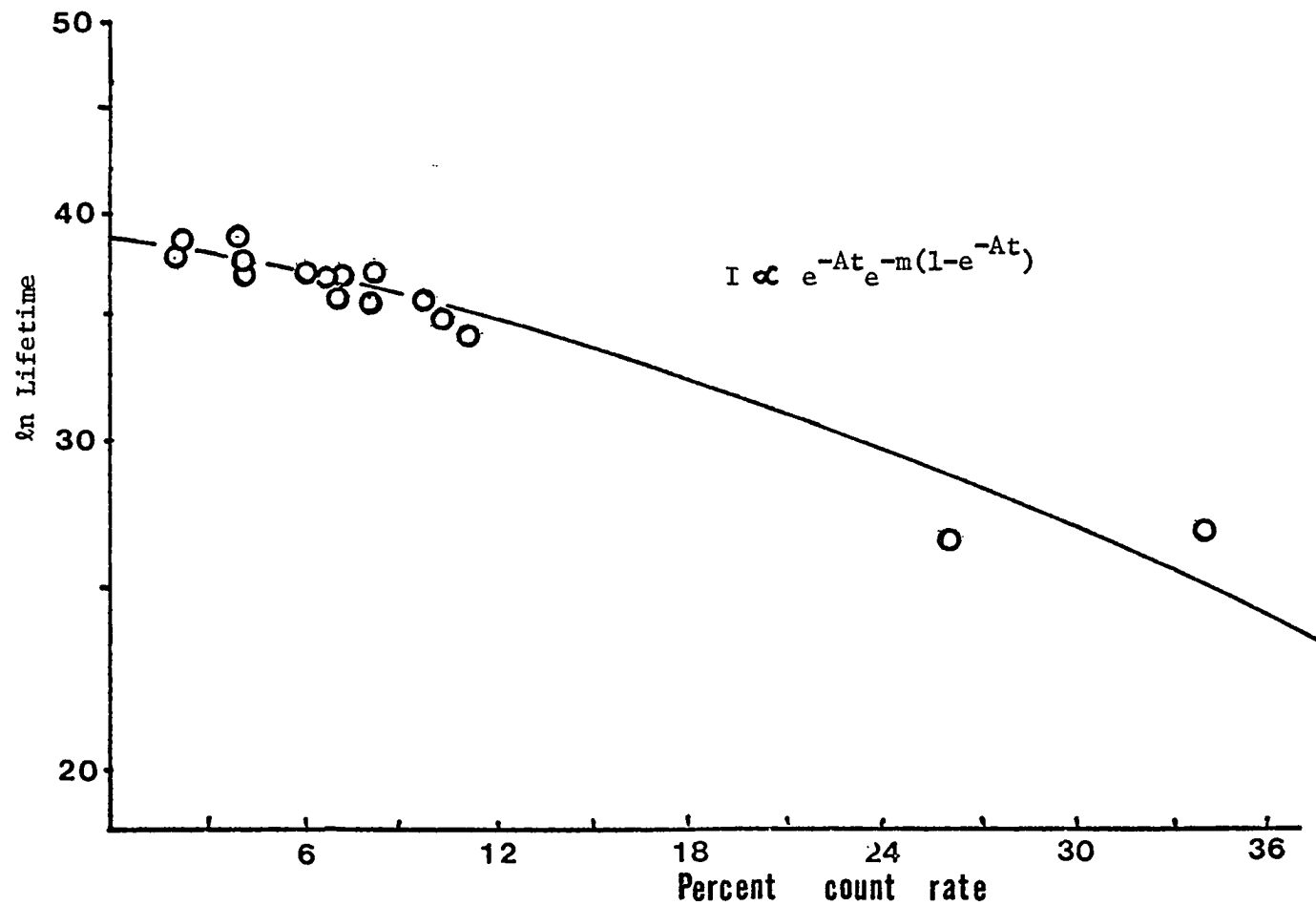
Fig. 37: Theoretical and Observed Dependence of the Lifetime on the Count Rate

CHAPTER V

Nitrogen Lifetimes

Nitrogen was chosen for this series of experiments because
the $B^2\Sigma_u^+$ state of N_2^+ and the $C\ ^3\Pi_u$ state of N_2 have been extensively
studied by many different techniques and Johnson[3] completed some
very precise work using the hot cathode invertron with which this
work was compared. Also, the $C\ ^3\Pi_u$ state appears to be pressure
independent and does not possess a cascade component. This state
then provides a clean single exponential of 38.4 nsec mean life with
which to calibrate the cold cathode system and to determine any
equipment dependences. Likewise, the $B^2\Sigma_u^+$ state of N_2^+ provides a
single exponential (59 nsec), but exhibits a pressure dependence
which should be useful in determining depopulation mechanisms.

It is felt that an adequate understanding now exists such
that experimental results are reliable and reproducable. A reca-
pitulation of the major experimental problems will be presented in
this section followed by tables of this work compared with that pre-
viously reported in the literature.

"Typical" data in the form of pressure vs the transition pro
probability is presented in Fig. 38 which represents the quality of
early data acquired on the unmodified system for the $B^2\Sigma_u^+$ state of
N_2^+. Suffice to say that this quality of data could not be tolerated.

Most of this problem was cleared up by recognizing the sever-
ity of the count rate distortion discussed earlier. This distortion
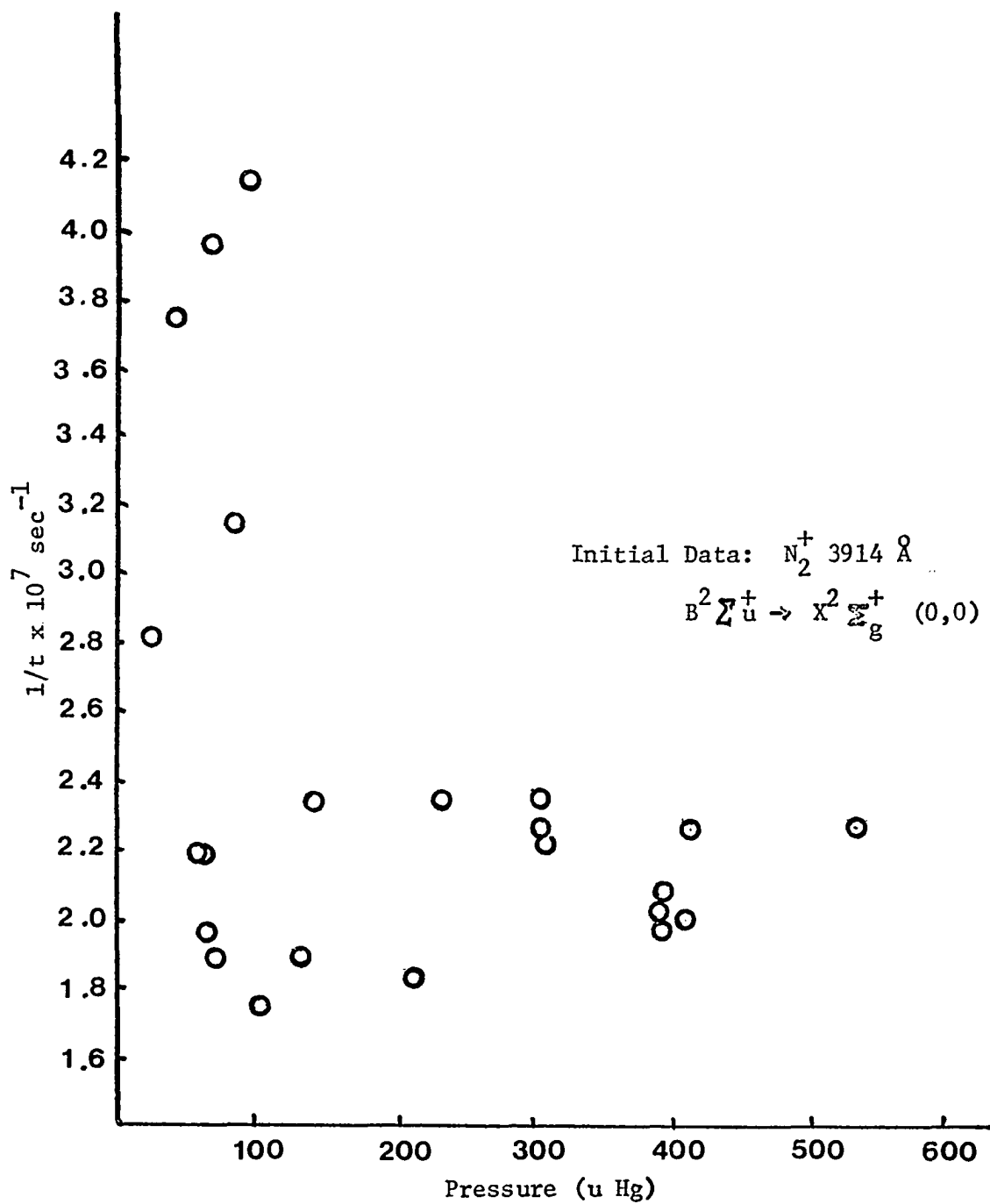
Fig. 38 Initial lifetime data for $B^2\Sigma_u^+$ N_2^+ (v'=0).

was expecially rampant in the earlier stages of these experiments
since the excitation electronics system did not pulse at the repeti-
tion rates indicated by the monitor, i.e. the discharge tube did not
fire every time it was pulsed. For example, it the repetition rate
was set at 500 Hz, the discharge tube might fire anywhere from 200-
300 Hz regularly, and at any other value sporadically. Also, the
vacuum system, primarily the discharge tube, leaked. The boron ni-
tride spacers were found to be quite porous. It was not clear if this
was a problem of age, or if the spacers were worn out due to removal
and reinsertion of the anode for cleaning. The leaking system was
the easiest to remedy, the boron spacers were replaced with Teflon
sleeves and subsequently the whole discharge tube was redesigned as
described in Chapter II-D. The problem of the discharge tube mis-
firing was at first tolerated by inserting the Canberra scalers as
shown in Chapter II-C and directly measuring the events counted vs
the number of times the system fired (i.e. the count rate) for a
given experiment. Later the difficulty was removed by properly modi-
fying the excitation electronics to give dependable firing rates.
(See Chapter II-B)

With these two corrections, our data were now much improved
as Fig. 39 indicates. It was then determined that the data were of
sufficient quality for the more subtle problems of the glow discharge
to be approached. With the help of Fig. 40 a rather interesting
problem was recognized. At low pressures it was found that both the
$B^2\Sigma_u^+$ and the C $^3\Pi_u$ states of N_2^+ and N_2 exhibited an increase in their
observed lifetimes which appeared at first glance to be equipment
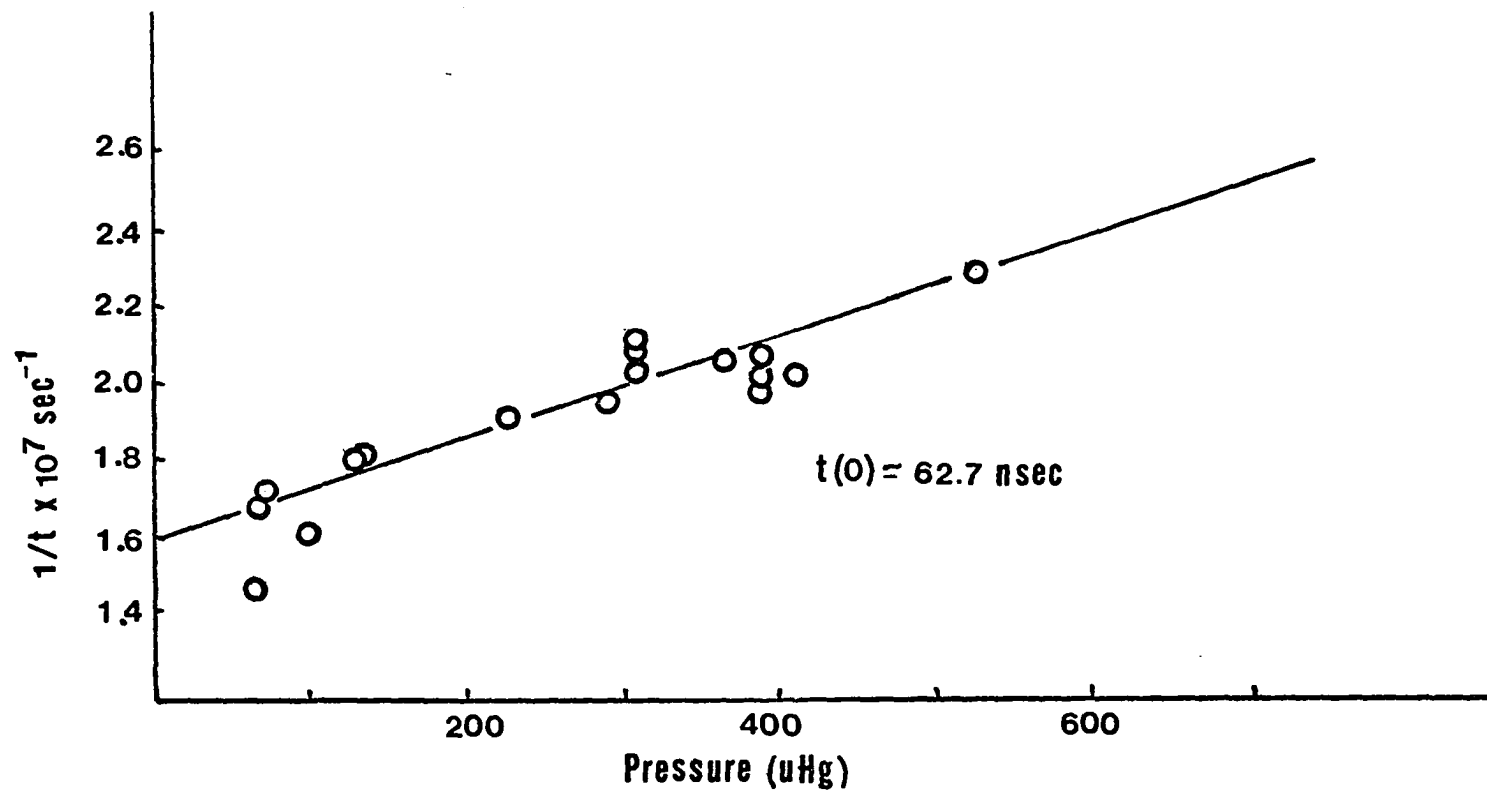
Fig. 39: Improved Lifetime Data for B $^2\Sigma_u^+$ N_2^+ (v'=0)
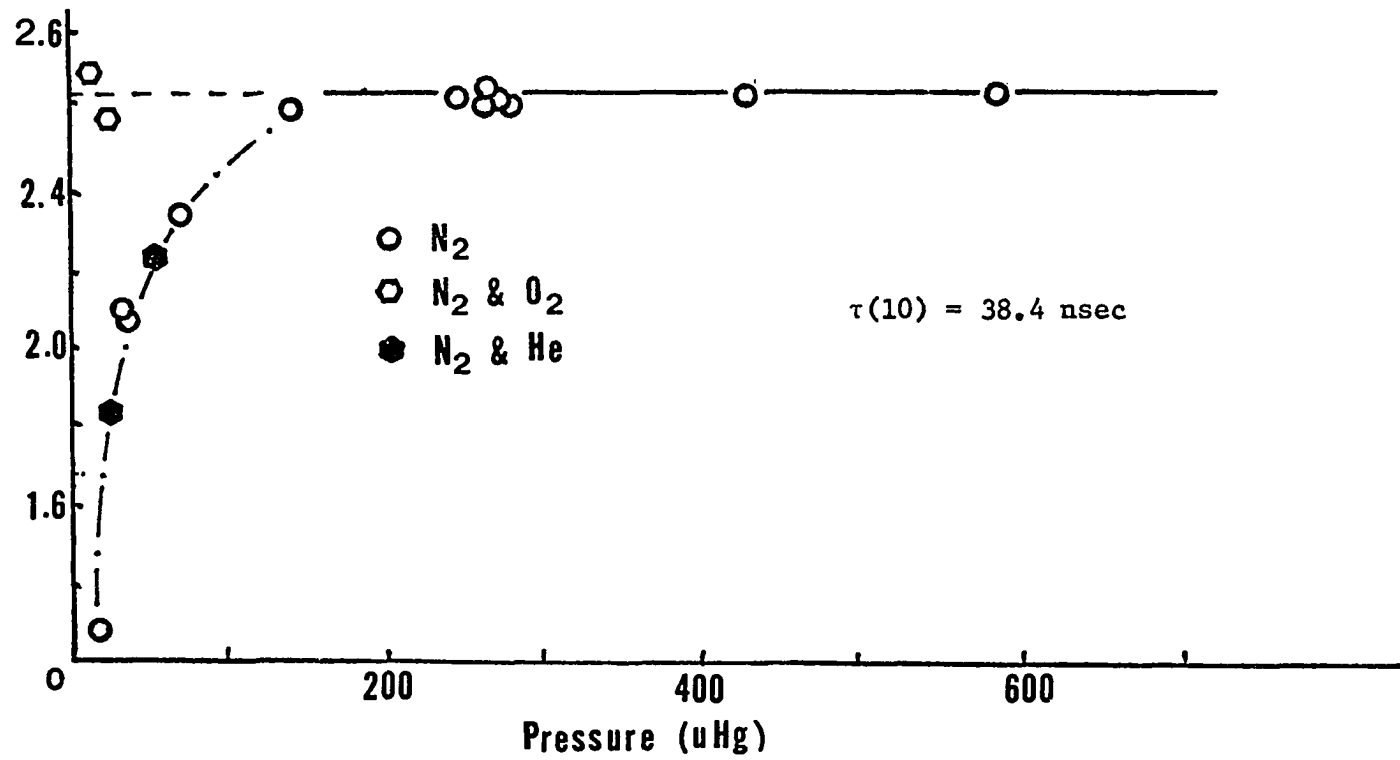
Fig. 40: Low Pressure Distortion of Lifetime Data of the $C^3\Pi_u$ $N_2(v'=0)$

oriented. As Fig. 40 indicates, this problem could be solved by the addition of small amounts of oxygen to the system, while the addition of helium did absolutly nothing. It was determined therefore that the pressure was not really the controlling variable, but rather the presence or absence of an electronegative gas capable of clearing the electrons out of the system after cut-off, in conjunction with an inability of the cathode structure to sweep these electrons.

This inability to sweep the field properly was also indicated by the probability decay curves which exhibited a "hump", and in severe cases, a peak in the lead to middle channels depending on the diameter and structure of the cathodes used as shown in Fig. 41. This was corrected after extensive cathode design studies were completed and cathode inserts of helix-grove or parallel-rod design were used (see Chapter II-E). These improvements then make possible the data shown in Fig. 42. Note however, that the problem at low pressures is still not completely solved. It probably cannot be solved while working with pure nitrogen as the attachment coefficient for pure nitrogen matches that of the noble gases...zero. However, studies in oxygen indicate that work at these lower pressures is indeed possible if the gas under study is electronegative.

Our attention was then turned to that of the magnetic field's influence on the observed results. The only effect observed with increasing field was an increasingly poor electrical cut-off of the discharge, and therefore an increase in the errors of data reduction. This effect was found to be random and it was therefore concluded merely that the magnetic field should be kept as low as necessary to sustain the discharge at low pressures (and off when possible)
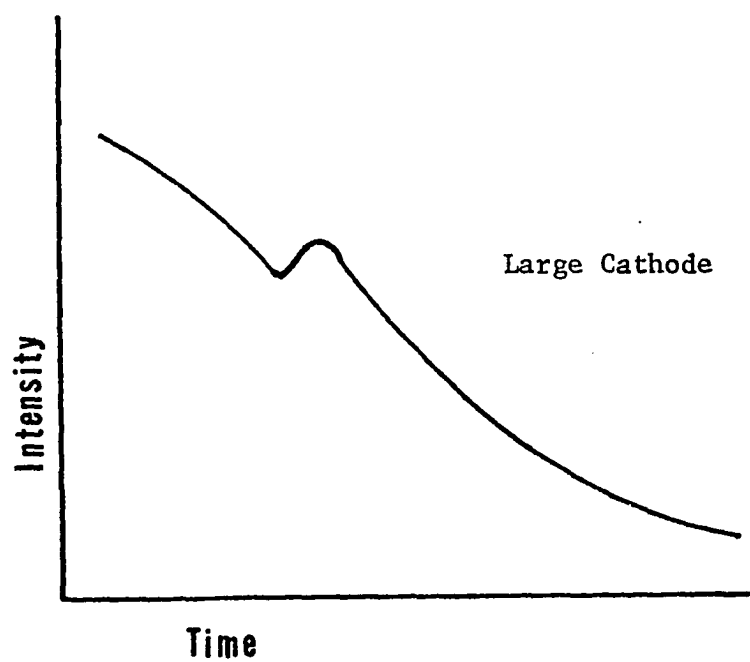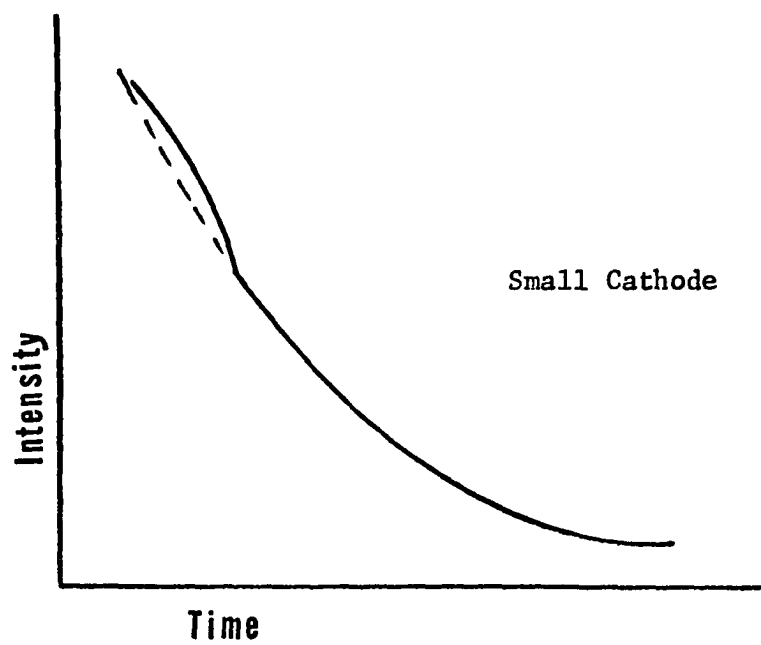
Fig. 41: Distorted Decay Curves Due to Improper Electron Quenching
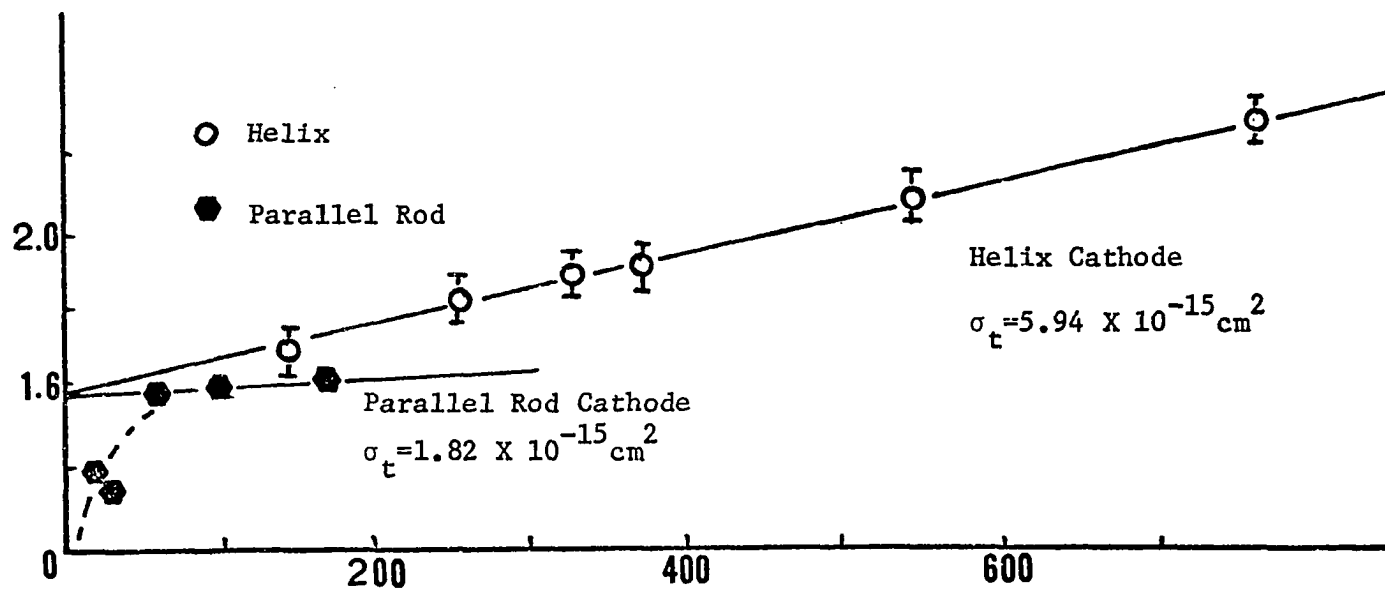
Fig. 42: Improved Lifetime Data Using the Helix and Parallel-Rod Cathodes

to reduce the errors in the data reduction.

A high applied voltage affected the results adversely in a manner similar to that of the magnetic field. At higher applied voltages larger numbers of electrons made cut-off difficult to achieve and consequently, the data reduction errors were increased. This occured only when the applied voltages were sufficient to cause the discharge to exist in the abnormal glow region. If this was not the case, i.e. the glow remained in the normal region, the increased voltage did not effect the results appreciably.

In conclusion, Table II and Table III list the reported lifetimes for the $B^2\Sigma_u^+$ and $C^3\Pi_u$ states of N_2^+ and N_2 as reported by other workers for a comparison of results.

Table II: Reported Lifetimes for $B^2\Sigma_u^+$ ($\nu'=0$) N_2^+

Experimentalist	τ (Nanoseconds)
Bennett & Dalby[33]	65.8 ± 3.5
Fowler & Holzberlein[34]	70 ± 15
Jeunehomme[35]	71.5 ± 5
Johnson[3]	59.2 ± 4
Hesser & Dressler[36]	59 ± 6
Nichols & Wilson[37]	65.9 ± 1
Sebacher[38]	65 ± 2
This Work	62.7 ± 2.5

Table III
Measured lifetimes of $C^3\Pi_u$ ($\nu'=0$) level of N_2

Experimentalist	(sec.)
Bennett & Dalby[33]	44.5 ± 6
Jeunehomme[35]	49 ± 5
Johnson[3]	39 ± 2.5
Nichols & Wilson[37]	45.4
This Work	38.4 ± 2.5

CHAPTER VI

SO_2

Introduction

Sulfur dioxide is a tri-atomic planar non-linear molecule belonging to the symmetry group C_{2v} and classed as an asymmetric top. This implies that the molecule SO_2 has two vertical planes of reflective symmetry, σ_v and σ_v' , and has a two-fold axis of cyclic or rotational symmetry, C_2. The planes of symmetry are refered to as vertical planes since by convention the main axis of symmetry is assumed to be the vertical (z) axis, and C_2 refers to a rotation by 180° about the z-axis. The vertical planes σ_v are sometimes written $\sigma_v(x,y)$ and $\sigma_v(y,z)$ to denote in which plane the reflection is considered.

Since there are four different ways of assigning plus and minus signs to the two reflections, the point group is represented by the four characters A_1, A_2, B_1, B_2 which denote symmetry or anti-symmetry with respect to the operation C_2. The characters of this group are given below in Table IV.

Table IV: C_{2v} Character table

C_{2v}	I(or E)	$C_2(z)$	$\sigma_v(x,y)$	$\sigma_v(y,z)$
A_1	+1	+1	+1	+1
A_2	+1	+1	-1	-1
B_1	+1	-1	+1	-1
B_2	+1	-1	-1	+1

The notation I and E are interchangable depending on the reference used and represent the identity element (E=Einheit), i.e. C_2^2 = I or E. The plus and minus signs refer to the preservation of the symmetry in a given operation.

As a matter of caution, the following notation will be observed to prevent confusion. A_1, A_2 etc. will refer as mentioned to symmetry or antisymmetry operations with respect to the cyclic rotation C_n. This is not to be confused with A_u, A_g, B_u, B_g, (u = ungerade, g = garade) which denote symmetry or antisymmetry with respect to the center of symmetry (as in the planar X_2Y_2 of the group C_{2h}), nor should these be confused with A_1', A_1'', etc. which refer to symmetry or antisymmetry with respect to the plane σ_h (reflection in a plane perpendicular to the principle axis, i.e., horizontal reflection) as in a planar XY_3 molecule from the group D_{3h}. Also, the symbol I should be used for the identity operator to avoid confusion with the degenerate species E_1, E_2, etc. found in higher order degenerate groups. One last word on notation, the symbol $\tilde{A}$ or $\tilde{X}$ refers to a particular molecular level and not to the symmetry species. Consequently, a state may be refered to as $\tilde{X}\ ^1A_1$ or $\tilde{A}\ ^3B_1$

without confusion. For further clarification, see ref. 39, 40.

Since a non-linear molecule does not have an axis about which the moment of inertia vanishes (as in linear molecules), there are three mutually perpendicular directions about which the moment of inertia has a maximum or a minimum.[41] These are termed the principle axes (or principle moments of inertia) and are designated ℓ_A, ℓ_B, ℓ_C where generally $\ell_A < \ell_B < \ell_C$. If the molecule has an axis of symmetry then this axis will be a principle axis. Likewise, any plane of symmetry the molecule possess must have a principle axis perpendicular to it. If two of the principle moments are equal, the molecule is refered to as a symmetric top. If $\ell_A = \ell_B$, it is called an oblate top and if $\ell_B = \ell_C$, it is refered to as a prolate top. If all three are equal, it is called a spherical top. In the case of SO_2, where none of the three moments are equal, the molecule is termed an asymmetric top.

The vibration of tri-atomic molecules can be broken down into three normal modes of vibration v_1, v_2 and v_3 as shown in Fig. 43. These modes are termed symmetrical valance (v_1), deformation (v_2), and anti-symmetrical (v_3) by Metropolis[42]. These vibrations cause what are termed vibronic species. These vibronic eigenfunctions ψ_{ev} are to a first approximation

$$\psi_{ev} = \psi_e(q,o)\psi_v(Q) \qquad\qquad 43$$

where $\psi_e(q,0)$ refers to the electronic wave function for the equilibrium position Q=0. This implies that the vibronic species are simply the direct products of the electronic species with the vibrational species. As an example consider an SO_2 molecule (C_{2v} symmetry) which is in the B_1 electronic state. If a B_2 vibration is excited (i.e.)

similar to $_3$ in Fig. 43) the resultant vibronic state is

$$B_1 \ X \ B_2 \ = \ A_2.$$
44

Degenerate vibrations will not be considered as they do not

occur except by accident for molecules with only two-fold symmetry

or less[43].
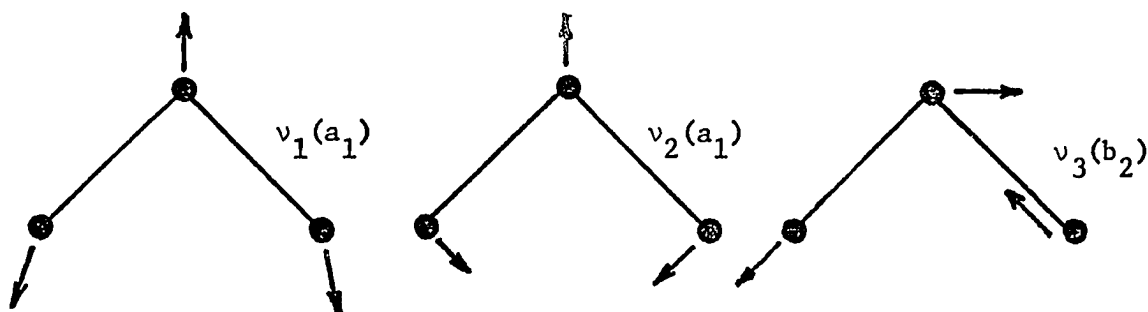
Fig. 43: Normal modes of vibration for SO_2

SO_2 SPECTRAL ANALYSIS

Pearse[44] has grouped the emission spectra of SO_2 into three

catagories, all of which are degraded to the red. These are: group

A, 4340 to 2700 Å; group B, 2640 to 2350 Å; and group C 2343 to 2170

Å. The work presented here has dealt exclusively with the second

and third groups.

With the MCA used in the MS mode, the spectra illustrated in

Fig's. 44-46 were obtained. Fig. 44 shows how important it is to

keep out trace quantities of nitrogen. A multiple distillation using

liquid nitrogen traps as described earlier (see Chapter II Sec. A)

X 2.5

SO & SO_2

N$_2$ C$^3\Pi_u$

2976   3136 3159   3371

Å   Å   Å   Å
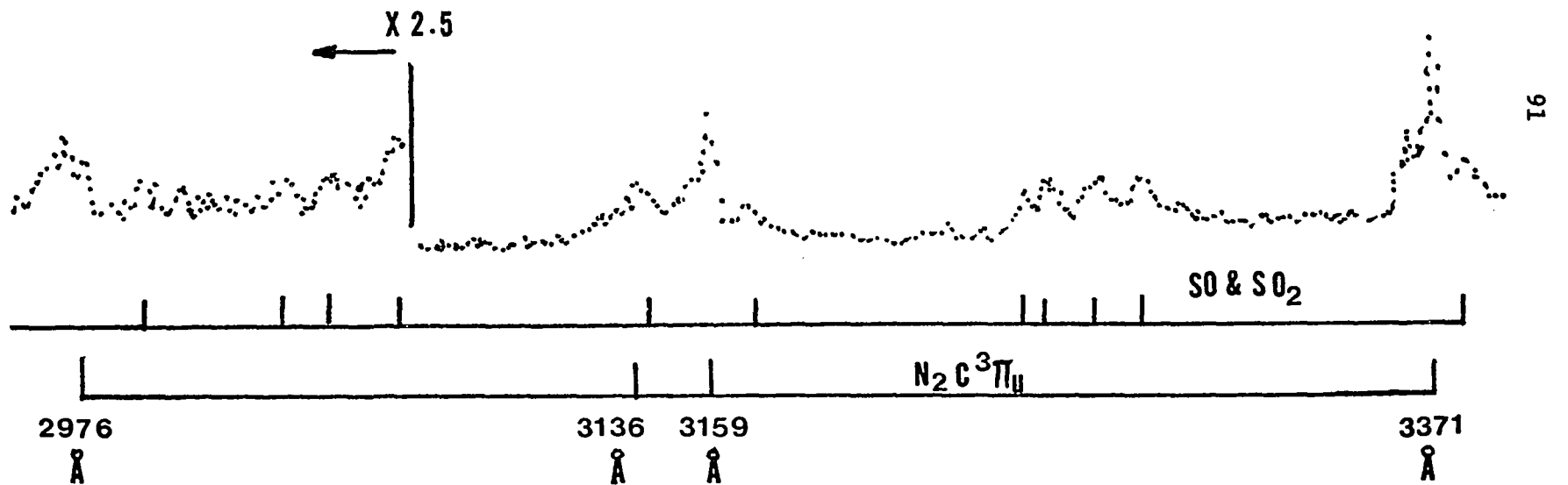
Fig. 44: SO_2 Spectra With Trace Nitrogen Contamination
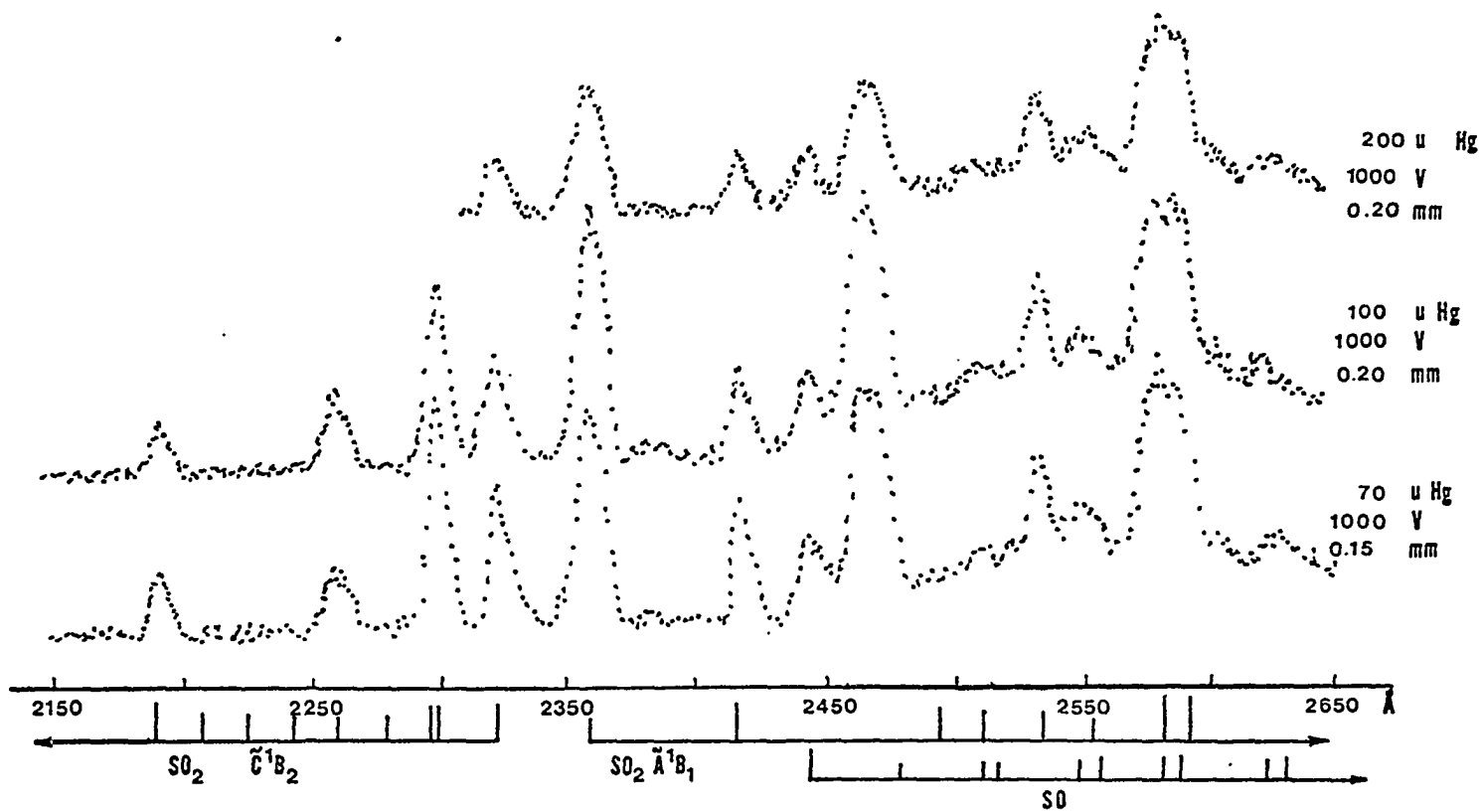
Fig. 45: SO$_2$ Spectra Showing Pressure Dependence
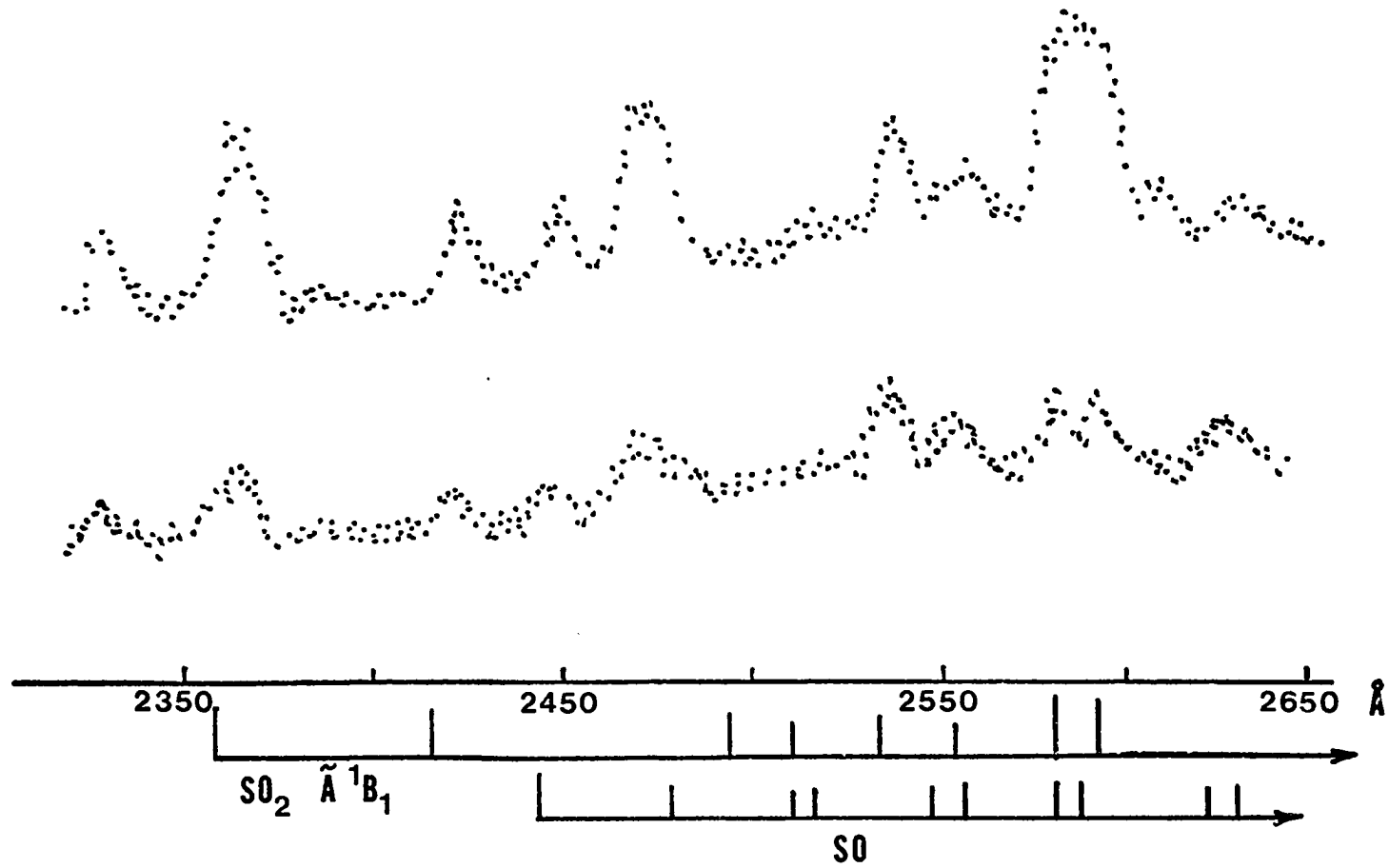
Fig. 46: SO_2 Spectra Illustrating Voltage Dependence

was used to eliminate these unwanted lines and subsequent spectra were free of N_2 emmision spectra. Fig. 45 and 46 illustrate the pressure and applied voltage dependence of the spectra. Please note the slit width change. It appears from Fig. 45 that at least two of the peaks, i.e. those centered around 2365 and 2263 Å, are not due to the emission of SO_2 as they gain relative intensity with pressure with respect to the other peaks. Also, in Fig. 46, these peaks suffer severe attenuation with a drop in applied voltage of 200 volts. It is felt that these peaks are due to the dissociation of SO_2 and the subsequent decay of excited atomic oxygen. This idea will be discussed later.

All of these spectra were obtained using a static gas sample, operating from 800 to 1000 volts. Very little sulfur deposition was observed except at high pressures (400+ μHg). The MCA was operated in the MS mode with a dwell time of 0.8 seconds per channel and 256 channels were used on each sweep.

PREVIOUS LIFETIME WORK
$$\tilde{a}\ ^3B_1\ \underline{SO_2}$$
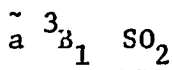
Previous lifetime determinations [45-47] have associated the region of group A with the first excited state, designated $\tilde{a}\ ^3B_1$. I determined this level to be very long lived (>200μsec) and consequently could not study it further. However, for completeness and to help illustrate the inconsistencies in the reported lifetimes for this molecule, the known work for this level is presented below in Table V.

Table V: Reported lifetimes for $\tilde{a}\ ^3B_1\ SO_2$.

Worker	Pressure	Lifetime
Caton & Duncan[45]	30 μ - 1.5 mm (no pressure dep. found)	7 $\pm$ 1 msec
Levitt & Sheen[46]	not stated in work (a few torr?)	0.2 msec.
Greenough & Duncan[47]	solid at 77° K	0.5 msec.

$$\underline{\tilde{A}\ ^1B_1\ SO_2}$$
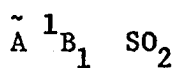
The second excited state designated $\tilde{A}\ ^1B_1$ from the electron

confirguration $(1a_2)^2(3b_2)^2(4a_1)(2b_1)\ ^{1,3}B_1$, has been reported to have

very diverse lifetimes and even to possess a non-exponential decay.

Mettee[48] alone presents a lifetime varying from 12 μsec to 128 μsec.

Greenough and Duncan give a lifetime of 45 μsec, while Levitt and

Sheen[46] list a value of only 7 μsec. In his work, Sidebottom[49] found

a nonexponential decay which had a time dependent decay varying from

14 to 33 μsec, and Hui and Price[50] simply state that the decay is

non-exponential for the $^1B_1$ state. Several arguments have been put

forth by the collective authors as to why their data do, or do not,

appear to agree. Mettee for example feels that perhaps his frequency

dependent lifetimes should all have the value of 64 μsec and the

variations are due to a frequency dependent excitation cross section.

However, a correlation does exist which these authors seem to over-

look. Table VI presents their data and Fig. 47 is a lifetime versus

wavelength plot of this data on semi-log paper.
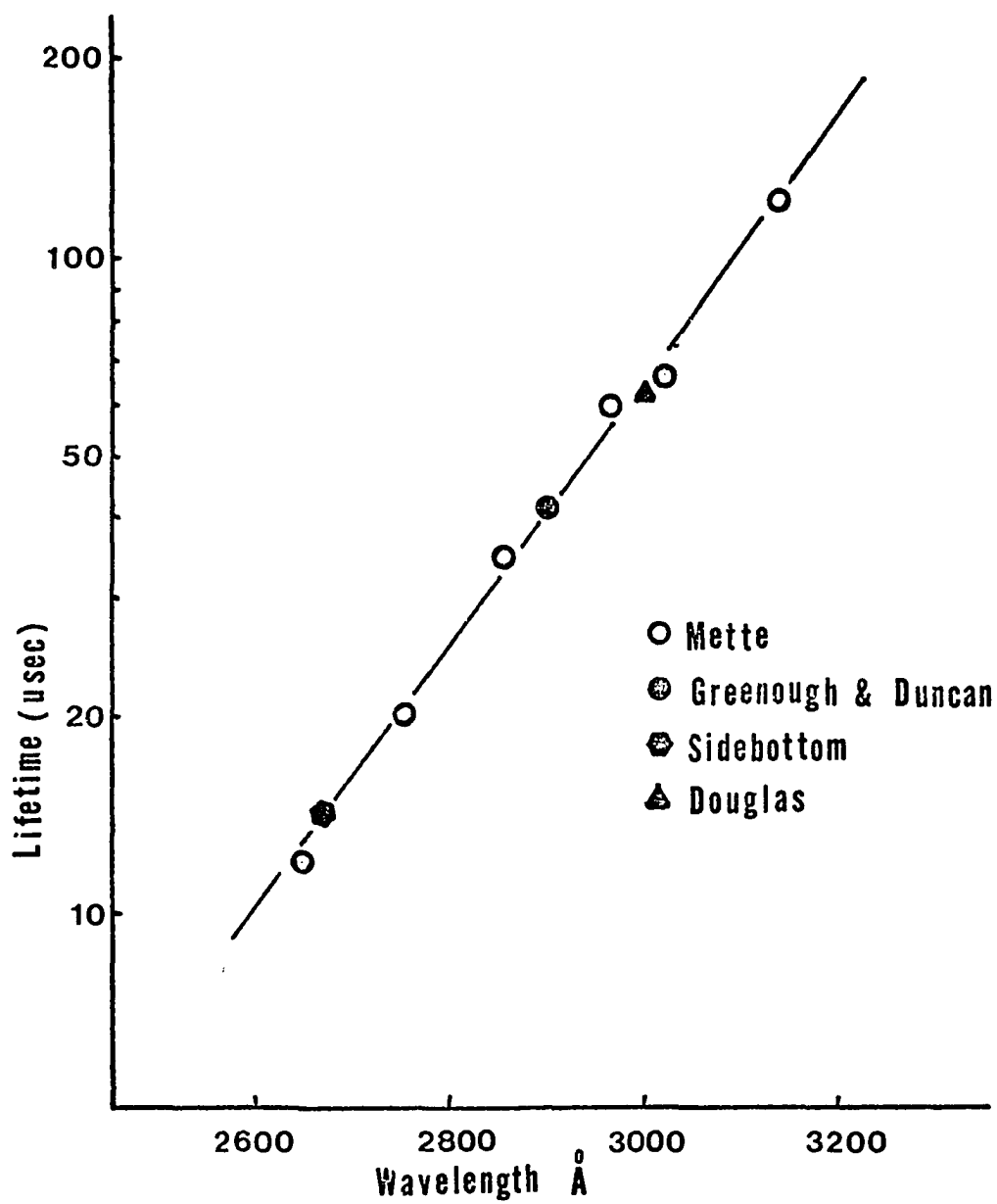
Fig. 47: Lifetime $\underline{VS}$ Wavelength for the $\tilde{A}\ ^1B_1\ SO_2$

Table VI: Reported lifetimes for $\tilde{A}\ ^1B_1$ SO_2

Worker	Wavelength	Pressure	Lifetime
Levitt & Sheen[46]	4360(?)	not stated	7 usec
Greenough & Duncan[47]	2700-3100	solid at 77°K	42 usec
Mettee[48]	3130	1--1000 µHg	128 usec
	3020		68
	2960		60
	2850		35
	2750		20
	2650		12
Sidebottom[49]	2662 (Laser)	2- 80 µHg	33 usec
			14 usec
		calculated values	36±4 usec 18±6 usec
Douglas[57]	3000	?	63 usec

The double value given by Sidebottom refers to the non-exponential nature of the observed decay and is an attempt to analyze the apparent time dependency of the decay. His calculated values correspond to levels which are partially and totally vibrationally equilibriated. The values stated for Douglas is based on his statement that his lifetime was approximately 50% higher than that of Greenough and Duncan.

Fig. 47 would seem to be more than a coincidence. This is obviously not due to the ν^3 factor and can perhaps be explained by considering interelectronic level mixing. Douglas[51] has stated four requirements for this type of effect to occur which are:

1) A strong electronic transition moment existing between
levels $\tilde{B}$ and $\tilde{X}$ (see Fig. 48).

2) A weak or no electronic transition moment existing between

levels $\tilde{A}$ and $\tilde{X}$,

3) A strong interaction existing between $\tilde{A}$ and $\tilde{B}$, i.e., vibronic

or Coriolis, or if they have different multiplicities, strong

spin-orbit interactions,

4) Density of vibrational levels of $\tilde{A} \gg \tilde{B}$.
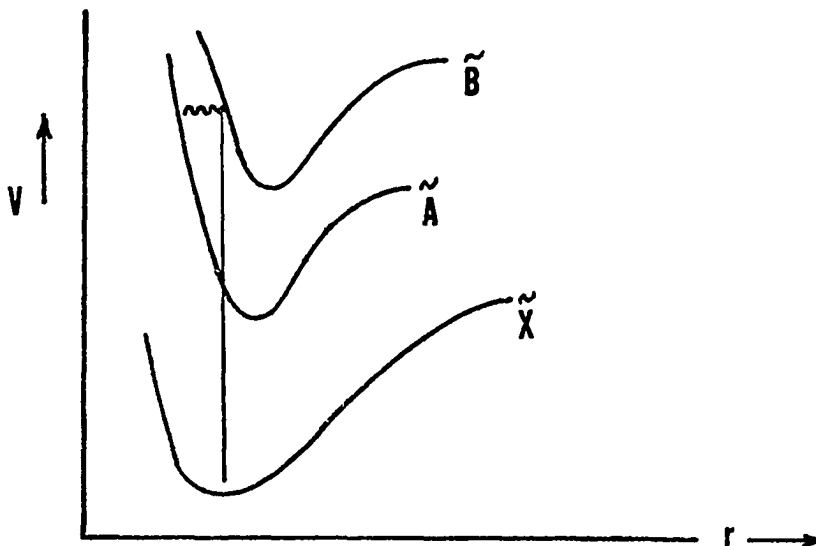
Fig. 48: Schematic potential wells for
interelectronic level mixing.

This type of system will add large numbers of extra vibrational

levels which can be reached by absorbing radiation from the ground

state, i.e. several levels from $\tilde{A}$ may be reached by one level from $\tilde{B}$.

This will produce a spectrum in which a large number of weak lines

are seen instead of a few strong lines. This in turn increases the

apparent degeneracy, alters the line strengths and consequently in-

creases the observed lifetime. The degree of mixing will obviously

depend on the extent of the interaction and on the type of interaction

present. In the limit of large interaction, Douglas states that the increase in the observed lifetimes will vary as the density of the levels $\tilde{A}$ and $\tilde{B}$.

This criterion seems applicable to SO_2. The $\tilde{B}$ ($\tilde{A}$ $^1B_1$)——— $X(X$ $^1A_1)$ transition is quite strong while the $\tilde{A}$ (a^3B_1)——— $\tilde{X}(\tilde{X}^1A_1)$ transition involves a different multiplicity and are reportedly very weak. This multiplicity difference could also provide the interaction necessary (spin-orbit for example) between $\tilde{a}$ and $\tilde{A}$.

One other effect is mentioned by Douglas. If the interaction is fairly weak and if it varies with the rotational and vibrational quantum numbers of the excited state, then even closely spaced levels may differ in their observed lifetimes. This implies that the decay of flourscence excited with even a narrow band of radiation (Sidebottom's LASER) will be a mixture of the various lifetimes and will be observed as non-exponential. Sidebottom[49] and Hui[50] report such decays for the $\tilde{A}$ $^1B_1$ level of SO_2. Perhaps the graph in Fig. 47 will be useful in determining the extent and type of interaction between the levels $\tilde{a}$ $^3B_1$ and $\tilde{A}$ $^1B_1$ of SO_2 in the future.

$$\tilde{C} \; ^1B_2 \quad \& \quad \tilde{D} \; ^3B_2$$
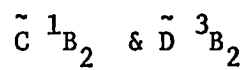
The last reported states of SO_2, the $\tilde{C}$ and $\tilde{D}$ states have been reported on by Hui and Price[50], who used single photon counting techniques and concluded that these states were not as strongly coupled to any other states as were the lower levels. An extrapolation of their data reveals a zero pressure lifetime for the composite system of 55 ± 8 nsec.

PRESENT LIFETIME WORK

$$\tilde{a}\ ^3B_1$$

The first excited level of SO_2, the $\tilde{a}\ ^3B_1$ state was not mea-
sured in this work as the levels are too long lived to allow accurate
work with the present equipment. It is hoped that the level can be
studied in the future after modification of the apparatus and will
be reported on in the future elsewhere.

$$\tilde{A}\ ^1B_1$$

The $\tilde{A}\ ^1B_1$ state has been observed in a flowing gas system at
several frequencies to determine if the same frequency dependence was
present as was reported earlier. It was not. However a reciprocal
transfer or close coupling of near states was observed as is apparent
in Fig. 49. A complete theoretical description of this process may
be found in Morton[7] and in Thompson[5]. Essentially, the process is as
follows (see Fig. 50).
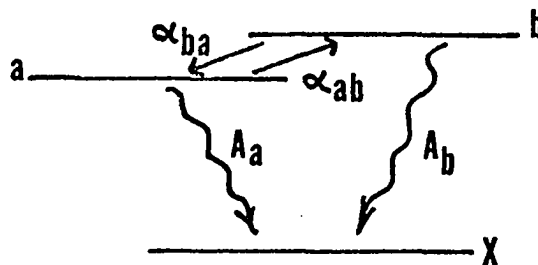
Fig. 50: Energy level diagram for close
coupling of states.
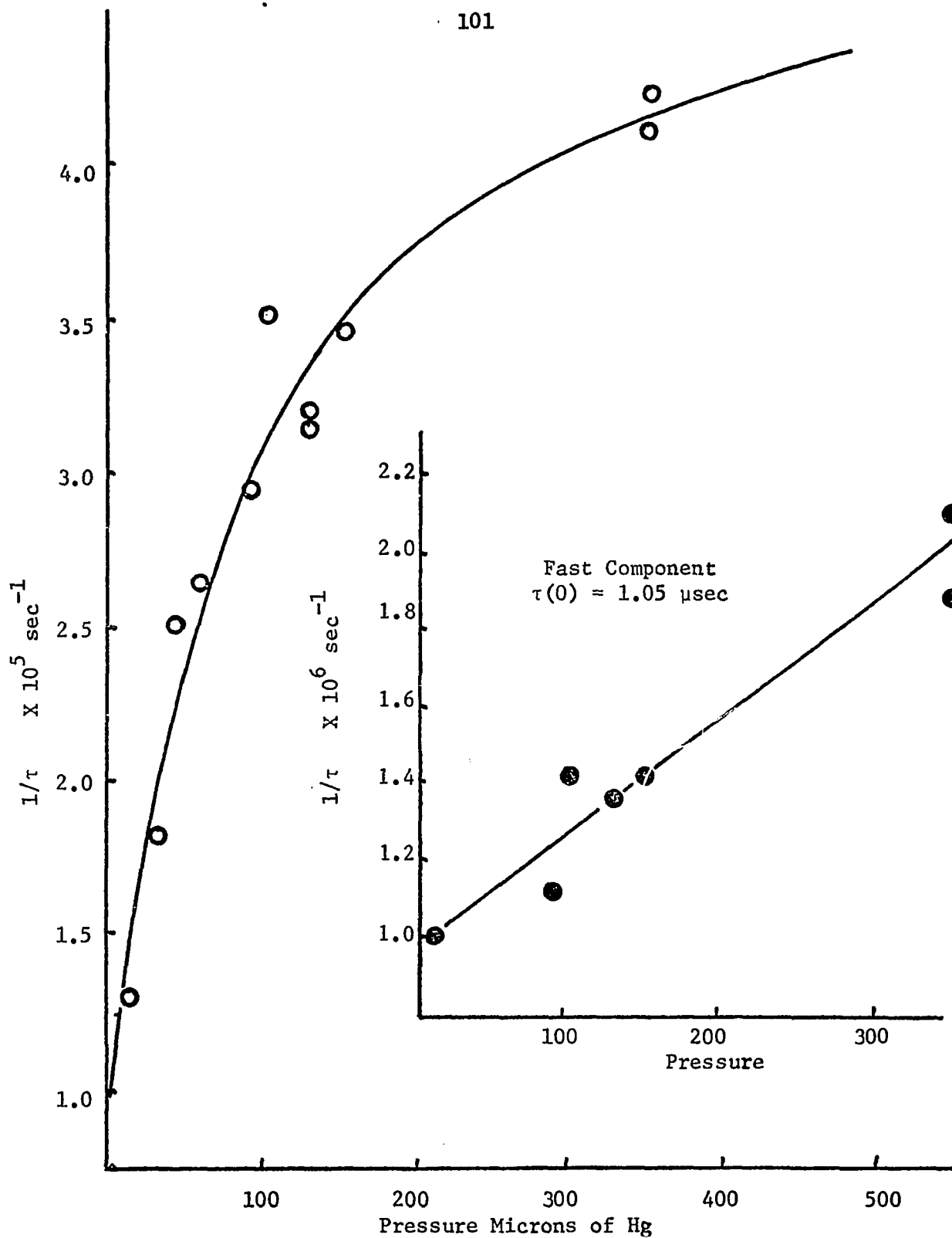
Fig. 49:   Inverse Lifetime VS Pressure for $\tilde{A}\ ^{1}B_{1}$ SO_{2}

Levels a and b are nearly the same energy above the ground state and allow a collisional resonance, i.e.,

$$\frac{dN_a}{dt} = -\alpha_a N_a + \alpha_{ba} N_b + P_a \qquad \text{45a}$$

$$\frac{dN_b}{dt} = -\alpha_b N_b + \alpha_{ab} N_a + P_b \qquad \text{45b}$$

where P_a and P_b are production rates important only during the discharge on-time, and where

$$\alpha_a = A_a + \sigma_a \bar{v}N + \sigma_{ab}\bar{v}N, \qquad \text{46a}$$

$$\alpha_b = A_b + \sigma_b \bar{v}N + \sigma_{ba}\bar{v}N, \qquad \text{46b}$$

$$\alpha_{ab} = \sigma_{ab}\bar{v}N. \qquad \text{46c}$$

The basic solution to these equations is a double exponential (where after cut-off we have $P_a = P_b = 0$), i.e.,

$$N_a = C_1 e^{-\lambda_1 t} + C_2 e^{-\lambda_2 t} \qquad \text{47}$$

and

$$N_b = -\frac{\alpha^1 + \alpha_b}{\alpha_{ba}} C_1 e^{-\lambda_1 t} + \frac{\alpha^1 - \alpha_b}{\alpha_{ba}} C_2 e^{-\lambda_2 t} \qquad \text{48}$$

where

$$\alpha^1 = (\alpha_b^2 - 2\alpha_b \alpha_a + \alpha_a^2 + 4\alpha_{ab}\alpha_{ba})^{\frac{1}{2}}$$

As we are interested in the population of N_a only (N_b will decay at a different frequency) and we expect $\lambda_1 \gg \lambda_2$ such that λ_1 will be an unobservably rapid buildup in the amplitude of the state of interest, we may consider the exponential form of λ_2;

$$\lambda_2 = \frac{1}{2}\{A_a + A_b + (\sigma_a + \sigma_b + \sigma_{ab}\sigma_{ba})\bar{v}N\}$$

$$-\frac{1}{2}\{|A_a - A_b + (\sigma_a - \sigma_b + \sigma_{ab} - \sigma_{ba})\bar{v}N|^2 + 4\sigma_{ab}\sigma_{ba}\bar{v}^2 N^2\}^{\frac{1}{2}} \qquad \text{49}$$

as being responsible for the observed curve in Fig. 49. The solid

line in Fig. 51 represents the analytic fit of λ_2 to the observed

data. The parameters used in the fit were:

$$A_a = 5.98 \times 10^5 \text{ sec}^{-1}$$

$$A_b = 0.8 \times 10^5 \text{ sec}^{-1}$$

$$\sigma_a = \sigma_b = 9 \times 10^{-16} \text{ cm}^2$$

$$\sigma_{ab} = 7.5 \times 10^{-15} \text{ cm}^2; \quad \sigma_{ba} = 7.0 \times 10^{-15} \text{ cm}^2$$

$$v = 3.18 \times 10^4 \text{ cm/sec} \quad (T = 300^\circ \text{ K})$$

$$N = 8.05 \times 10^{15} \text{ p (torr)/cc}$$

It is felt that this process is similar to the interelectronic

mixing apparently responsible for the frequency dependency observed

by previous workers working in the absorption region.

This level did exhibit a double exponential decay; however, the

fast component (~ 1 μsec decay) observed is believed[53] to be due to the

underlying recombination continium caused by $SO + O \longrightarrow SO_2 + h\nu$, and

not to be the level in collisional resonance with the $^1B_1$ level since

the zero pressure lifetime for such a collisional state should be

around 1.7 μsec. Fig. 52 shows a schematic representation for such a

double exponential system and illustrates why the mixed state should

be around 1.7 μsec.

The intercept of the dashed lines should be half the sum of the

decay probabilities (high pressure extrapolation of the terms λ_1 and

λ_2, where λ_1 differs from λ_2 only in the sign of the second term).

Table VII lists the wavelengths of the observed levels of the

$\tilde{A}$ $^1B_1$ state of SO_2. The measurements made in this work would then

indicate a zero pressure lifetime of 12.5 ± 2.5 μsec which is in good

$\tau(0) = 12.5 \pm 2.5$ μsec

$\sigma_a = 9 \times 10^{-16}$ cm^2

$\sigma_{ab} = 7.5 \times 10^{-15}$ cm^2
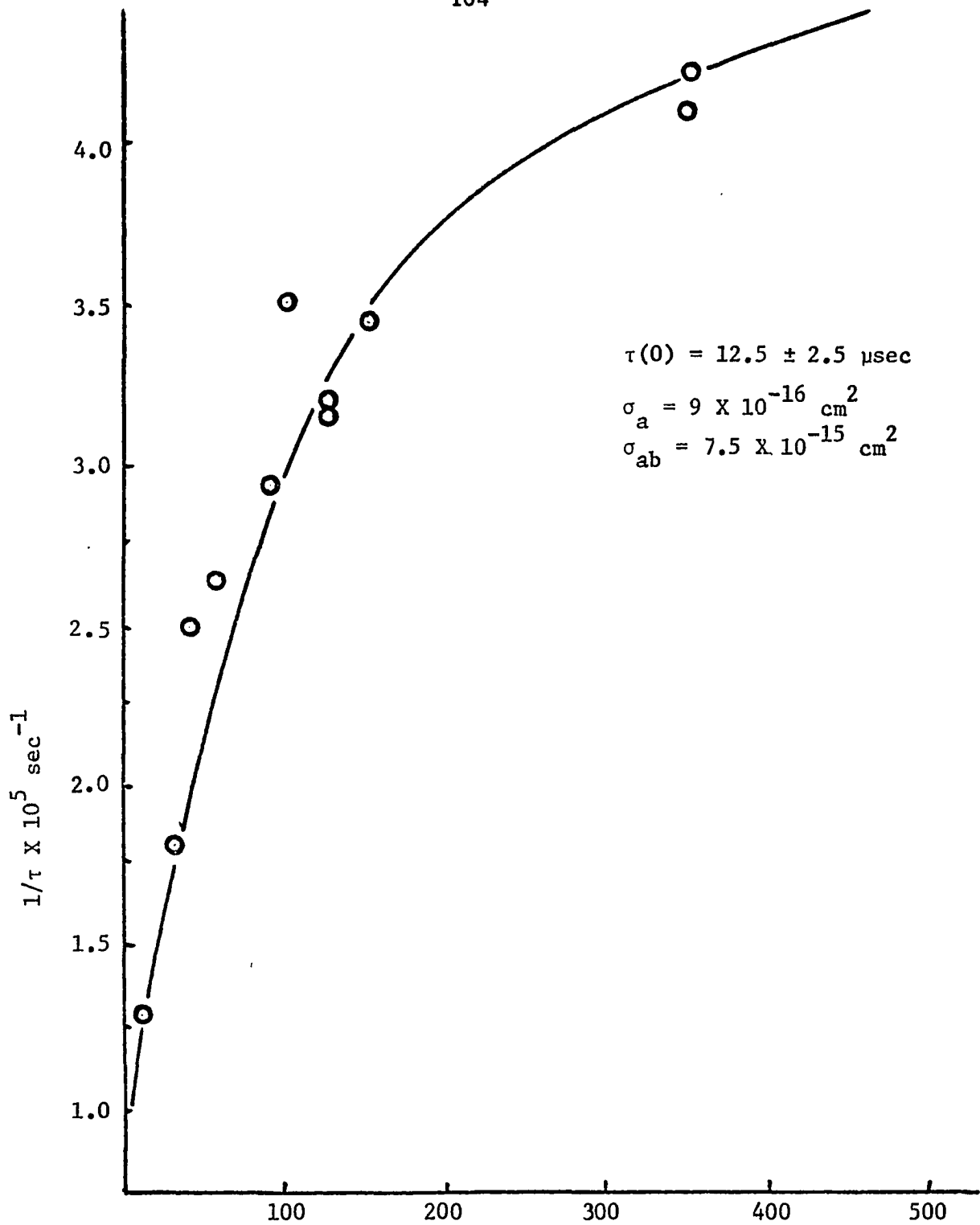
Fig. 51: Analytic Fit to inverse Lifetime $\underline{VS}$ Pressure Curve $\tilde{A}\ ^1B_1$ SO_2

agreement with the lowest level observed by Mettee[48] and with the

faster value (14 µsec) listed by Sidebottom. Recall that Sidebottom

calculated a value for the lifetime of 18 µsec for a vibrationally

equilibriated system. It would perhaps be safe to assume that the

level measured by Mettee at 2650 $\overset{o}{A}$ was also in vibrational equilib-

rium, and by the nature of the excitation used in these experiments,

our levels should also be in vibrational equilibrium.

Table VII: A $^1B_1$ levels of SO_2

WAVELENGTH ($\overset{o}{A}$)	PRESSURE	LIFETIME (usec)
2593		
2561		
2493	15 -400 u Hg	12.5±2.5
2415	flowing	
2383		
2263		
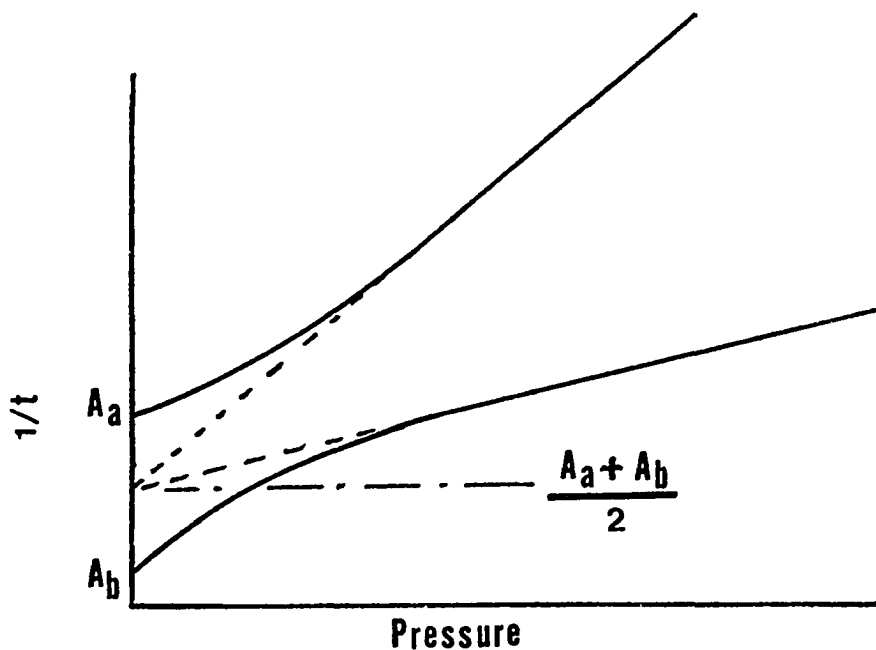
Fig. 52: Decay of collisionally resonance states.

$$\tilde{C} \text{ and } \tilde{D} \; ^{1,3}B_2$$

The $\tilde{C}$ and $\tilde{D}$ states of SO_2 ($^{1,3}B_2$) proved to be a straight forward measurement with results in good agreement with those of Hui and Price[50]. A fast single exponential was observed with a linear pressure dependence indicating a total collisional depopulation cross section of $\sigma_t = 2.72 \times 10^{-15}$ cm^2. Fig. 53 is a reciprocal lifetime vs pressure curve for the $\tilde{C}$ state which indicates a zero pressure lifetime of 60.6 ± 1.8 nsec. This is a count rate corrected curve. This value compares well to that extrapolated for Hui and Price of 55 ± 8 nsec. This level did not exhibit any frequency dependence similar to that seen for the $\tilde{A}$ state.

OII LINES

The oxygen lines observed in this work have been studied elsewhere and are mentioned here only because of the quadratic pressure dependence they seem to possess. Three ionized oxygen lines have been observed, the $3p \; ^2D^o_{3/2} - 3d^1 \; ^2P_{\frac{1}{2}}$ (2365.15 Å) the $3p \; ^2D^o_{3/2} - 3d^1 \; ^2P_{3/2}$ (2365.03 Å) and the $3p \, ^2P^o_{3/2} - 5s \; ^2P_{\frac{1}{2}}$ (2263 Å) with lifetimes ranging from 5.3 µsec at 600 µ Hg to 1.18 msec at 30 µ Hg. This data is presented in Fig. 54. Note that the data is quadratic in pressure. This would tend to indicate a three body collision, the molecule SO_2 and two slow electrons with excited ionized atomic oxygen as one of the products. We then observe the decay of the OII atom not at its characteristic decay rate, but at the rate of production of the ions.
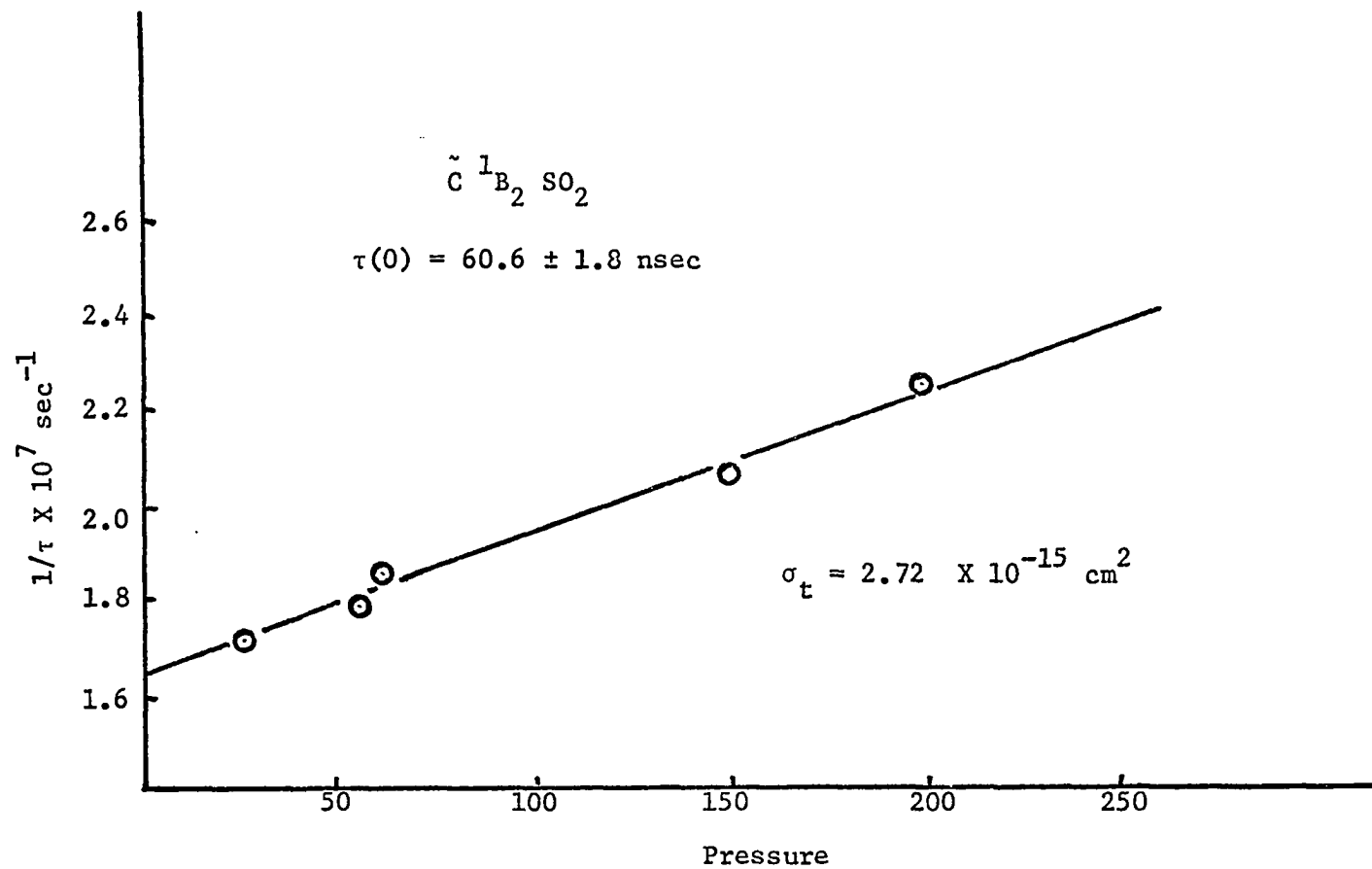
Fig. 53:   Inverse Lifetime <u>VS</u> Pressure Curve for $\tilde{C}\ ^1B_2$ of SO_2
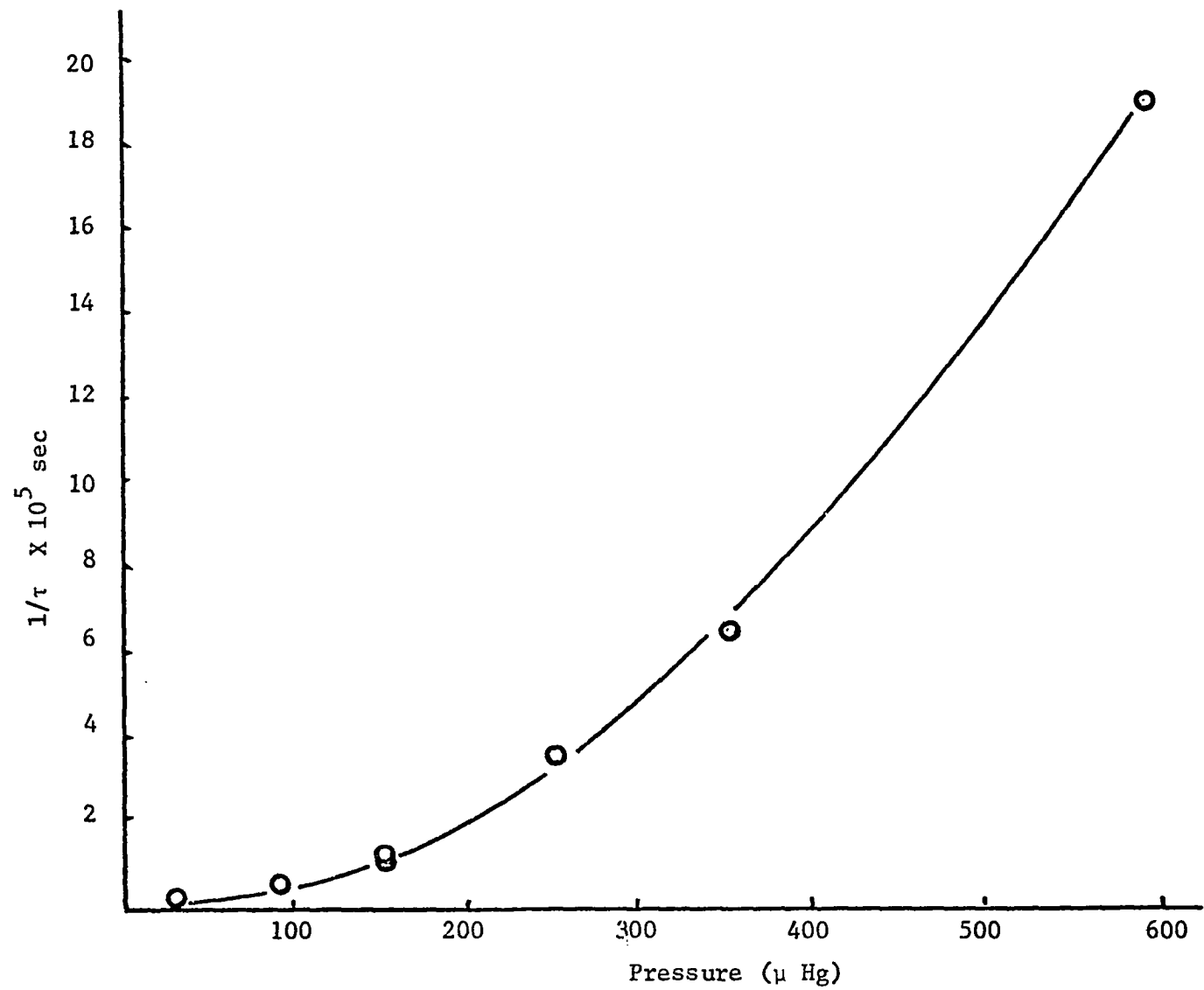
Fig. 54. Quadratic Pressure Dependence Of Recombination OII (2365 and 2265 Å)

CHAPTER VII

CONCLUSIONS

It is the opinion of the author that with a little care and patience, the cold cathode invertron can be a very useful tool in examining the lifetimes and related parameters of polyatomic molecules. It has been shown to be accurate in reproducing the known lifetimes of He, OI and N_2 which were initially determined on entirely different equipment, some determinations even being made on equipment using entirely different concepts of physics.

The observed lifetimes of SO_2 are well within the experimental errors reported by some (i.e., the $\tilde{C}$ and $\tilde{D}$ $^{1,3}B_2$) and are consistent with the reported values of thers ($\tilde{A}$ $^1B_1$), while improving the precision of both considerably ($\pm$ 3% as apposed to their $\pm$ 15%). By combining the results obtained through the absorption spectra and that obtained in emission, it is felt that a better understanding of the molecule has been achieved. Also, data has been collected which perhaps in the future will help determine the extent and the type of vibrational and interelectronic level mixing.

Future work is still required in the visible region of SO_2 and will be completed after modification of the apparatus to allow millisecond investigations. At present the lifetime of the ã $^3B_1$ excited level of SO_2 is too long for accurate measurement on the existing apparatus. Finally a thorough investigation of the visible and perhaps the infrared regions will reveal the state which appears to

be close coupled with the $\tilde{A}\ ^1B_1$ level (assuming that it is not the excited state $\tilde{a}\ ^3B_1$).

This equipment should now be useful in measuring lifetimes for other easilly dissociated polyatomic molecules.

REFERENCES

1. G.E. Copeland, Ph. D. Dissertation, University of Oklahoma (1970).

2. T.M. Holzberlein, Ph.D. Dissertation, University of Oklahoma (1963).

3. A.W. Johnson, Ph. D. Dissertation, University of Oklahoma (1968).

4. A.R. Schaefer, Ph. D. Dissertation, University of Oklahoma (1970).

5. R.T. Thompson, Ph. D. Dissertation, University of Oklahoma (1972).

6. R. Anderson, private communication.

7. L. Morton (Editor),Advances in Electronics and Electron Physics (New York: Acedemic Press, Inc.,1970),p.115.

8. G. Herzberg, Atomic Spectra and Atomic Structure,(New York: Dover Publications, Inc.,1945).

9. G. Herzberg, Spectra of Diatomic Molecules, (New York: Van Nostrand Reinhold Company, 1950).

10. G. Herzberg, Infrared and Raman Spectra, (New York: Van Nostrand Reinhold Co.,1945).

11. G. Herzberg,Electronic Spectra and Electronic Structure of Polyatomic Molecules,(New York: D. Van Nostrand co., 1966) .

12. G. Herzberg, Spectra and Structure of Free Radicals; an Introduction to Molecular Spectroscopy, (Ithaca: Cornell Univ. Press.,1971).

13. R.G. Fowler, "Radiation From Low Pressure Discharges",Handbuch der Physik, Gas Discharges II, XXII (1956).

14. H. Brian Dunford, Elements of Diatomic Molecular Spectra,(Reading, Mass.:Addison-Wesley Publishing Co., 1968).

15. E.U. Condon and G.H. Shortly, Theory of Atomic Spectra,(Cambridge: Cambridge University Press, 1963).

16. H.G. Kuhn, Atomic Spectra, (New York: Academic Press, 1969).

17. P.B. Coats, J. Phys. D. 6, 1959 (1973); 5, 915 (1972).

18. P.B. Coats, J. Phys. E. 4, 201 (1971).

19. G.A. Morton, H.M. Smith and R. Wasserman, Trans IEEE Nucl. Sci. NS-14 (1), 443 (1967).

REFERENCES
(cont'd)

20. W.C. Paske, R.S.I., <u>45</u>, No.8, 1001 (1974).

21. G.E. Copeland, J. Chem. Phys. <u>54</u>, 3482 (1971).

22. J.D. Cobine, <u>Gaseous Conductors</u>, (New York: Dover Publications, Inc., 1958) p. 216.

23. J.D. Cobine, Ibid. p.96.

24. A. von Engel, <u>Ionized Gases</u>, (Oxford University Press, 1965) p.163.

25. G. Valle, Nuovo Cemento , <u>7</u>, 174 (1950); <u>9</u>, 145 (1952).

26. J.M. Somerville, Proc. Phys. Soc. B. <u>65</u>, 620 (1952).

27. F, Llewellyn-Johns, <u>Ionization and Breakdown in Gases</u>,(New York: John Wiley and Sons, Inc., 1957).

28. D.W. Marquardt, J. Soc. Indust. Appl. Math. <u>11</u>, 2 (1963).

29. H. Margenan and G.M. Murphy, <u>The Mathematics of Physics and Chemistry</u>, 2nd Ed. (Princeton, N.J.: Van Nostrand Co., Inc., 1956) pp. 504-19.

30. W.E. Deming, <u>Statistical Adjustment of Data</u>,(New York: Dover Publications Inc., 1964).

31. P.R. Bevington, <u>Data Reduction and Error Analysis for the Physical Sciences</u>, (New York: McGraw-Hill Book Co., 1969).

32. Chr. Holzapfel, R.S.I. <u>45</u>, 894 (1974).

33. R.G. Bennett and F.W. Dalby, J. Chem.Phys. <u>31</u>, 434 (1959).

34. R.G. Fowler and T.M. Holzberlein, J. Chem. Phys. <u>43</u>, 1124 (1966).

35. M. Jeounehomme , J. Chem. Phys. <u>44</u>, 2672 (1966).

36. J.E. Hesser and K. Dressler, J. Chem. Phys. <u>45</u>, 3149 (1966).

37. L.L. Nichols and W.E. Wilson, Applied Optics <u>7</u>, 167 (1968).

38. D.I. Sebacher, J. Chem. Phys. <u>42</u>, 1368 (1965).

39. Morton Hamermesh, <u>Group Theory and its Application to Physical Problems</u>, (Reading, Mass.: Addison-Wesley Pub. Co., 1962)

40. G. Herzberg, Op. Cit. Chapter IV.

41. G, Herzberg, Ibid. p.151.

42. N.Metropolis, Phys. Rev. <u>60</u>, 295 (1941).

43. G. Herzberg, Ibid. p.144.

44. P.W.B. Pearse and A.G. Gaydon, <u>Identification of Molecular Spectra</u>, (New York: John Wiley and Sons, Inc.,1963) p. 267.

REFERENCES

(cont'd)

45. R.B. Caton and A.B.F. Duncan, J. Am. Chem. Soc. 90, 1945 (1967)

46. B.P. Levitt and D.B. Sheen, Trans Faraday Soc., 61, 2404 (1965); and 63, 540, (1967).

47. K.F. Greenough and A.B.D. Duncan, J. Am. Chem. Soc., 83,555 (1961).

48. H.D. Mettee, J.Chem. Phys. 49, 1784 (1963).

49. H.W. Sidebottom et. al. Chem. Phys. Letts. 13, 337, (1972).

50. M.H. Hui and S.A. Rice, Phys. Letts. (Netherlands) 17, No. 4, 474, (1972).

51. A.E. Douglas, J.Chem. Phys. 45, 1007 (1966).

52. L.Morton, Ibid. p.144 ff.

53. G. Herzberg, Electronic Spectra and Electronic Structure of Polyatomic Molecules, (New York: D. Van Nostrand Co. 1966) p. 455.

54. A.R. Strigancv and N.S. Sventitskii, Tables of Spectral Lines of Neutral and Ionized Atoms, (New York: IFI/Plenum Data Corp., 1968).

LPLOT   20:08   THU.   FEB 05, 1974

```
      DIMENSION Y(512),A(5),YP(512)
      DIMENSION CHAN(10),TIM(10)
      REAL INCR,L1,L2
      DATA A/"X","+",".","  ","*"/
C DATA INPUT
      CALL INPAK(N,NTC,CHAN,TIM,TIME,Y)
      PRINT1234,
 1234 FORMAT(1H ,"ENTER PLOT INCREMENT")
    1 INPUT ,K
      IF (K)2,2,3
    2 PRINT999
      CALL EXIT
C HEADING
    3 CONTINUE
C Y VALUES TO BE PLOTTED
 9201 FORMAT(1H ,2A6,3X,"DATE-",A2,A3,A4,3X,"RUN #",I2)
C SEARCH FOR MAXIMUM AND MINIMUM VALUES
      B=Y(1)
      S=10000.
      DO 20 I=2,N
      IF (Y(I)-B)15,15,11
   11 B=Y(I)
      GO TO 20
   15 IF (Y(I)-S)16,20,20
   16 IF(Y(I).EQ.0.0)GO TO20
      S=Y(I)
   20 CONTINUE
C CALCULATION OF SCALING FACTOR AND RANGE
      PRINT 910,S,B
      INPUT,S,B
      PRINT 201,S,B
      B=ALOG(B)
      S =ALOG(S)
      SC=(B-S)/63.0
C SET UP BORDER AND PRINT SCALE
      PRINT903
      PRINT 902,(A(5),I=1,65)
C PLOTTING OF DATA
      DO 30 I=1,N,K
      I1=I-1
      NY=1
      IF(Y(I)-S.LE.0.0)GO TO 30
      NY=(ALOG(Y(I))-S)/SC+1
      DO 21 J=1,NY
   21 YP(J)=A(4)
```

```
        YP(NY)=A(2)
     30 PRINT 293,I1,(YP(J),J=1,NY)
C FINAL BORDER
        PRINT 902,(A(5),I=1,65)
        PRINT 202,SC
        GO TO 1
    902 FORMAT(1H ,3X,65A1)
    201 FORMAT(1H1,F8.0,52X,F8.0)
    202 FORMAT(1H0,"SCALE=",F8.5,"LN(COUNTS)/PRINT CHANNEL")
    293 FORMAT(I4,"*",64A1)
    903 FORMAT(1H ,3X,"*",63X,"*")
    910 FORMAT("ENTER SCALE LIMITS,DEFAULT VALUES ARE ",I6,I8)
    999 FORMAT(1H0,"END OF JOB")
        END
```

```
        SUBROUTINE INFAK(N1,NTC,CHAN,TIM,TIME,Y)
        DIMENSION CHAN(10),TIM(10),Y(256)
       1,DATE(3)
        INTEGER CHAN
        REAL L1,L2
        CALL DATIME(TIMED,TIMEB,DATE)
        CALL OPENF(1,"INPUT")
        READ(1,9101)L1,L2,DA,XMO,YR,RN,SA,VL,P
        READ(1,9102)N1,NTC,(CHAN(I),I=1,NTC)
        READ(1,9103)(TIM(I),I=1,NTC)
   9101 FORMAT(2A6,A2,A3,A4,I2,A6,F5.0,F5.1)
   9102 FORMAT(I3,I1,8I3)
   9103 FORMAT(8F7.2)
        N=N1
        READ(1,7000)TIME,(Y(I),I=1,N)
   4000 FORMAT(15F4.0)
   5000 FORMAT(14F5.0)
   6000 FORMAT(10F7.0)
   7000 FORMAT(I6,9I7)
        CALL CLOSEF(1,"INPUT")
        PRINT9201,L1,L2,DA,XMO,YR,RN
        PRINT9202,SA,VL,P,TIMED,DATE
   9201 FORMAT(1H0,//////,2A6,3X,"DATE-",A2,A3,A4,3X,"RUN #",I2)
   9202 FORMAT(1H ,"SAMPLE-",A6,3X,"WAVELENGTH=",F5.0," A",
       13X,"PRESSURE=",F5.1," MICRONS"//" CALCULATED AT",
       21X,A6,1X,3A6/)
        RETURN
        END
```

```
      SUBROUTINE RGRES (V,U,A,B,N1,N2,R2,SWTCH)
      DIMENSION U(512),V(512)
      REAL M1,M2
120 FORMAT("ZERO    (STD ERROR OF ESTIMATE EXCEEDS STD DEV
   1OF Y ")
      N=N2-N1+1
100 FORMAT(1X,"SIMPLE LINEAR REGRESSION
   1 EQUATION: LOG(Y-F(X))=A+B*X",//1X,"INDX R*R VALUE     95%
   2CONF LIMITS BEGIN END DIFF")
150 FORMAT (1H1)
200 FORMAT(F9.5,4H   A=,3F12.8,I4,I6,I6/,9X,4
   1H  B=,3F12.8)
      IF(SWTCH.EQ.2.)GO TO 11
      IF(A) 8,10,8
  8 IF (ICNT-25) 11,11,9
  9 PRINT 150
 10 ICNT=1
      IF(SWTCH.EQ.1)GO TO 101
102 PRINT110,
110 FORMAT(1H ,"ITERATIONS NOT DISPLAYED")
      GO TO 11
101 PRINT 100,
 11 CONTINUE
      S1=0
      S2=0
      S3=0
      S4=0
      S5=0
      DO 20 I=N1,N2
      S1=S1+U(I)
      S2=S2+U(I)*U(I)
      S3=S3+V(I)
      S4=S4+V(I)*V(I)
 20 S5=S5+U(I)*V(I)
      M1=S1/N
      M2=S3/N
      D1=S2/N-M1*M1
      D2=S4/N-M2*M2
      D3=S5/N-M1*M2
      C1=N*D1
      R8=0
      B=D3/D1
      A=M2-B*M1
      D4=D2-B*D3
      D44=D4
      IF(D4-D2) 2070,2040,2040
```

```
2040 R8=1
     R2=0
     GO TO 2080
2070 R2=1-(D4/D2)
2080 CONTINUE
     IF(R8) 2110,2130,2110
2110 PRINT 120
     GO TO 2160
2130 D2M4=D2-D4
     D4SCR=SQRT(D4)
2160 D4=N*D4/(N-2)
     T=1.95996+2.37226/(N-2)+2.82250/(N-2)*(N-2)
     D5=SQRT(D4/C1)
     D6=SQRT(D4/N)
     B1=B-T*D5
     B2=B+T*D5
     A1=A-T*D6
     A2=A+T*D6
     IF(SWTCH.NE.1)GO TO 56
     PRINT 200,R2,A,A1,A2,N1,N2,N,B,B1,B2
  56 CONTINUE
     IF(SW TCH.NE.2.0)GO TO 57
     R2=D5
     SW TCH=D6
  57 CONTINUE
     RETURN
     END
```

```
         SUBROUTINE DSPAK
C PLOT ROUTINE
         COMMON N, IK, IW, M, IB, ITEST, IDUM, NDUM, IPR, IFG, IM, YT, TEST,
        1WVAR, SSQ, IDF, DET, ISW, IPLT, ISC, Y(300), X(1, 300), W(300), IX(10),
        2PG(10), P(10), SP(10), YC(300), DY(300), BM(10, 11), ALAB(10), INTT,
        3PART(10), NSETS
         EQUIVALENCE (IDUM, IN1), (NDUM, NN2)
         DIMENSION ICH(10), APLT(65)
         INTEGER APLT
         DATA IBCH, ISCH, ICH/" ", "*", "A", "B", "C", "D", "E", "T", "U", "V"
        1, "W", "X"/
         DATA IOCH/"0"/
  500 FORMAT (1X, I3, 65A1)
  901 FORMAT( 1H0)
  905 FORMAT (2X, F7.3, 53X, F7.0)
         K=IK-1
         KK=IK/2-1
         YQ=Y(1)
         DO 5 I=1, N
    5 YQ=AMAX1(YQ, Y(I))
         SCALE=63./ALOG(1000.)
         CHKZ=EXP(1./SCALE)*YQ/1000.
         J=   -IPLT
         PRINT 901
         YQLN1=(YQ/1000.)
         PRINT 905, YQLN1, YQ
  170 IXPLT=0
         N1=65
  200 DO 210 I=1, 65
  210 APLT(I)=ISCH
         APLT(32)=IOCH
         J=J+1
         GO TO 250
  215 J=J+IPLT
         IF(J-N) 216, 216, 170
  216 CONTINUE
         IXPLT=IN1+J-1
         DO 220 I=2, 64
  220 APLT(I)=IBCH
         DO 240 I=1, KK
         DUM=Y(J)-P(K)
         DO 230 IJ=1, KK
         IF(IJ-1) 225, 230, 225
  225 DUM=DUM-P(2*IJ-1)*EXP(-X(1, J)/P(2*IJ))
  230 CONTINUE
         IF(DUM-CHKZ) 237, 237, 235
  235 NMBR =(ALOG(DUM)-ALOG(YO/1000.))*SCALE+1.
         IF(NMBR-64) 238, 238, 236
  236 NMBR=64
         GO TO 238
```

```
237 NMBR = 2
238 APLT(NMBR) = ICH(I)
    IF (N1.LT.NMBR) N1=NMBR
240 CONTINUE
    NMBR=(DUM-P(K-2)*EXP(-X(1,J)/P(2*KK)))/(Y(J)**.5)*2.+32.
    IF(NMBR-1         )247,247,245
245 CONTINUE
    IF(NMBR-64)248,248,246
246 NMBR=64
    GO TO 248
247 NMBR = 2
248 APLT(NMBR) = ICH(KK+1)
    IF(N1.LT.NMBR)N1=NMBR
250 PRINT 500,IXPLT,(APLT(I),I=1,N1)
    N1=2
    IF (J-N)215,170,251
251 CONTINUE
    RETURN
    END
```

W C PASKE   DATE-JUN 21.73   RUN   1
SAMPLE-N2 2PS   WAVELENGTH=3159.A   PRESSURE=325.0MICRONS

CALCULATED AT 08 00   THU. JUN. 21.1973

ENTER PLCT INCREMENT.LOWER SCALE LIMIT. UPPER SCALE LIMIT.BACKGROUND.
     2   0.   0.   0.

       22.   1447.
       *
       ****
     1*+
     3*+
     5*+
     7*+
     9*+
    11*
    13*
    15*
    17*
    19*
    21*
    23*
    25*
    27*
    29*
    31*
    33*
    35*
    37*
    39*
    41*
    43*
    45*
    47*
    49*
    51*
    53*
    55*
    57*
    59*
    61*
    63*
    65*
    67*
    69*
    71*
    73*
    75*
    77*
    79*
    81*
    83*
    85*
    87*
    89*
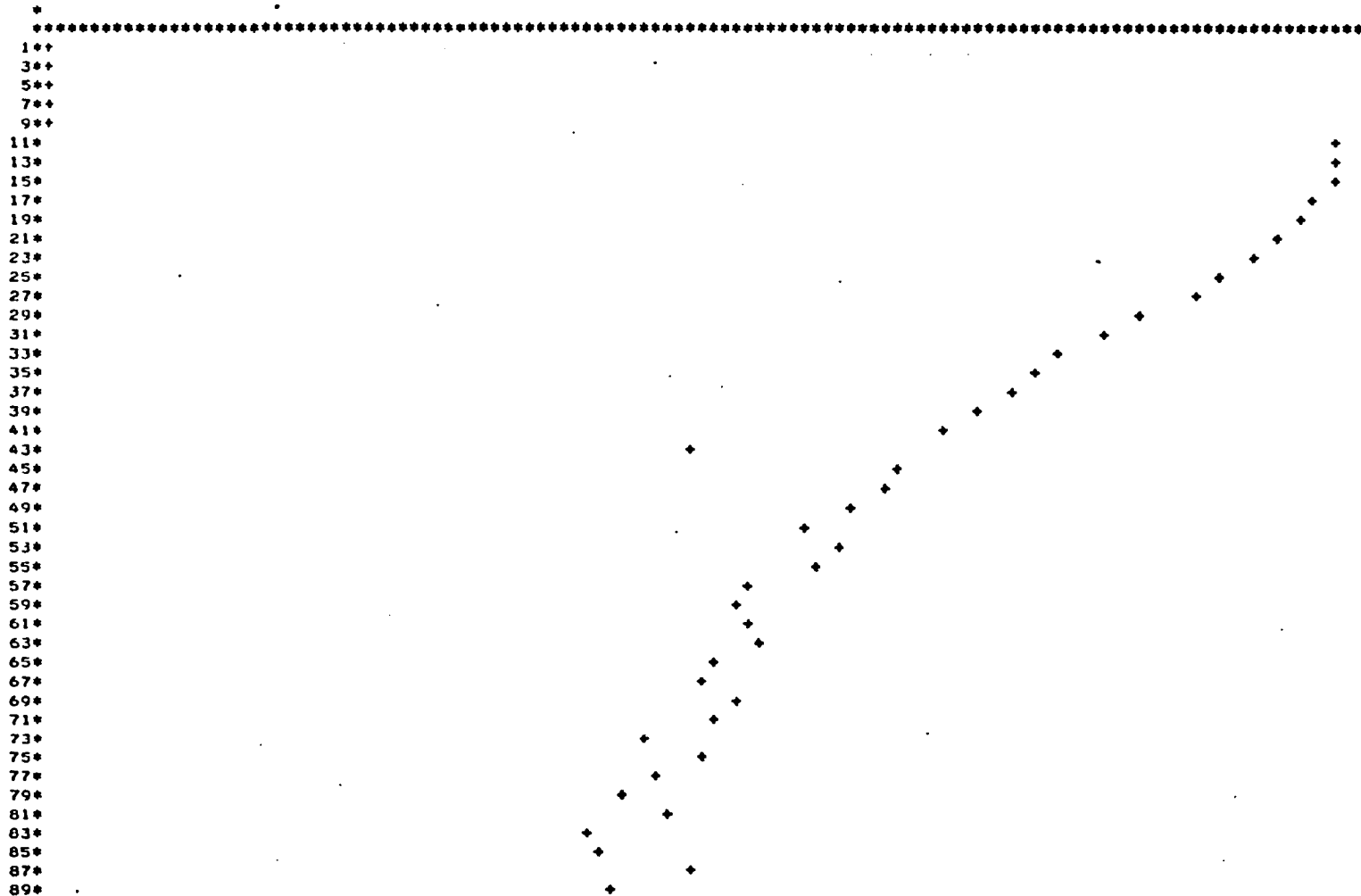
```
//      EXEC  FORTGCLG.PARM.FORT='NAME=LASL'

//FORT.SYSIN   DD  *

C     MAIN PROGRAM FOR NONLINEAR LEAST SQ. EXP. FIT. FROM LASL
      DOUBLE PRECISION YT.WVAR
      DOUBLE PRECISION W.P.SP.YC.DY.PART.BM.DET.ALAB
      COMMON N.IK.IW.M.IB.ITEST.IDUM.NDUM.IPR.IFG.IM.TEST.YT.WVAR.SSQ.
     1IDF.DET.ISW.IPLT.ISC.INTT.Y(300).X(1.300).W(300).IX(10).PG(10).P(
     210).SP(10).YC(300).DY(300).    BM(10.11).ALAB(10).PART(10).NSETS.
     3DUM(1).Z(1)
      EQUIVALENCE (IDUM.IN1).(NDUM.NN2)
      READ(5.930) NRD
  930 FORMAT(2I4)
      READ(NRD.920)(ALAB(I).I=1.4)
      IPLT=0
C     CLEAR DUM. PART
    1 DUM(1)=0.
      DO 20 K=1.10
   20 PART(K)=0.0
C     CALL INPUT ROUTINE
      ALAB(10)=NRD
      READ(NRD.920)
      READ(NRD.920)
      IN1=0
      NN2=5
      CALL ISPAK
C     CALL CALCULATION ROUTINE
```

```
      CALL PSPAK
C     CALL OUTPUT ROUTINE
      CALL RSPAK
C     CALL PLOT ROUTINE
  900 FORMAT(' ENTER PLOT INCR IF PLOT IS DESIRED THEN 0 FOR NEXT CASE.1
     1 TO RERUN WITH NEW PARAMETERS.-1 TO CALL EXIT')
      WRITE(6.900)
      READ(NRD.910)IPLT.JPLT
      WRITE(6.910)IPLT.JPLT
  910 FORMAT(2I3)
  920 FORMAT(4A6)
      IF(IPLT.GT.0)CALL DSPAK
      IPLT=JPLT
      IF(IPLT.LT.0)CALL EXIT
      GO TO 1
      END
      SUBROUTINE ISPAK
C     INPUT ROUTINE
      DOUBLE PRECISION W,P,SP,YC,DY,PART,BM,DET,ALAB
      DOUBLE PRECISION YT,WVAR
      COMMON N,IK,IW,M,IB,ITEST,IDUM,NDUM,IPR,IFG,IM,TEST,YT,WVAR,SSQ,
     1IDF,DET,ISW,IPLT,ISC,INTT,Y(300),X(1,300),W(300),IX(10),PG(10),P(
     210),SP(10),YC(300),DY(300),    BM(10,11),ALAB(10),PART(10),NSETS,
     3DUM(1),Z(1)
      EQUIVALENCE (IDUM,IN1),(NDUM,NN2)
      NRD=ALAB(10)
```

```
      IF(IPLT.EQ.1) GO TO 4

      CALL INPAK(N,IB,IX,P,TIME,Y,ALAB,NRD)

      NSAV=N

      IF(P(1)) 350,355,360

350 CLBRTR=-P(1)

      GO TO 4

355 CLBRTR=1.0

      GO TO 4

360 DET=2.0

      DO 3 I=1,IB

      DY(I)=P(I)

  3 W(I)=IX(I)

      CALL RGRES(DY,W,TEST,CLBRTR,1,IB,AI,DET)

940 FORMAT(' ENTER NUMBER OF PARAMS, FIRST POINT,LAST POINT,WEIGHT POW
     6ER, IPR=0,1,2 OR 3 FOR INCREASED OUTPUT. IM=I HOLD CONSTANT.'/,' A
     6ND ENTER REP. RATE OF PULSING SYSTEM IF PILE UP CORRECTION IS DESI
     6RED')

  4 WRITE(6,940)

      N=NSAV

      READ(NRD,950)IK,IN1,IN2,WEIT,IPR,IM,TDCR

950 FORMAT(3I4,F4.1,2I4,F10.2)

      WRITE(6,950)IK,IN1,IN2,WEIT,IPR,IM,TDCR

      IX(2)=IK

      NSETS=0

      IB=0

      ITEST=0
```

```
      IK=IK+1

      ISW=0

      M=1

      IF(IM.NE.2)IM=1

      IX(1)=IK

      IFG=2

      KK=IK-2

      KI=IK-1

960   FORMAT(' ENTER LIFETIMES(SHORT,LONG),COEFFS(SHORT,LONG),CONSTANT')

      WRITE(6,960)

      READ(NRD,970)(PG(K),K=2,KK,2),(PG(J),J=1,KI,2)

970   FORMAT(1P10E8.1)

971   FORMAT(1X,1P10E10.1)

      WRITE(6,971)(PG(K),K=2,KK,2),(PG(J),J=1,KI,2)

      PG(IK)=0.0

      PG(IK-1)=PG(IK-1)+.5

980   FORMAT('  CALIBRATION IS',F10.5,'  NS/CHAN +OR-',F10.7)

      WRITE(6,980)CLBRTR,AI

      DO 11 I=1,N

      AI=I-1

11    X(1,I)=AI*CLBRTR

C     PHOTON PILE-UP CORRECTION ROUTINE

      IDCR=TDCR

      IF(IDCR.EQ.0)GO TO 80

      YSUM=Y(1)

      SDCR=TDCR
```

```
      TDCR=SDCR*TIME

      DO 81 I=2,NSAV

      YTEMP=Y(I)/(1.0-(YSUM/TDCR))

      YSUM=YSUM+Y(I)

      Y(I)=YTEMP

   81 CONTINUE

      CNRT=(YSUM/TDCR)*100.

      YMAX=Y(1)

      DO 83 J=2,NSAV

      IF(YMAX-Y(J))82,83,83

   82 YMAX=Y(J)

   83 CONTINUE

      PMAX=YMAX/TDCR

      WRITE(6,981)CNRT,PMAX

  981 FORMAT(' COUNTRATE FOR THIS RUN IS ',F5.2,' PER CENT'/,' MAXIMUM P
     6ROBILITY OF A COUNT OCCURRING IN A CHANNEL, IN ONE CYCLE, IS ',F8.
     66)

   80 N=IN2-IN1+1

C     SET UP WEIGHTS

      WRITE(6,950)IN1,NN2

      WRITE(6,971)Y

      IF(WEIT.NE.0)GO TO 6

      DO 40 I=1,N

   40 W(I)=1.0

      GO TO 8

    6 DO 50 I=1,N
```

```
        J=IN1-I+I
  50 W(I)=Y(J)/Y(IN1)
        WRITE(6,950)I,J,IN1
        IF(WEIT.EQ.1.0) GO TO 8
 405 FORMAT (' WEIGHT RANGES FROM 1.0 TO',F7.3,' FOR CHAN ',I3)
    7 DO 60 I=2,N
        IF(W(I).EQ.0.0)GO TO 59
        W(I)=W(I)**WEIT
        GO TO 60
  59 W(I)=0.0
  60 CONTINUE
    8 TEST=1.0E-08
        WRITE(6,405)W(N),IN2
        DO 55 I=1,N
        IN1M1=I+IN1-1
  55 Y(I)=Y(IN1M1)
        RETURN
    1 CALL EXIT
        END
        SUBROUTINE RSPAK
C       OUTPUT ROUTINE
        REAL*8   DSQRT
        DOUBLE PRECISION W,P,SP,YC,DY,PART,BM,DET,ALAB
        DOUBLE PRECISION YT,WVAR
        COMMON N,IK,IW,M,IB,ITEST,IDUM,NDUM,IPR,IFG,IM,TEST,YT,WVAR,SSQ,
       1IDF,DET,ISW,IPLT,ISC,INTT,Y(300),X(1,300),W(300),IX(10),PG(10),P(
```

```
    210),SP(10),YC(300),DY(300),        BM(110),ALAB(10),PART(10),NSETS,
  . 3DUM(1),Z(1)
      DIMENSION TS(40)
C     PAGE 1 OF THE STANDARD OUTPUT
      I=-1
      CALL YPS(I)
      WRITE (6,200)WVAR,TEST,SSQ
200 FORMAT(/26H THE WEIGHTED VARIANCE IS 1PE14.7,/
   1,' THE UNWEIGHTED SIGMA IS ',1PE14.7
   2,' AND THE UNWEIGHTED SUM OF SQUARES OF THE DEVS IS ',1PE14.7)
300 FORMAT('       GUESS OF   FINAL VAL OF    S.D. OF          EXACT LST S
   1QRS EQNS',/,'   K  K-TH PARAM  K-TH PARAM  K-TH PARAM      FITTED FC
   2TN   INPUT DATA')
      WRITE(6,300)
      KFREE=IK-IM
      DO 40 K=1,KFREE
   2 A=0.0
      B=0.0
      DO 30 I=1,N
      A=A+W(I)*YC(I)*PART(K)
  30 B=B+W(I)*Y(I)*PART(K)
      WRITE(6,500)K,PG(K),P(K),SP(K),A,B
500 FORMAT(I3,1X,1P3E12.4,3X,1P2E12.4)
  40 CONTINUE
C     CAL AND RITE  CORR MATRIX
      IF(IPR.LT.1) GO TO 70
```

```
      WRITE(6,700)
700 FORMAT(//////' MATRIX OF CORRELATIONS BETWEEN FREE PARAMS')
      DO 60 K1=1,KFREE
      DO 50 K2=1,KFREE
      IJ=K2*KFREE+K1
      JJ=K1*KFREE+K1
      KJ=K2*KFREE+K2
50 TS(K2)=BM(IJ)/DSQRT(BM(JJ)*BM(KJ))
851 FORMAT(I3,10F8.3 )
56 WRITE (6,851)K1,(TS(K),K=1,KFREE)
60 CONTINUE
70 RETURN
      END
      SUBROUTINE LAMBDA (NM,PC,LBDA,DP,IT,AN)
      REAL LBDA,NU
      DOUBLE PRECISION YT,WVAR,PHI
      DOUBLE PRECISION W,P,SP,YC,DY,PART,BM,DET,ALAB,PC,DP,AN,AM
      DIMENSION PC(10),AM(110),DP(10)
      DIMENSION AN(100)
      COMMON N,IK,IW,M,IB,ITEST,IDUM,NDUM,IPR,IFG,IM,TEST,YT,WVAR,SSQ,
     1IDF,DET,ISW,IPLT,ISC,INTT,Y(300),X(1,300),W(300),IX(10),PG(10),P(
     210),SP(10),YC(300),DY(300),      BM(110),ALAB(10),PART(10),NSETS,
     3DUM(1)
      KFREE=IK-IM
      NU=10
      NI=KFREE*(KFREE+1)
```

```
      PHI=0.0

      H=1.0

      GO TO (10,100),NM

   10 DO 20 K=1,KFREE

      IJ=(K-1)*KFREE+K

      BM(K)=BM(K)/DSQRT(AN(IJ))

      DO 20 KK=1,KFREE

      KJ=(KK-1)*KFREE+KK

      I=K*KFREE+KK

      BM(I)=BM(I)/DSQRT(AN(IJ)*AN(KJ))

   20 AM(I)=BM(I)

      IF(IPR.GT.2)WRITE(6,940)(BM(J),J=1,KFREE)

      IF(IPR.GT.2)WRITE(6,950)(AN(J),J=1,IJ,IK)

      GO TO 500

  100 D=0.

      GD=0.

      G=0.

      DO 120 J=1,KFREE

      G=BM(J)**2+G

      D=SP(J)**2+D

  120 GD=BM(J)*SP(J)+GD

      GD=GD/SQRT(D*G)

      IF(IPR.NE.0) WRITE(6,900)GD

  160 PHI=0.0

      DO 200 J=1,N

      VT=PC(IK-1)
```

```
            IN=IK-3

            DO 150 K=1,IN,2

            JJ=K

150  YT=YT+PC(K)*DEXP(-X(1,J)/PC(K+1))

200  PHI=W(J)*(Y(J)-YT)**2+PHI

            IF(PHI.LE.WVAR) GO TO 600

            IF(GD.LT..707.AND.LBDA.GT.0)GO TO 400

            H=H/2.0

            K=0

            IF(IPR.NE.0) WRITE(6,920)H,PHI

            DO 220 I=1,KFREE

            DP(I)=H*DP(I)

            PC(I)=P(I)+DP(I)

            CHK=DABS((PC(I)-P(I))/P(I))

            IF(CHK.LT.TEST)K=K+1

220  CONTINUE

            IF(KFREE-K)600,600,160

400  LBDA=LBDA*NU

            IF(IPR.NE.0) WRITE(6,910)LBDA,IT,PHI

            IJ=KFREE+1

            DO 300 K=IJ,NI

300  BM(K)=AM(K)

            GO TO 520

500  IF(LBDA.LE..00001) GO TO 520

            LBDA=LBDA/NU

520  IJ=KFREE+1
```

```
      DO 530 K=IJ,NI,IJ
  530 BM(K)=AM(K)+LBDA
      RETURN
  600 NM=1
      RETURN
  900 FORMAT(' COS(GAMMA)= ',1PE11.4)
  910 FORMAT(' LAMBDA= ',1PE7.1,'   ITER NO. ',I2,' PHI= ',1PE15.9)
  920 FORMAT(' H= ',1PE8.2,' PHI= ',1PE15.9)
  930 FORMAT(2I4,1PE10.3)
  940 FORMAT(' BM(J)=   ',1P7E17.8)
  950 FORMAT(' AN(J,J)= ',1P7E17.8)
      END
      SUBROUTINE YPS(I)
C     FUNCTION AND PARTIAL DERIVATIVE ROUTINE
      DOUBLE PRECISION W,P,SP,YC,DY,PART,BM,DET,ALAB
      DOUBLE PRECISION YT,WVAR
      COMMON N,IK,IW,M,IB,ITEST,IDUM,NDUM,IPR,IFG,IM,TEST,YT,WVAR,SSQ,
     1IDF,DET,ISW,IPLT,ISC,INTT,Y(300),X(1,300),W(300),IX(10),PG(10),P(
     210),SP(10),YC(300),DY(300),     BM(10,11),ALAB(10),PART(10),NSETS,
     3DUM(1),Z(1)
  900 FORMAT(' SUM OF EXPONENTIALS. Y(I)=P(1)*EXP(-X(I)/P(2))+...+P(',I1
     1,')')
      IF (I)1,3,3
    1 K=IK-1
      WRITE(6,900)K
      GO TO 4
```

```
      3 YT=0.0

        KI=IK-2

        DO 10 K=2,KI,2

        PART(K-1)=DEXP(-Z(1)/P(K))

        PART(K)=P(K-1)*PART(K-1)

        YT=YT+PART(K)

     10 PART(K)=PART(K)*Z(1)/P(K)**2

        YT=YT+P(IK-1)

        PART(IK-1)=1.0

      4 RETURN

        END

        SUBROUTINE PSPAK

C       CALCULATION ROUTINE

        DIMENSION AM(100),DP(10),PC(10),AN(10)

        DIMENSION MA(10),MB(10),IIW(200),JIW(100)

        EQUIVALENCE(IIW(101),JIW(1))

        REAL*8   DSQRT

        DOUBLE PRECISION YT,WVAR

        DOUBLE PRECISION W,P,SP,YC,DY,PART,BM,DET,ALAB,AM,DP,PC,AN

        COMMON N,IK,IW,M,IB,ITEST,IDUM,NDUM,IPR,IFG,IM,TEST,YT,WVAR,SSQ,

       1IDF,DET,ISW,IPLT,ISC,INTT,Y(300),X(1,300),W(300),IX(10),PG(10),P(

       210),SP(10),YC(300),DY(300),      BM(110),ALAB(10),PART(10),NSETS,

       3DUM(1),Z(1)

        REAL LBDA

        EQUIVALENCE(ITEST,LASTIT)

C       INITIAL OUTPUT OPTION
```

```
      IF(IPR.EQ.0) GO TO 1

      WRITE(6,400) TEST

  400 FORMAT(/8H TEST = ,1PE15.7/)
C     INITIALIZATION FOR MAIN ITERATION LOOP
    1 KFREE=IK-IM    .

      KP=KFREE+1

      IDF=N-KFREE

      DF=IDF

      IT=0

      LADA=.0001

      XSVAR=1.0E+15

      IREJ=0.

      DO 10 K=1,IK

      DP(K)=0.0

      SP(K)=0.0

      PC(K)=PG(K)

   10 P(K)=PG(K)

      LASTIT=0

      M25C=0

      IF(KFREE.EQ.0)GO TO 3
C     MAIN ITERATION LOOP
    2 IT=IT+1

      H=1

      DO 30 K=1,KFREE

      DO 20 KK=1,KFREE

      JJ=K+(KK-1)*KFREE
```

```
      AM(JJ)=0.
   20 BM(JJ)=0.
      JJ=K+(KP-1)*KFREE
      BM(JJ)=0.
      JJ=K+K*KFREE
   30 BM(JJ)=0.
    3 VAR=0.0
      SSQ=0.0
C     LOOP TO SET UP NORMAL EQUATIONS
      DO 90 I=1,N
C     CALL YP ROUTINE. CALCULATE SUM OF SQUARES
      DO 40 J=1,M
   40 Z(J)=X(J,I)
      CALL YPS(I)
      YC(I)=YT
      DY(I)=Y(I)-YC(I)
      DEL=DY(I)**2*W(I)
      IF(DEL.LT.X5VAR)GO TO 35
      W(I)=0.0
      IREJ=IREJ+1
      IIW(IREJ)=I+IDUM-1
      IIW(IREJ+100)=Y(I)
   35 VAR=VAR+W(I)*DY(I)**2
      SSQ=SSQ+DY(I)**2
      IF(KFREE.EQ.0) GO TO 90
C     SET UP AN AS VECTOR OF PARTIAL DERIVATIVES
```

```
      K1=0

      DO 60 K=1,IK

      IF(IM.EQ.0) GO TO 4

      DO 50 KK=1,IM

      IF(K.EQ.IX(KK)) GO TO 5

  50 CONTINUE

   4 K2=K-K1

      AN(K2)=PART(K)

      GO TO 60

   5 K1=K1+1

  60 CONTINUE

C     FORM A AND B MATRICES

      DO 80 K=1,KFREE

      DO 70 KK=1,KFREE

      JJ=K+(KK-1)*KFREE

      AM(JJ)=AM(JJ)+AN(K)*AN(KK)*W(I)

      IJ=JJ+KFREE

  70 BM(IJ)=AM(JJ)

  80 BM(K)=BM(K)+AN(K)*DY(I)*W(I)

  90 CONTINUE

      WVAR=VAR

      XSVAR=12.*WVAR/DF

      IF(KFREE.EQ.0) GO TO 23

      IF(LASTIT.EQ.1)LBDA=0.

      CALL LAMBDA(1,PC,LBDA,DP,IT,AM)

      NM=2
```

```
C       OPTIONAL PRINTOUT OF A AND B MATRICES ON LAST ITERATION
        IF(LASTIT.EQ.0) GO TO 6
        IF(IPR.LT.3) GO TO 6
        WRITE(6,500)
    500 FORMAT(///,3X,1HK,19X,6HA(K,L),28X,4HB(K)//)
        DO 110 K=1,KFREE
        WRITE(6,600)BM(K)
    600 FORMAT(//1H+,1P1E67.5)
        JJ=(K-1)*KFREE+1
        IJ=K*KFREE
    110 WRITE(6,700)K,(AM(II),II=JJ,IJ)
    700 FORMAT(I4,1P10E12.4)
C       SOLVE THE NORMAL EQUATIONS
      6 IF(KFREE.GT.1) GO TO 7
        DET=AM(1)
        BM(2)=1.0/AM(1)
        GO TO 8
      7 CONTINUE
        CALL MINV(BM(KP),KFREE,DET,MA,MB)
        IF(DET.EQ.0)LASTIT=1
        IF(DET.EQ.0) WRITE(6,750)IT
    750 FORMAT(' SINGULAR SYSTEM ITER NO  ',I2)
        CALL GMPRD(BM(KP),BM,DP,KFREE,KFREE,1)
        DO 115 I=1,KFREE
        IJ=(I-1)*KFREE+I
        SP(I)=DP(I)
```

```
         DP(I)=DP(I)/DSQRT(AM(IJ))

 ·115 PC(I)=P(I)+DP(I)

 C       WRITE THE VALUE OF THE DETERMINANT, A INVERSE, AND NO. OF ITERATIONS

         CALL LAMBDA(NM,PC,LDDA,DP,IT,AM)

         IF(NM.EQ.2) GO TO 7

       8 IF (LASTIT.EQ.0) GO TO 11

         WRITE(6,800)IT,DET

     800 FORMAT(I6,' ITERATIONS, DET. OF PART. DERIV. MATRIX =',1PE14.6)

 C       CALCULATE NEW PARAMETER VALUES AND CHECK FOR SIGN CHANGES IF NECESSARY

      11 K1=0

         DO 140 K=1,IK

         IF(IM.EQ.0) GO TO 12

         DO 130 KK=1,IM

         IF(K.EQ.IX(KK)) GO TO 16

     130 CONTINUE

      12 K2=K-K1

      13 PC(K)=P(K)+H*DP(K)

         IF(LASTIT.NE.0) GO TO 140

         IF(IFG-1)14,140,15

      14 IF(IT.GT.5) GO TO 140

      15 IF(P(K)*PC(K).GE.0) GO TO 140

         H=H/2

         IF(H.GE.1.0E-10) GO TO 11

         WRITE(6,1500)

    1500 FORMAT(' PROG. QUIT ITERATING DUE TO PARAMETER',I3,' CHANGED SIGN'
        1)
```

```
      H=0

      LASTIT=1

      GO TO 8

   16 KI=KI+1

  140 CONTINUE

C     OPTIONAL PRINTOUT FOR EACH ITERATION

      IF(LASTIT.NE.0) GO TO 19

      IF(IPR.LT.1) GO TO 17

      WRITE(6,1300) IT,H,VAR

 1300 FORMAT( 1H0,I3,1P2E17.7)

 1400 FORMAT( 1P6E11.3)

      IF(IPR.LT.2) GO TO 17

      WRITE(6,1400) (PC(K),K=1,IK)

C     TEST FOR CONVERGENCE

   17 KK=0

      DO 160 K=1,IK

      IF(P(K).EQ.0) GO TO 18

      IF(DABS((PC(K)-P(K))/P(K))-TEST)160,160,19

   18 KK=KK+1

  160 CONTINUE

      IF(KK.EQ.IK) GO TO 19

      M25C=1

C     SET PARAMETER VALUES FOR THE NEXT ITERATION

   19 DO 170 K=1,IK

  170 P(K)=PC(K)

C     AFTER LAST ITERATION GO BACK FOR FINAL CALCULATION OF YC,DY,ETC.
```

```
      IF(LASTIT.EQ.0) GO TO 21

    . KFREE=0

      GO TO 3

C     TEST WHETHER 25 ITERATIONS HAVE BEEN TAKEN

   21 IF(M25C.EQ.1) GO TO 22

      IF(IT.LT.25) GO TO 2

C     GO BACK FOR LAST ITERATION

   22 LASTIT=1

      GO TO 2

C     CALCULATE WEIGHTED VARIANCE, STANDARD DEV. OF THE PARAMS.

   23 WVAR=VAR/DF

      TEST = SQRT(SSQ/DF)

      K1=0

      DO 190 K=1,IK

      IF(IM.EQ.0) GO TO 24

      DO 180 KK=1,IM

      IF(K.EQ.IX(KK)) GO TO 25

  180 CONTINUE

   24 K2=K-K1

      K3=K2+K2*(IK-IM)

      K4=K3-IK+IM

      SP(K)=DSQRT(BM(K3)*WVAR/AM(K4))

      GO TO 190

   25 K1=K1+1

  190 CONTINUE

      IF(IREJ.EQ.0)GO TO 200
```

```
      WRITE(6,1600)IREJ
      WRITE(6,1901) (IIW(J),JIW(J) ,J=1,IREJ)
1901 FORMAT(10(I4,I8))
1600 FORMAT(20X,'THE FOLLOWING',I4,'  POINTS ARE OUTSIDE 3.46 SIGMA')
 200 CONTINUE
      RETURN
      END
      SUBROUTINE MINV(A,N,D,L,M)                                      MINV 033
C                                                                     MINV 001
C     ...........................................................     MINV 002
C                                                                     MINV 003
C     SUBROUTINE MINV                                                 MINV 004
C                                                                     MINV 005
C     PURPOSE                                                         MINV 006
C        INVERT A MATRIX                                              MINV 007
C                                                                     MINV 008
C     USAGE                                                           MINV 009
C        CALL MINV(A,N,D,L,M)                                         MINV 010
C                                                                     MINV 011
C     DESCRIPTION OF PARAMETERS                                       MINV 012
C        A - INPUT MATRIX, DESTROYED IN COMPUTATION AND REPLACED BY   MINV 013
C            RESULTANT INVERSE.                                       MINV 014
C        N - ORDER OF MATRIX A                                        MINV 015
C        D - RESULTANT DETERMINANT                                    MINV 016
C        L - WORK VECTOR OF LENGTH N                                  MINV 017
C        M - WORK VECTOR OF LENGTH N                                  MINV 018
```

```
C                             .                            MINV 019

C   .    REMARKS                        .                  MINV 020

C         MATRIX A MUST BE A GENERAL MATRIX                MINV 021

C                    .                                     MINV 022

C         SUBROUTINES AND FUNCTION SUBPROGRAMS REQUIRED    MINV 023

C            NONE                                          MINV 024

C            .                                             MINV 025

C         METHOD                                           MINV 026

C            THE STANDARD GAUSS-JORDAN METHOD IS USED. THE DETERMINANT  MINV 027

C            IS ALSO CALCULATED. A DETERMINANT OF ZERO INDICATES THAT   MINV 028

C            THE MATRIX IS SINGULAR.                       MINV 029

      DIMENSION A(1),L(1),M(1)                             MINV 034

      REAL*8 DABS

      DOUBLE PRECISION A,D,BIGA,HOLD                       MINV 042

C                                                          MINV 030

C      ...................................................MINV 031

C                                                          MINV 032

C                                                          MINV 035

C      ...................................................MINV 036

C                                                          MINV 037

C         IF A DOUBLE PRECISION VERSION OF THIS ROUTINE IS DESIRED, THE  MINV 038

C         C IN COLUMN 1 SHOULD BE REMOVED FROM THE DOUBLE PRECISION      MINV 039

C         STATEMENT WHICH FOLLOWS.                         MINV 040

C                                                          MINV 041

C                                                          MI-V 043

C         THE C MUST ALSO BE REMOVED FROM DOUBLE PRECISION STATEMENTS    MINV 044
```

```
C       APPEARING IN OTHER ROUTINES USED IN CONJUNCTION WITH THIS      MINV 045
C       ROUTINE.                                                       MINV 046
C                                                                      MINV 047
C       THE DOUBLE PRECISION VERSION OF THIS SUBROUTINE MUST ALSO      MINV 048
C       CONTAIN DOUBLE PRECISION FORTRAN FUNCTIONS.  ABS IN STATEMENT  MINV 049
C       10 MUST BE CHANGED TO DABS.                                    MINV 050
C                                                                      MINV 051
C       ..............................................................MINV 052
C                                                                      MINV 053
C       SEARCH FOR LARGEST ELEMENT                                     MINV 054
C                                                                      MINV 055
        D=1.0                                                          MINV 056
        NK=-N                                                          MINV 057
        DO 80 K=1,N                                                    MINV 058
        NK=NK+N                                                        MINV 059
        L(K)=K                                                         MINV 060
        M(K)=K                                                         MINV 061
        KK=NK+K                                                        MINV 062
        BIGA=A(KK)                                                     MINV 063
        DO 20 J=K,N                                                    MINV 064
        IZ=N*(J-1)                                                     MINV 065
        DO 20 I=K,N                                                    MINV 066
        IJ=IZ+I                                                        MINV 067
   10 IF(DABS(BIGA)-DABS(A(IJ))) 15,20,20                              MINV 068
   15 BIGA=A(IJ)                                                       MINV 069
        L(K)=I                                                         MINV 070
```

```
      M(K)=J                                        MINV 071
   20 CONTINUE                                      MINV 072
C                                                   MINV 073
C           INTERCHANGE ROWS                        MINV 074
C                                                   MINV 075
      J=L(K)                                        MINV 076
      IF(J-K) 35,35,25                              MINV 077
   25 KI=K-N                                        MINV 078
      DO 30 I=1,N                                   MINV 079
      KI=KI+N                                       MINV 080
      HOLD=-A(KI)                                   MINV 081
      JI=KI-K+J                                     MINV 082
      A(KI)=A(JI)                                   MINV 083
   30 A(JI) =HOLD                                   MINV 084
C                                                   MINV 085
C           INTERCHANGE COLUMNS                     MINV 086
C                                                   MINV 087
   35 I=M(K)                                        MINV 088
      IF(I-K) 45,45,38                              MINV 089
   38 JP=N*(I-1)                                    MINV 090
      DO 40 J=1,N                                   MINV 091
      JK=NK+J                                       MINV 092
      JI=JP+J                                       MINV 093
      HOLD=-A(JK)                                   MINV 094
      A(JK)=A(JI)                                   MINV 095
   40 A(JI) =HOLD                                   MINV 096
```

```
C                                                        MINV 097
C          DIVIDE COLUMN BY MINUS PIVOT (VALUE OF PIVOT ELEMENT IS    MINV 098
C          CONTAINED IN BIGA)                            MINV 099
C                                                        MINV 100
    45 IF(BIGA) 48,46,48                                 MINV 101
    46 D=0.0                                             MINV 102
       RETURN                                            MINV 103
    48 DO 55 I=1,N                                       MINV 104
       IF(I-K) 50,55,50                                  MINV 105
    50 IK=NK+I                                           MINV 106
       A(IK)=A(IK)/(-BIGA)                               MINV 107
    55 CONTINUE                                          MINV 108
C                                                        MINV 109
C          REDUCE MATRIX                                 MINV 110
C                                                        MINV 111
       DO 65 I=1,N                                       MINV 112
       IK=NK+I                                           MINV 113
       HOLD=A(IK)                                        MINV M01
       IJ=I-N                                            MINV 114
       DO 65 J=1,N                                       MINV 115
       IJ=IJ+N                                           MINV 116
       IF(I-K) 60,65,60                                  MINV 117
    60 IF(J-K) 62,65,62                                  MINV 118
    62 KJ=IJ-I+K                                         MINV 119
       A(IJ)=HOLD*A(KJ)+A(IJ)                            MINV M02
    65 CONTINUE                                          MINV 121
```

```
C                                                    MINV 122
C          DIVIDE ROW BY PIVOT                        MINV 123
C                                                    MINV 124
      KJ=K-N                                          MINV 125
      DO 75 J=1,N                                     MINV 126
      KJ=KJ+N                                         MINV 127
      IF(J-K) 70,75,70                                MINV 128
   70 A(KJ)=A(KJ)/BIGA                                MINV 129
   75 CONTINUE                                        MINV 130
C                                                    MINV 131
C          PRODUCT OF PIVOTS                          MINV 132
C                                                    MINV 133
      D=D*BIGA                                        MINV 134
C                                                    MINV 135
C          REPLACE PIVOT BY RECIPROCAL                MINV 136
C                                                    MINV 137
      A(KK)=1.0/BIGA                                  MINV 138
   80 CONTINUE                                        MINV 139
C                                                    MINV 140
C          FINAL ROW AND COLUMN INTERCHANGE           MINV 141
C                                                    MINV 142
      K=N                                             MINV 143
  100 K=(K-1)                                         MINV 144
      IF(K) 150,150,105                               MINV 145
  105 I=L(K)                                          MINV 146
      IF(I-K) 120,120,108                             MINV 147
```

```
108 JO=N*(K-1)                                          MINV 148

    JR=N*(I-1)                                          MINV 149

    DO 110 J=1,N                                        MINV 150

    JK=JO+J                                             MINV 151

    HOLD=A(JK)                                          MINV 152

    JI=JR+J                                             MINV 153

    A(JK)=-A(JI)                                        MINV 154

110 A(JI) =HOLD                                         MINV 155

120 J=M(K)                                              MINV 156

    IF(J-K) 100,100,125                                 MINV 157

125 KI=K-N                                              MINV 158

    DO 130 I=1,N                                        MINV 159

    KI=KI+N                                             MINV 160

    HOLD=A(KI)                                          MINV 161

    JI=KI-K+J                                           MINV 162

    A(KI)=-A(JI)                                        MINV 163

130 A(JI) =HOLD                                         MINV 164

    GO TO 100                                           MINV 165

150 RETURN                                              MINV 166

    END                                                 MINV 167

    SUBROUTINE GMPRD(A,B,R,N,M,L)                       GMPRD037

C                                                       GMPRD001

C   ...................................................GMPRD002 .

C                                                       GMPRD003

C       SUBROUTINE GMPRD                               GMPRD004

C                                                       GMPRD005
```

```
C     PURPOSE                                                      GMPRD006

C        MULTIPLY TWO GENERAL MATRICES TO FORM A RESULTANT GENERAL  GMPRD007

C        MATRIX                                                     GMPRD008

C                                                                   GMPRD009

C     USAGE                                                         GMPRD010

C        CALL GMPRD(A,B,R,N,M,L)                                    GMPRD011

C                                                                   GMPRD012

C     DESCRIPTION OF PARAMETERS                                     GMPRD013

C        A - NAME OF FIRST INPUT MATRIX                             GMPRD014

C        B - NAME OF SECOND INPUT MATRIX                            GMPRD015

C        R - NAME OF OUTPUT MATRIX                                  GMPRD016

C        N - NUMBER OF ROWS IN A                                    GMPRD017

C        M - NUMBER OF COLUMNS IN A AND ROWS IN B                   GMPRD018

C        L - NUMBER OF COLUMNS IN B                                 GMPRD019

C                                                                   GMPRD020

C     REMARKS                                                       GMPRD021

C        ALL MATRICES MUST BE STORED AS GENERAL MATRICES            GMPRD022

C        MATRIX R CANNOT BE IN THE SAME LOCATION AS MATRIX A        GMPRD023

C        MATRIX R CANNOT BE IN THE SAME LOCATION AS MATRIX B        GMPRD024

C        NUMBER OF COLUMNS OF MATRIX A MUST BE EQUAL TO NUMBER OF ROWGMPRD025

C        OF MATRIX B                                                GMPRD026

C                                                                   GMPRD027

      DOUBLE PRECISION A,B,R

      DIMENSION A(1),B(1),R(1)                                      GMPRD038

C     SUBROUTINES AND FUNCTION SUBPROGRAMS REQUIRED                 GMPRD028

C        NONE                                                       GMPRD029
```

```
C                                                              GMPRD030
C        METHOD                                                GMPRD031
C           THE M BY L MATRIX B IS PREMULTIPLIED BY THE N BY M MATRIX A GMPRD032
C           AND THE RESULT IS STORED IN THE N BY L MATRIX R.   GMPRD033
C                                                              GMPRD034
C        ......................................................GMPRD035
C                                                              GMPRD036
C                                                              GMPRD039
         IR=0                                                  GMPRD040
         IK=-M                                                 GMPRD041
         DO 10 K=1,L                                           GMPRD042
         IK=IK+M                                               GMPRD043
         DO 10 J=1,N                                           GMPRD044
         IR=IR+1                                               GMPRD045
         JI=J-N                                                GMPRD046
         IB=IK                                                 GMPRD047
         R(IR)=0                                               GMPRD048
         DO 10 I=1,M                                           GMPRD049
         JI=JI+N                                               GMPRD050
         IB=IB+1                                               GMPRD051
   10    R(IR)=R(IR)+A(JI)*B(IB)                               GMPRD052
         RETURN                                                GMPRD053
         END                                                   GMPRD054
         SUBROUTINE PGRES (V,U,A,B,N1,N2,R2,SWTCH)
         DOUBLE PRECISION V,U,SWTCH
         DIMENSION U(255),V(255)
```

```
      REAL M1,M2
120 FORMAT(' ZERO          (STD ERROR OF ESTIMATE EXCEEDS STD DEV OF Y
   1)'/)
      N=N2-N1+1
100 FORMAT (   3X,''S I M P L E   L I N E A R   R E G R E S S I O N
   1EQUATION    LOG(Y-F(X)) = A + B*X' ,//1X,'INDX R*R  EXPL VAR   UNEX
   2P VAR  STD ERR        VALUE       95 PCT CONF LIMITS  BEGIN  END
   3DIFF'   )
150 FORMAT (1H1)
200 FORMAT (F9.5,2F10.6,F9.6,4H  A=,3F12.8,I4,I6,I6./,38X,4H  B=,3F12.
   18)
     IF(SWTCH.EQ.2.0)GO TO 11
      IF (A) 8,10,8
  8 IF (ICNT-25) 11,11,9
  9 WRITE (6,150)
 10 ICNT = 1
     IF(SWTCH.EQ.1)GO TO 101
102 WRITE(6,110)
110 FORMAT(1H ,'ITERATIONS NOT DISPLAYED')
     GO TO 11
101 WRITE(6,100)
 11 ICNT = ICNT+1
      S1=0
      S2=0
      S3=0
      S4=0
```

```
      S5=0

      DU 20 I=N1,N2

      S1=S1+U(I)

      S2=S2+U(I)*U(I)

      S3=S3+V(I)

      S4=S4+V(I)*V(I)

   20 S5=S5+U(I)*V(I)

      M1=S1/N

      M2=S3/N

      D1=S2/N-M1*M1

      D2=S4/N-M2*M2

      D3=S5/N-M1*M2

      C1=N*D1

      RB=0

      B=D3/D1

      A=M2-B*M1

      D4=D2-B*D3

      D44 = D4

      IF (D4-D2)2070,2040,2040

 2040 RB=1

      R2=0

      GO TO 2080

 2070 R2=1-(D4/D2)

 2080 CONTINUE

      IF(R8)2110,2130,2110

 2110 WRITE (6,120)
```

```
      GO TO 2160

2130 D2M4=D2-D4

      D4SQR=SQRT(D4)

2160 D4=N*D4/(N-2)

      T=1.95996+2.37226/(N-2)+2.82250/(N-2)*(N-2)

      D5=SQRT(D4/C1)

      D6=SQRT(D4/N)

      B1=B-T*D5

      B2=B+T*D5

      A1=A-T*D6

      A2=A+T*D6

      IF(SWTCH.NE.1)GO TO 56

      WRITE (6,200)B2,D2M4,D44,D4SQR,A,A1,A2,N1,N2,N,B,B1,B2

   56 IF(SWTCH.NE.2.0)GO TO 57

      B2=D5

      SWTCH=D6

   57 CONTINUE

      RETURN

      END

      SUBROUTINE DSPAK

C     PLOT ROUTINE

      DOUBLE PRECISION W,P,SP,YC,DY,PART,BM,DET,ALAB

      DOUBLE PRECISION YT,WVAR

      COMMON N,IK,IW,M,IB,ITEST,IDUM,NDUM,IPR,IFG,IM,TEST,YT,WVAR,SSQ,
     1IDF,DET,ISW,IPLT,ISC,INTT,Y(300),X(1,300),W(300),IX(10),PG(10),P(
     210),SP(10),YC(300),DY(300),    BM(10,11),ALAB(10),PART(10),NSETS
```

```
      EQUIVALENCE (IDUM,IN1),(NDUM,NN2)

      DIMENSION ICH(10),APLT(128)

      INTEGER APLT

      DATA IBCH,ISCH,ICH/' ','*','A','B','C','D','E','T','U','V','W','X'
     1/

      DATA IOCH/'0'/

  500 FORMAT (1X,I3,128A1)

  901 FORMAT(1H1)

  905 FORMAT(2X,F7.3,116X,F7.0)

      K=IK-1

      KK=IK/2-1

      IJ=1

      J=1

      WVAR=DSQRT(WVAR)

      DO 5 I=1,N

      IF(Y(J).LT.Y(I))J=I

  5 CONTINUE

      DO 7 I=1,KK

      SP(I)=P(2*I-1)*DEXP(-X(1,J)/P(2*I))

      IF(SP(I).GT.SP(IJ))IJ=I

  7 CONTINUE

      YQ=Y(J)-P(K)

      DO 8 I=1,KK

      IF(I.EQ.IJ)GO TO 8

      YQ=YQ-SP(I)

  8 CONTINUE
```

```
      SCALE=115./ALOG(1000.)

      CHKZ=EXP(1./SCALE)*YO/1000.

      J=-IPLT

      WRITE(6,901)

      YOLN1=(YO/1000.)

      WRITE(6,905)YOLN1,YO

170   IXPLT=0

      N1=116

200   DO 210 I=1,116

210   APLT(I)=ISCH

      APLT(58)=IOCH

      J=J+1

      GO TO 250

215   J=J+IPLT

      IF(J-N) 216,216,170

216   CONTINUE

      IXPLT=IN1+J-1

      DO 220 I=2,115

220   APLT(I)=IBCH

      DO 240 I=1,KK

      DUM=Y(J)-P(K)

      DO 230 IJ=1,KK

      IF(IJ-1)225,230,225

225   DUM=DUM-P(2*IJ-1)*DEXP(-X(1,J)/P(2*IJ))

230   CONTINUE

      IF(DUM-CHKZ)237,237,235
```

```
235 NMBR=(ALOG(DUM)-ALOG(YO/1000.))*SCALE+1.

    IF(NMBR-116)238,238,236

236 NMBR=116

    GO TO 238

237 NMBR=2

238 APLT(NMBR)=ICH(I)

    IF(N1.LT.NMBR) N1=NMBR

240 CONTINUE

    NMBR=((DUM-P(K-2)*DEXP(-X(1,J)/P(2*KK)))*W(J)**.5*.1)+64

    IF(NMBR-1)247,247,245

245 CONTINUE

    IF(NMBR-115)248,248,246

246 NMBR=115

    GO TO 248

247 NMBR=2

248 APLT(NMBR)=ICH(KK+1)

    IF(N1.LT.NMBR)N1=NMBR

250 WRITE(6,500)IXPLT,(APLT(I),I=1,N1)

    N1=2

    IF(J-N)215,170,251

251 CONTINUE

    RETURN

    END

    SUBROUTINE INPAK(N1,NTC,CHAN,TIM,TIME,Y,DATE,NRD)

    DIMENSION CHAN(10),TIM(10),Y(512),DATE(4)

    INTEGER RN
```

```
      INTEGER CHAN

      DOUBLE PRECISION LA,LB,DATE,SA,TIM

      NP=7

      NPU=NI

      READ(NRD   ,9101)LA,LB,DA,XMO,YR,RN,SA,VL,P

      READ(NRD   ,9102)N1,NTC,(CHAN(I),I=1,NTC)

      READ(NRD   ,9103)(TIM(I),I=1,NTC)

 9101 FORMAT(2A6,A2,A3,A4,I2,A6,F5.0,F5.1)

 9102 FORMAT(I3,I1,8I3)

 9103 FORMAT(8F7.2)

      N=N1

      IF(NRD.NE.5) GO TO 10

      READ(NRD,7000) TIME,(Y(I),I=1,N)

      GO TO 7500

   10 READ(NRD,6000)TIME,(Y(I),I=1,N)

 6000 FORMAT(F6.0,9F7.0)

 7000 FORMAT(10F8.0)

      IF(NPU.NE.1) GO TO 7500

      WRITE(NP,9101)LA,LB,DA,XMO,YR,RN,SA,VL,P

      WRITE(NP,9102)N1,NTC,(CHAN(I),I=1,NTC)

      WRITE(NP,9103)(TIM(I),I=1,NTC)

      WRITE(NP,7000)TIME,(Y(I),I=1,N)

 7500 CONTINUE

      WRITE(6,9201)LA,LB,DA,XMO,YR,RN

      WRITE(6,9202)SA,VL,P,DATE

 9201 FORMAT(1H1,//////,1H ,2A6,3X,'DATE-',A2,A3,A4,3X,'RUN  ',I2)
```

```
9202 FORMAT(1H ,'SAMPLE-',A6,3X,'WAVELENGTH=',F5.0,'A',3X,'PRESSURE=',F
     15.1,'MICRONS'//' CALCULATED AT',1X,A6,1X,3A6/)
     RETURN
     END
/*
//GU.SYSIN DD *
```

W C PASKE   DATE-JUN 30.73   RUN 3
SAMPLE-N2 2PS   WAVELENGTH=3371.A   PRESSURE=400.0MICRONS

CALCULATED AT 14 00 MON. JUL. 02.1973

ENTER NUMBER OF PARAMS, FIRST POINT,LAST POINT,WEIGHT POWER, IPR=0,1,2 OR 3 FOR INCREASED OUTPUT. IM=1 HOLD CONSTANT
  3 30 250-1.0   0   0
ENTER LIFETIMES(SHORT,LONG),COEFFS(SHORT,LONG),CONSTANT
  4.0E 01   6.0E 02   7.0E 01
CALIBRATION IS   1.66512 NS/CHAN +OR- 0.0078660
30 250

0.0	0.0	0.0	0.0	0.0	0.0	0.0	0.0	0.0	0.0
8.8E 02	8.7E 02	8.7E 02	8.7E 02	8.2E 02	8.8E 02	8.6E 02	8.8E 02	8.3E 02	9.0E 02
7.7E 02	8.2E 02	8.0E 02	8.0E 02	8.6E 02	7.9E 02	8.1E 02	8.3E 02	8.3E 02	7.7E 02
6.5E 02	6.6E 02	4.0E 02	6.0E 02	6.0E 02	7.4E 02	8.0E 02	7.1E 02	7.5E 02
5.5E 02	1.2E 02	4.8E 02	4.6E 02	5.7E 02	6.0E 02	5.8E 02	5.8E 02	5.6E 02
3.4E 02	3.7E 02	3.6E 02	3.5E 02	3.7E 02	4.6E 02	4.2E 02	3.3E 02	4.3E 02
2.9E 02	2.8E 02	2.7E 02	2.9E 02	3.2E 02	3.5E 02	3.3E 02	3.3E 02
2.4E 02	2.5E 02	2.4E 02	1.9E 02	2.7E 02	2.5E 02	2.8E 02	2.6E 02
1.8E 02	1.9E 02	1.7E 02	1.7E 02	1.9E 02	2.1E 02	1.9E 02	1.9E 02
1.6E 02	1.4E 02	1.4E 02	1.7E 02	1.7E 02	1.7E 02	1.6E 02	1.7E 02
1.5E 02	1.3E 02	1.3E 02	1.3E 02	1.6E 02	1.3E 02	1.3E 02	1.5E 02
1.3E 02	1.0E 02	1.1E 02	1.2E 02	1.3E 02	1.3E 02	1.2E 02	1.1E 02
1.0E 02	1.1E 02	1.2E 02	1.2E 02	9.4E 01	1.1E 02	1.1E 02	1.1E 02
1.1E 02	9.6E 01	1.1E 02	1.2E 02	9.2E 01	1.2E 02	1.0E 02	9.5E 01
8.9E 01	1.1E 02	1.0E 02	9.9E 01	1.2E 02	9.3E 01	9.9E 01	9.7E 01
8.0E 01	8.7E 01	1.1E 02	1.1E 02	8.7E 01	1.0E 02	1.2E 02	1.0E 02
1.0E 02	7.6E 01	9.3E 01	8.0E 01	8.0E 01	1.0E 02	1.0E 02
7.9E 01	6.4E 01	9.0E 01	9.8E 01	9.5E 01	9.3E 01	6.8E 01	8.5E 01
7.8E 01	8.6E 01	8.1E 01	8.2E 01	8.2E 01	9.8E 01	8.8E 01	1.0E 02
9.3E 01	9.0E 01	8.3E 01	8.2E 01	8.6E 01	8.7E 01	7.7E 01
8.1E 01	7.3E 01	8.2E 01	8.3E 01	9.3E 01	8.5E 01	7.5E 01	7.3E 01
6.7E 01	7.7E 01	8.7E 01	9.7E 01	7.3E 01	8.7E 01	9.3E 01	6.7E 01
6.7E 01	7.4E 01	7.7E 01	7.7E 01	7.7E 01	7.9E 01	7.1E 01	9.4E 01
9.4E 01	7.5E 01	7.3E 01	6.9E 01	7.0E 01	7.6E 01	7.0E 01
7.1E 01	8.8E 01	6.9E 01	6.8E 01	6.0E 01	8.4E 01	6.9E 01	7.3E 01
6.0E 01	9.0E 01	6.6E 01	6.9E 01	3.4E 03	9.9E 01	5.9E 01	8.6E 37	-1.9E 22
2.5E-01	-1.4E 01	-1.1E 42	9.5E-07	2.0E-79	2.8E-72	5.1E-85	3.0E 53
5.1E-85	3.0E 53	9.8E-03	5.1E-85	5.1E-85	3.0E 53	9.8E-03	5.1E-85
3.0E 53	5.1E-85	1.3E-79	5.0E 52	-6.6E-80	1.3E-85	1.3E-79	5.0E 52
5.1E-85	1.3E-79	3.0E-80	-6.8E-80	5.1E-05	5.1E-85	3.0E 53	-9.8E-03	5.1E-85

221 250 30
WEIGHT RANGES FROM 1.0 TO 10.329 FOR CHAN 250
6 ITERATIONS. DET. OF PART. DERIV. MATRIX = 2.5461280-01
      THE FOLLOWING 2 POINTS ARE OUTSIDE 3.46 SIGMA
      403
43 124 34
SUM OF EXPONENTIALS. $Y(I)=P(1)*EXP(-X(I)/P(2))+...+P(3)$

THE WEIGHTED VARIANCE IS 9.47183110 02
THE UNWEIGHTED SIGMA IS 3.29579016E 01 AND THE UNWEIGHTED SUM OF SQUARES OF THE DEVS IS 2.36796681E 05
        GUESS OF   FINAL VAL OF   S.D. OF   EXACT LST SQRS EQNS
K   K-TH PARAM   K-TH PARAM   K-TH PARAM   FITTED FCTN   INPUT DATA
1   6.0000E 02   6.41750 02   9.36280 00   1.0430E 02   1.0630E 02
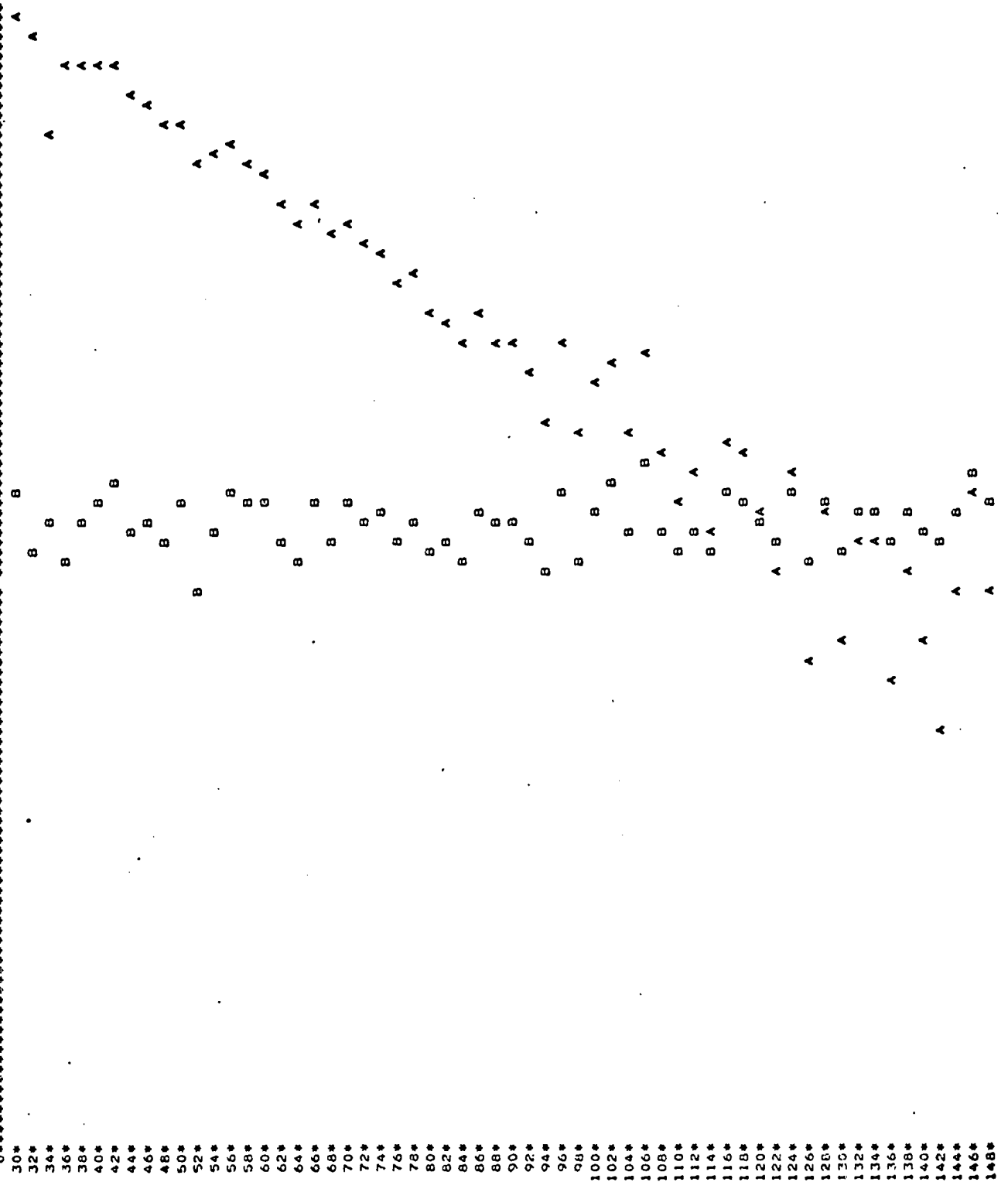2   4.0000E 01   4.97240 01   8.50870-01   9.91670 03   9.9168E 03
3   7.0500E 01   8.0461D 01   1.0786D 00   1.6512E 05   1.6513E 05
ENTER PLOT INCR IF PLOT IS DESIRED THEN 0 FOR NEXT CASE.1 TO RERUN WITH NEW PARAMETERS.-1 TO CALL EXIT
2   0

W C PASKE   DATE-JUN 30,73   RUN   4
SAMPLE-N2 2PS   WAVELENGTH=3371.A   PRESSURE=400.0MICRONS

CALCULATED AT 14 00 MON. JUL. 02,1973

ENTER NUMBER OF PARAMS, FIRST POINT,LAST POINT,WEIGHT POWER, IPR=0,1,2 OR 3 FOR INCREASED OUTPUT, IM=1 HOLD CONSTANT
   3 35 250-1.0   0   0
ENTER LIFETIMES(SHORT,LONG),COEFFS(SHORT,LONG),CONSTANT
   4.0E 01   1.5E 03   2.0E 02
CALIBRATION IS   1.66512 NS/CHAN +OR- 0.0078660
  35 250
     0.0   0.0   0.0   0.0   1.0E 00   1.3E 03   1.6E 03   1.7E 03   1.6E 03   1.7E 03
     1.7E 03   1.8E 03   1.7E 03   1.7E 03   1.6E 03   1.7E 03   1.6E 03   1.7E 03   1.6E 03   1.7E 03
     1.7E 03   1.6E 03   1.7E 03   1.7E 03   1.5E 03   1.6E 03   1.5E 03   1.5E 03   1.5E 03   1.5E 03
     1.5E 03   1.5E 03   1.4E 03   1.4E 03   1.3E 03   1.3E 03   1.3E 03   1.3E 03   1.3E 03   1.2E 03
     1.2E 03   1.1E 03   1.1E 03   1.1E 03   1.1E 03   1.0E 03   9.9E 02   9.4E 02   9.7E 02   9.0E 02
     8.9E 02   7.8E 02   8.1E 02   8.3E 02   7.4E 02   8.7E 02   7.2E 02   7.9E 02   6.5E 02   6.6E 02
     7.3E 02   6.8E 02   6.7E 02   6.7E 02   6.7E 02   6.7E 02   5.8E 02   5.6E 02   5.9E 02   5.6E 02
     5.5E 02   5.5E 02   4.8E 02   5.4E 02   5.1E 02   4.8E 02   5.0E 02   4.5E 02   4.5E 02   4.7E 02
     4.4E 02   4.5E 02   4.3E 02   4.3E 02   4.5E 02   3.8E 02   4.2E 02   4.0E 02   3.9E 02   4.0E 02
     3.7E 02   3.7E 02   3.4E 02   3.7E 02   3.4E 02   3.3E 02   1.1E 02   3.5E 02   3.0E 02   3.1E 02
     3.7E 02   3.3E 02   3.3E 02   3.3E 02   3.1E 02   3.2E 02   3.1E 02   3.1E 02   2.9E 02   2.7E 02
     8.4E 01   3.0E 02   3.1E 02   2.9E 02   2.7E 02   2.9E 02   2.9E 02   3.0E 02   2.6E 02   2.6E 02
     2.8E 02   2.7E 02   2.9E 02   2.8E 02   2.9E 02   2.6E 02   2.6E 02   2.6E 02   2.4E 02   2.8E 02
     2.5E 02   2.2E 02   2.5E 02   2.7E 02   2.4E 02   2.7E 02   2.6E 02   2.5E 02   2.6E 02   2.4E 02
     2.6E 02   2.5E 02   2.4E 02   2.4E 02   2.7E 02   2.5E 02   2.4E 02   2.7E 02   2.1E 02   2.2E 02
     2.3E 02   2.6E 02   2.4E 02   2.2E 02   2.4E 02   2.4E 02   2.3E 02   2.3E 02   1.2E 02   2.2E 02
     2.5E 02   2.5E 02   2.4E 02   2.2E 02   2.3E 02   2.1E 02   2.4E 02   2.3E 02   2.3E 02   2.5E 02
     2.3E 02   2.2E 02   2.3E 02   2.4E 02   2.3E 02   2.1E 02   2.3E 02   2.0E 02   2.2E 02   2.3E 02
     2.4E 02   2.3E 02   2.3E 02   2.6E 02   2.2E 02   2.6E 02   2.3E 02   2.1E 02   2.3E 02   2.0E 02
     2.0E 02   2.5E 02   2.4E 02   2.3E 02   2.4E 02   2.3E 02   2.0E 02   2.3E 02   2.1E 02   2.0E 02
     1.9E 02   2.1E 02   2.3E 02   2.3E 02   2.0E 02   2.3E 02   2.2E 02   2.1E 02   2.2E 02   2.2E 02
     2.2E 02   2.3E 02   1.9E 02   1.9E 02   2.4E 02   1.9E 02   2.2E 02   2.1E 02   2.4E 02   1.9E 02
     2.2E 02   2.4E 02   2.3E 02   2.0E 02   2.0E 02   1.9E 02   2.3E 02   2.1E 02   2.1E 02   1.9E 02
     2.0E 02   1.8E 02   2.0E 02   2.0E 02   2.0E 02   2.1E 02   1.9E 02   2.1E 02   1.6E 02   1.9E 02
     2.0E 02   1.9E 02   2.0E 02   2.0E 02   2.3E 02   2.3E 02   1.9E 02   1.8E 02   2.1E 02   2.0E 02
     1.9E 02   1.9E 02   1.9E 02   2.1E 02   1.9E 02   -3.4E 03   -8.9E 05   8.6E 37   -5.8E 22   -1.9E 22
     2.5E-01   2.5E-01   2.5E-01   -1.4E 01   -1.1E 42   9.5E-07   2.0E-79   2.8E-72   5.1E-85   3.0E 53
    -9.8E-03   5.1E-85   5.1E-85   3.0E 53   -9.8E-03   5.1E-85   5.1E-85   3.0E 53   -9.8E-03   5.1E-85
     5.1E-85   3.0E 53   -9.8E-03   5.1E-85   1.3E-79   3.0E 52   -6.8E-80   5.1E-85   1.3E-79   5.0E 52
    -6.4E 02   5.1E-85   1.3E-79   3.0E 52   -6.8E-80   5.1E-85   5.1E-85   3.0E 53   -9.8E-03   5.1E-85
 216 250 35
WEIGHT RANGES FROM 1.0 TO 6.613 FOR CHAN 250
     5 ITERATIONS, DET. OF PART. DERIV. MATRIX = 2.5676150-01
              THE FOLLOWING   3 POINTS ARE OUTSIDE 3.46 SIGMA
  97   112 111   84 159   115
SUM OF EXPONENTIALS, Y(I)=P(1)*EXP(-X(I)/P(2))+...+P(3)

THE WEIGHTED VARIANCE IS 1.7355181D 03
THE UNWEIGHTED SIGMA IS 3.2627060E 01 AND THE UNWEIGHTED SUM OF SQUARES OF THE DEVS IS 2.2674394E 05
         GUESS OF   FINAL VAL OF   S.D. OF   EXACT LST SQRS EQNS
  K K-TH PARAM K-TH PARAM K-TH PARAM   FITTED FCTN   INPUT DATA
  1   1.5000E 03 1.1572D 03 1.2953D 01   1.8370E 02   1.8369E 02
  2   4.0000E 01 4.8838D 01 7.0280D-01   3.1906E 04   3.1906E 04
  3   2.0050E 02 2.1023D 02 1.7897D 00   2.8030E 05   2.8031E 05
ENTER PLOT INCR IF PLOT IS DESIRED THEN 0 FOR NEXT CASE,1 TO RERUN WITH NEW PARAMETERS,-1 TO CALL EXIT
  2 -1